Safety in CO_2 logistics

ConsenCUS-D8.6-Safety report on CO_2 logistics – version 1 - 2404

Date	Version	Status	Initials	Changes Marked
April 30, 2024	1	First issue	KHA, JCH, SCU	-

This project has received funding from the European Union's Horizon 2020 research and Innovation programme under grant agreement N° 101022484.

Version Control Sheet

WP	WP 8 CO_2 clusters & value chain design
Lead Author:	K. Harboe (DGC)
Contributing Author(s):	J.O. Christensen (DGC), S. Cuthbert (DGC)
Reviewed by:	Nikolai Andrianov (GEUS)
Due Date:	2024-04-30
Date:	2024-04-30
Version:	1
Contact:	kha@dgc.dk
Dissemination Level:	x PU: Public □ CO: Confidential, only for members of the consortium (including the Commission)

Table of contents

Abbreviations

ALARA	As Low As Reasonably Acceptable
CCS	Carbon Capture and Storage
CCUS	Carbon Capture, Utilization and Storage
DMI	Danish Meteorological Institute
EIGA	European Industrial Gas Association
EGIG	European Gas Pipeline Incident Data Group
EOR	Enhanced Oil Recovery
EOS	Equation of State
ERT	Emergency Response Team
FEED	Front-End Engineering Design
HSE	Health and Safety Executive
IDHL	Immediate dangerous to life or health
IRPA	Individual Risk per Annum
LNG	Liquefied Natural Gas
LPG	Liquefied Petroleum Gas
PHMSA	Pipeline Hazardous Material Safety Administration
PLL	Potential for Loss of Life
QRA	Quantitative risk assessment
SCBA	Self-Contained Breathing Apparatus
SLOD DTL	Significant likelihood of death dangerous toxic load
SLOT DTL	Specific level of toxicity dangerous toxic load

1 Extended summary

1.1 Objectives

As the European Commission strives towards net zero greenhouse gas emissions in 2050, it puts high pressure on energy-intensive and large emitting industries with a high amount of unavoidable process emissions. The application of Carbon Capture, Utilization and Storage (CCUS) technologies is essential for net zero CO_2 emissions. An important but often underestimated step to succeed in CCUS is the need for transporting CO_2 from one or more sources to a CO_2 storage facility or utilization site.

Delivery 8.6 examines the safety issues for CO_2 transportation related to the CCUS value chain. CO_2 is potentially toxic. It can displace oxygen in breathing air at high concentrations. This can lead to shortness of breathing, mild narcosis, confusion, headache, etc. Like all other means of moving gases or liquids, the transportation of CO_2 can and must be handled safely to avoid or minimize the risk of danger to the environment and human health.

To assess the risks associated with transportation of gases or liquids, including CO_2, the following questions can be asked:

Question 1: What can happen?
Question 2: How often can it happen?
Question 3: What are the consequences of an event?
Question 4: What is the risk?
Question 5: Is the risk acceptable and how can it be mitigated?

This report examines the above questions for transportation of CO_2.

Section 2 and 3 looks into **Question 1** about how CO_2 behaves and gives a qualitative representation of the safety and risk in CO_2 transport for pipeline, road, rail and shipping transportation as well as intermediate storage.
Section 3 gives a broader view for the safety in CO_2 transport leading to **Question 2** and **Section 4** about the failure frequencies of pipelines and tanks. A statistical analysis of pipeline incidents is presented using data 1) from CO_2 pipelines in the U.S. reported by the Pipeline Hazardous Material Safety Administration (PHMSA), and 2) incident data bases for the natural gas grid in the EU.

Section 5 gives to some considerations to **Question 3** by examining the consequence from a CO_2 pipeline rupture and rupture of intermediate storage tanks. The section is based on cases relevant to the CCUS value chain and presents a sensitivity analysis of selected parameters in consequence modeling. Consequence analysis for leakages was not studied in this report.

Risk is the combination of the probability of an incident to happen – as examined in Section 4 – and the consequence of the event – as examined in Section 5. Moving on to **Question 4**, the **Section 6** presents the risk assessment for selected cases and the model considerations and assumptions related to quantifying the risk.

Whether the risk is acceptable or not is country and company specific. To come around **Question 5,** considerations for the emergency management is described in **Section 7** as the emergency response plan will be one of the keys to success in the CCUS value chain. Lastly, the project conclusions are presented in **Section 8**.

1.2 Concluding remarks

The main highlights from this study are:

- The emergency preparedness of a community on the periphery of a CO_2 pipeline release event is critical to minimizing the negative effects on the community until the local emergency can effectively respond. This is due to the short time lapse from the initial release to the point where the CO_2 has dispersed to non-toxic levels.

- The weather conditions and the terrain are the key sensitivities for determining the extend of the toxicity of the released CO_2 cloud.

- Modeling with pure CO_2 without accounting for the solid formation and deposition during the release can skew the dispersion curves over the time period of the simulation. This skewness is evident in the eyewitness accounts from the Satartia incident.

1.3 Recommendations for future work

Through this study there is a qualitative indication of significant sensitivities for key assumptions that were not investigated. Therefore, the following main topics are recommendations for further studies.

- Inclusion of impurities in the toxic cloud dispersion for CO_2 release.
- Inclusion of realistic failure rates for isolation valves installed within the pipeline for safety segmentation.
- Tank failures leading to pool accumulations around the tank where the tank integrity is largely maintained – i.e. tank wall crack.
- Release scenarios from a pipeline with varying hole size.

Acknowledgement

This project has received funding from the European Union's Horizon 2020 research and innovation programme under grant agreement No 101022484.

The sole responsibility for the content of this publication lies with the authors. It does not necessarily represent the opinion of the European Union. Neither CINEA nor the European Commission are responsible for any use that may be made of the information contained therein.

2 General hazards of CO_2 in CCUS value chain

Carbon Capture, Utilization and Storage (CCUS) requires transportation of CO_2 from point source to utilization or storage site, and it is important to know the properties and hazards of CO_2 to ensure correct handling and transportation. CO_2 is naturally present in the air at a concentration around 0.04% by volume and is considered non-toxic at this concentration. At normal atmospheric pressure and temperature CO_2 is a colorless, odorless and non-flammable gas. As CO_2 is denser than air at standard conditions (ρ_{CO2} = 1.8 kg/m^3, ρ_{air} = 1.2 kg/m^3 at 1 bar and 20 °C), CO_2 from a leak will tend to accumulate in confined spaces or valleys and depressions near the ground. CO_2 is generally considered to have a low toxicity, however, at elevated concentrations CO_2 becomes toxic. CO_2 is a normal product of human metabolism and is released when we breath. Oxygen from the air enters the lungs and diffuses across the alveolar membrane into the blood. The CO_2 from the blood enters the alveoli at the same time. It is the concentration gradient across the membranes than drives the transport of CO_2 from the blood to the lungs. Higher concentration of CO_2 in the air we are breathing will lower the CO_2 concentration gradient and lower the quantities of CO_2 that leaves the blood stream. The body will respond to this but only to a limit. The increased CO_2 concentration in the lungs will decrease the space for oxygen, and this effect is called intoxication. It is possible to have a slightly lower oxygen concentration of 19%, which is not harmful, but an increased CO_2 concentration of 10% is very harmful over time (see Table 1) [1].

Properties of CO_2

Molecular weight: 44 g/mol
Critical point: 31 °C at 7.38 MPa
Density: 1.8 kg/m^3 at 1 bar and 20 °C
Colorless and odorless
Non-explosive
Toxic at elevated concentrations

Safety information from EIGA [1]***:***

"

Important to measure CO_2 concentration and not only the oxygen concentration.

Scenario:

Following a release of carbon dioxide into the air in a factory the oxygen concentration was measured on oxygen monitors as falling from the normal 21% to 19%.

What does this mean?

Based on the composition of air (21% oxygen and 79% nitrogen; ratio of 1:3.76) the 2%-point reduction in oxygen corresponds to a total amount of 9.5% air (2% oxygen and 7.5% nitrogen) which has been replaced by the carbon dioxide that was released. Therefore, a reduction of "only" 2%-point oxygen results in a concentration of 9.5% carbon dioxide and this represents a significant hazard of intoxication to any people in the area.
"

CO_2 transportation in relation to CCUS will take place at high concentrations, almost 100% pure CO_2 streams, which means that safety measures must be considered to avoid leakages of CO_2 to the surroundings. If high-pressure CO_2 is released into the atmosphere, the temperature will decrease due to the expansion (Joule-Thomson effect). In some cases, reaching the sublimation temperature of approximately -79 °C, which can lead to cryonic burns on the skin and in the respiratory tract in case of inhalation.

In cases where the CO_2 release plume causes the temperature to drop below the water dew point temperature at atmospheric conditions, the water vapor in the atmosphere will condense to form a cloud visible to humans.

Symptoms of CO_2 exposure include headaches, dizziness, confusion, loss of consciousness and ultimately death by suffocation. The symptoms depend on both the concentration of CO_2 in air and the time of exposure, see description in Table 1 [1, 2].

2.1 Dangerous toxic load

The Health and Safety Executive in UK defines toxic dose as

$$A = C^n t$$

where *t* is the exposure time in minutes, *C* is the concentration in ppm, and *n* is an exponent for *C*. For CO_2 *n* equals 8. The toxic dose, *A*, for CO_2 then has the unit '$ppm^8 min$'.

HSE UK defines an expression of "Specific level of toxicity dangerous toxic load (SLOT DTL)" and "Significant likelihood of death dangerous toxic load (SLOD DTL)" [4]. SLOT relates to a mortality of 1-5% and SLOD to a mortality of 50%. Both DTLs are based on studies on animals, with the limitations and difficulties in extrapolating animal data to humans. However, the recommended practice by DNV states that "unless the use of alternative harm criteria is justified, the SLOT and SLOD dangerous toxic load should be applied" [5]. Figure 1 shows the SLOT and SLOD DTL limits for CO_2 as defined by HSE UK [4] and correlates both CO_2 concentration and exposure time. The correlation is for pure CO_2, and the toxicity of other contaminants, such as H_2S, should be considered as part of the safety risk assessment.

Another definition by HSE UK and listed in Table 1 is the "Immediately dangerous to life or health" (IDHL). This is defined as "the maximum exposure concentration for a given chemical in the workplace from which one could escape within 30 minutes without any escape impairing symptoms or any irreversible health effect" [3]. IDHL for CO_2 is at an exposure concentration of 4% and corresponds to a toxic dose of 2E+38 ppm^8min. SLOT corresponds to a toxic dose of 1.5E+40 ppm^8min and SLOD corresponds to a toxic dose of 1.5E+41 ppm^8min.

Table 1 CO_2 concentration and related responses and exposure time. Reproduced from [3].

Exposure time	% CO_2	Responses
8 hours	4.5%	Reduced concentration capability
1 hour	5.5%	Breathing difficulty, headache, and increased heart rate
15 min	6.5%	Dizziness and confusion
6 min	7.0%	Anxiety caused by breathing difficulty effects becoming severe
30 min	10%	Approaches threshold of unconsciousness
30 min	4%	Immediate dangerous to life or health (IDLH)
5 min	12%	Threshold of unconsciousness reached
1 min	15%	Exposure limit
<1 min	20%	Unconsciousness occurs

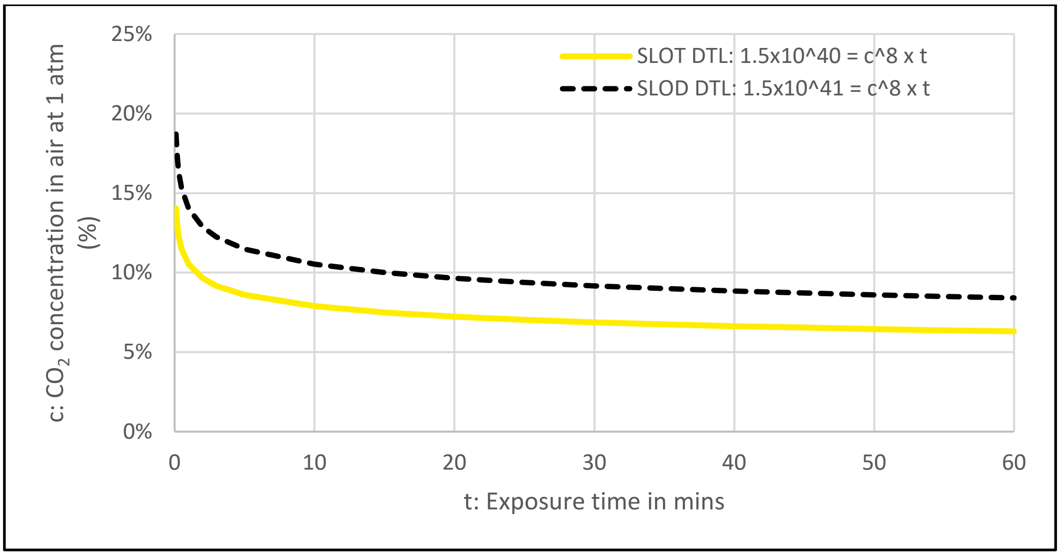

Figure 1 Specific level of toxicity dangerous toxic load (SLOT DTL) and significant likelihood of death dangerous toxic load (SLOD DTL) for CO_2. Reproduced from [4].

2.2 Probit function

The so-called "Purple Book" published by Dutch Committee for the Prevention of Disasters on risk analysis [6], shows how to relate the effect of an exposure to the given concentration and time of exposure with a probit function. The general form is:

$$\mathrm{Pr} = a + b\ln(C^N t) \qquad \text{Eq. 1}$$

where *a*, *b* and *N* are constants, *C* is the concentration (ppm), and *t* is the exposure time (min). The relation between the probability of effect, P_{death}, and the probit, *Pr,* is given by:

$$P_{death} = \frac{1}{2}\left\{1 + \mathrm{erf}\left(\frac{Pr-5}{\sqrt{2}}\right)\right\} \qquad \text{Eq. 2}$$

With the definition from HSE UK on SLOD, equal to a probability of death of 50%, the constants a, b, and n can be defined as $a = -90.778$, $b = 1.01$ and $n = 8$.
Figure 2 shows the lethality (probability of death) for given CO_2 concentrations at selected exposure times. Table 2 shows the related exposure time and CO_2 concentration for a probability of 50% lethality. It is evident that in case of an emergency, it matters whether we are exposed to 6% or 14% when it comes to the time allowed for escaping an CO_2 incident. It is these lethality curves that are used to estimate the toxicity of a CO_2 leakage and to implement proper safety measures to reduce the risk.

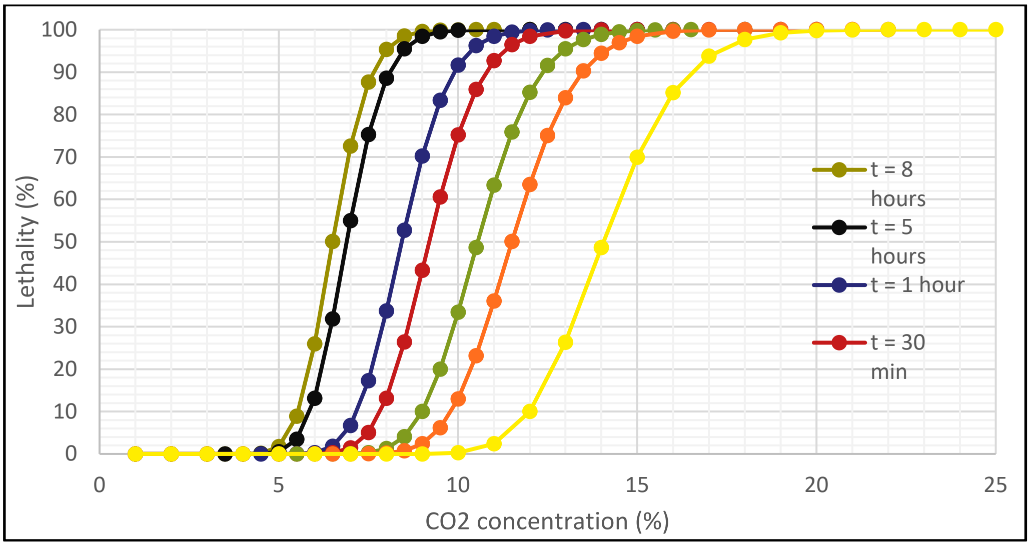

Figure 2 Lethality based on CO_2 concentration and selected time of exposure.

Table 2 Corresponding exposure time and CO_2 concentration for 50% lethality (equal to SLOD).

Exposure time	"SLOD"- CO_2 concentration (%)
1 min	14.1
5 min	11.5
10 min	10.5
30 min	9.2
1 hour	8.4
5 hours	6.9
8 hours	6.5

2.3 CO_2 historical incidents

A few historical CO_2 incidents are described here to highlight the importance of safe handling and proper emergency response plans when transporting large quantities of CO_2 in relation to CCUS.

Mississippi, US, February 2020

On February 22, 2020, a 24-inch CO_2 pipeline ruptured in Yazoo Country, Mississippi, less than a kilometer from the town Satartia. The pipeline was installed in 2009 and operated by Denbury Enterprises to transports CO_2 from natural CO_2 fields in the Jackson Dome, Mississippi, to oil fields, where the CO_2 is used in enhanced oil recovery. CO_2 is transported in pressured pipelines at 83-190 bar, ensuring that the CO_2 is in liquid form. Though not officially confirmed, the CO_2 stream was believed to be contaminated by up to 5% H_2S, which added to the severity of the incident. The locals reported a green plume and a smell of rotten eggs, which is typical for H_2S and contrary to CO_2 which is colorless and odorless. The failure investigation report states the cause of the pipeline rupture as "Heavy rains are believed to have led to a landslide, which created axial strain on the pipeline and resulted in a full circumferential girth weld failure" [7]. The girth weld failure was confirmed by metallurgical analysis. The total release volume of CO_2 was estimated to 31405 barrels corresponding to approximately 4400 ton.

No one died during the incident, but 46 people were hospitalized, some with

Figure 3 CO_2 pipeline rupture in Mississippi, US, Feb. 22, 2020.

severe breathing problems, and 300 people were evacuated from their homes.
Neither the first responders nor the hospital staff were trained in handling CO_2 pipeline incidents, and there was confusion about what the victims had been exposed to [7].
The incident is the most recent and most comparable to future CCUS projects. After this pipeline failure the U.S. Pipeline and Hazardous Material Safety Administration (PHMSA) announces on May 26, 2022, new safety measures to protect the Americans from CO_2 pipeline failures. This includes requirement to monitor land movements [8].

OCAP CO_2 pipeline to greenhouse, Netherlands, September 2018

Gaseous CO_2 is transported from a Shell refinery in Rotterdam to horticultural greenhouses in North and South Netherland [9]. In September 2018 a leakage in the transportation pipeline occurred during excavation work for the construction of a distribution network for geothermal heat. The CO_2 pipeline was immediately shut down. A nearby bicycle path was closed off and the staff in the nearby office buildings were told to stay indoors. The assessment report states that it took longer time than expected to dilute the area and reduce the CO_2 concentration. The office building has a lower parking area, and it was decided that the firefighters, wearing breathing apparatus, drove the car of the employees to the entrance of the building allowing the employees to drive off immediately. There was no casualties reported [10].

Worms, Germany, November 1988

A vessel containing liquid CO_2 at Proctor and Gambles' citrus facility in Worms, Germany, failed due to overpressure causing three fatalities and eight injured employees. The vessel had a capacity of 30 tonnes CO_2 and was designed for -50 °C and 20 bar. On inspection several causes that may have led to the failure were identified. The rupture happened close to a recent modification where a new flange was welded to a spare nozzle opening. Prior to the incident a vessel heater had failed causing the temperature to drop to -60 °C, which is below the design temperature. This could have caused the welded joint to become brittle and crack. The safety relief valve did not open probably due to freezing either from dry ice or from frozen atmospheric moisture blocking the valve seat [11].

Lake Nyos, Cameroon, August 1986

In August 1986 a limnic eruption, which is a very rare type of natural disaster, released CO_2 from Lake Nyos in Cameroon. The mass of release was enormous, among the largest accidents known, releasing up to 1.5 million tons, and killed 1,746 people [12], [13]. Even worst-case scenarios for CO_2 pipeline ruptures regarding CCUS will be of much smaller scale and should include proper safety plans for operating CO_2 infrastructure.

Menzengraben, Germany, July 1953

Less recently, but still relevant to CCS, is the outburst of CO_2 in a potash mine in 1953 in the former East Germany. Potash is mined from underground salt deposits and is used in fertilizers. In some salt mines, CO_2 is entrapped in the salt deposits and can be released during mining. The mine in Menzengraben was in a valley, and the amount of CO_2 emitted was estimated to 1100-3900 tonnes. The outburst lasted 20-25 minutes and led to high concentration of CO_2 in the valley. The miners and locals were warned of the outburst and escaped uphill, however three people lost their lives [12].

2.4 Typical operating conditions in CCUS value chain

It's important to understand the properties of CO_2 to ensure safe handling when pressurized CO_2 is transported. All pressurized medias encounter some measure to be handled safely. With CO_2, the change in phase must be evaluated in the CCUS value chain. Figure 4 shows the pressure-temperature phase diagram for pure CO_2. There are four phases: gas, liquid, solid and supercritical. Above the critical point at 74 bar and 31 °C, the CO_2 is in its supercritical form. In this form, the CO_2 behaves as a supercritical fluid occupying the volume of its container like a gas, but with a liquid-like density. The viscosity of a supercritical CO_2 is like that in the gaseous phase, which can be up to 100 times lower than in the liquid phase [14].

An increase or decrease in pressure or temperature above the saturation line, but below the critical point, will cause phase change from gas to liquid or vice versa. Figure 4 includes areas of typical operating conditions for CO_2 in CCUS value chain. The corresponding temperature and pressure are given in Table 3.

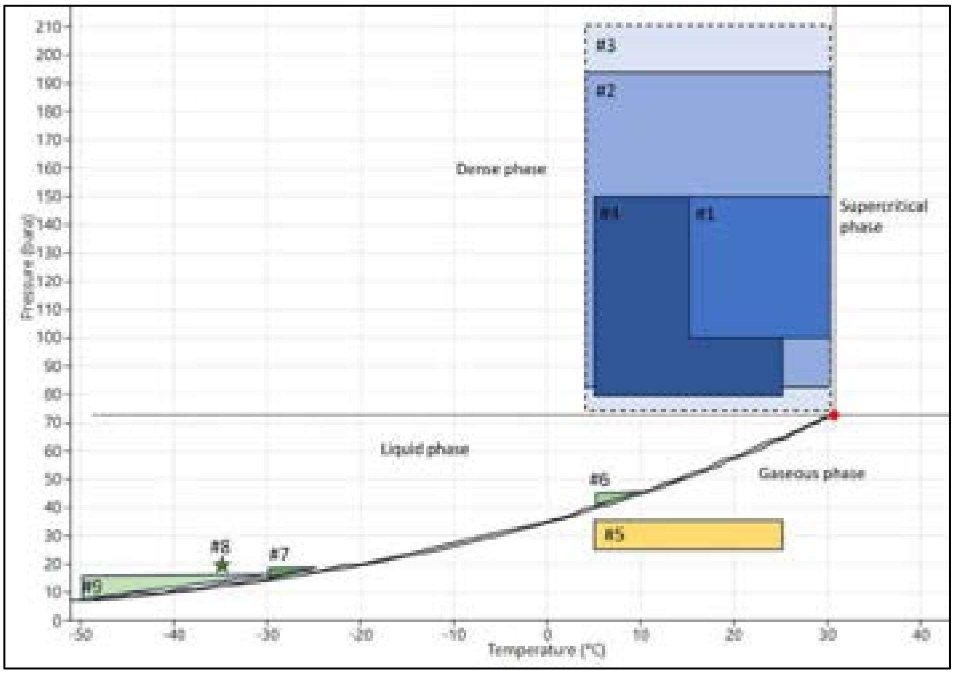

Figure 4 Phase diagram of pure CO_2 with typical operating conditions for pipeline and ship transport. See data in Table 3.

Table 3 Typical operating conditions for pipeline and ship transport. See also phase diagram in Figure 4.

Item no in Figure 4	Means of transport	Pressure	Temperature	Reference
#1	Dense phase pipeline	100-150 bar	15-30 °C	[15]
#2	Dense phase pipeline	83-193 bar	-	[16]
#3	Dense phase pipeline	74-210 bar	-	[17]
#4	Dense phase pipeline	80-150 bar	-	[18]
#5	Gaseous pipeline	25-35 bar	5 – 25 °C	[18]
#6	Ship	40-50 bar	5 – 15 °C	[18], [19]
#7	Ship	15-18 bar	(-30) – (-25) °C	[18]
#8	Ship	19 bar	(-35) °C	[20]
#9	Ship	7-15 bar	(-50) – (-30) °C	[19]

The corresponding mass density of pure CO_2 as a function of pressure and temperature is seen in Figure 5 Mass density of pure CO_2 as function of pressure and temperature (based on Peng Robinson EOS) [5].. As an example, we can see that transporting gaseous CO_2 in a buried pipeline around 10 °C and at 20 bar gives a density around 57 kg/m^3, but by increasing the pressure to 120 bar the density becomes around 945 kg/m^3. For ship transport and intermediate storage tanks, the CO_2 is often kept liquid with a density of around 1000 kg/m^3. With a high density, less material is needed to transport or store the same amount of CO_2 compared to low density, reducing the cost of material and space requirements.

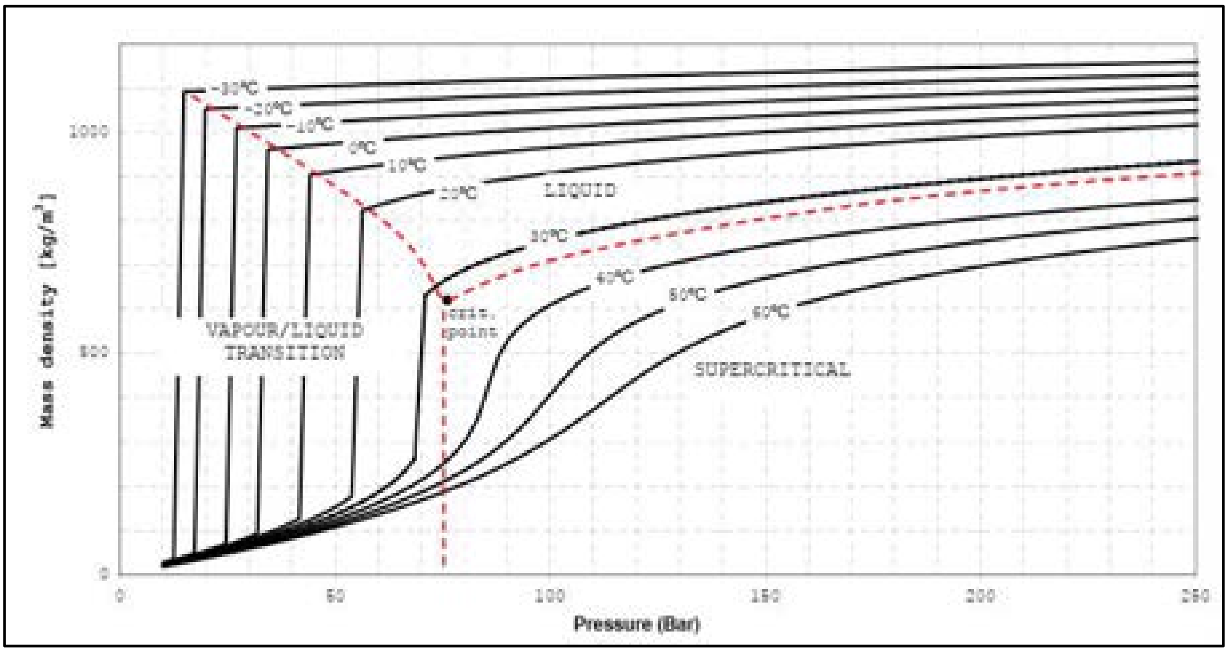

Figure 5 Mass density of pure CO_2 as function of pressure and temperature (based on Peng Robinson EOS) [5].

2.5 Effects of impure CO_2

The CO_2 captured in CCUS will not be 100% pure and the impurities play an important role, as well as the limitation of these, to ensure a safe transportation system.

The impurities in the CO_2 stream for transportation depends on the source, from which process CO_2 is captured, and the level of purification before transportation. It is difficult to give a universal specification for the maximum allowable impurities in the CO_2, as it depends on multiple factors, including but not limited to:

1) CO_2 source and upstream equipment prior to transportation

2) Temperature, pressure and material selection for the transportation
3) End use of CO_2, or storage site e.g. the specific geology.

Transportation of CO_2 in pipelines has been practiced since 1972, and there is currently more than 8000 km onshore CO_2 pipelines, mainly in the U.S. and Canada [21]. Most of these pipelines transport CO_2 from natural sources, and the CO_2 is used for enhanced oil recovery (EOR). The experience from the design and operation of CO_2 pipelines for EOR might be used for transport of CO_2 in the CCUS infrastructure, but attention should be paid to the impact of CO_2 quality, operating condition, and safety measures. CO_2 used in EOR in North America tends to be fairly pure [22], whereas CO_2 from hard-to-abate industries is often generated as a by-product or a waste stream. The CO_2 captured from these processes will often contain impurities originating from the flue gases, such as SO_2, NO_x, O_2, N_2, water, Ar, H_2 and others besides CO_2. When considering CO_2 for EOR there is an economic incentive to remove some impurities to enhance oil recovery by preventing reactions with hydrocarbons [23]. When CO_2 captured from hard-to-abate industries is transported solely for storage or utilization other requirements for CO_2 quality may apply.

The following sections describes how impurities can affect the design and choice of operating conditions for CO_2 transportation in different ways, for example:

1) Impurities that cause toxicity in humans and animals.
2) Impurities that affect the phase diagram.
3) Impurities that enhance corrosion and cause material damage.
4) Impurities that are of concern due to requirements at the CO_2 utilization unit or storage unit.

2.5.1 Impurities that cause concern due to toxicity in humans

The main impurities related to risk of toxic hazards are H_2S, SO_2, CO, NO, NO_2, amines and glycol [5]. The limits of these components are based on health, safety and environment regulations [24]. The project DYNAMIS recommended limits of H_2S (200 ppm), CO (2000 ppm), SO_x (100 ppm) and NO_x (100 ppm) based on health and safety in the event of a sudden release. It did not consider pipeline integrity such as cross-chemical reactions resulting in corrosive products. Other research and CCS projects have found that these limits are too high when considering cross-reaction between impurities and the pipeline integrity [23].

2.5.2 Impurities that affect the phase diagram

It is critical to ensure that CO_2 is transported in one phase (gas or liquid phase) during pipeline transportation, especially for long-distance transportation where intermediate boosting stations are required. A compressor or pump operating close the two-phase boundary will experience operational difficulties such as cavitation [25]. Looking at the phase diagram of pure CO_2 (Figure 4) it is evident at which temperatures and pressures pure CO_2 is in either the gas or liquid phase. However, the phase diagram changes when CO_2 contains impurities. Even trace amounts of an impurity may cause substantial changes in the phase behavior of the mixture, this may lead to uncertainties in the operating conditions required to stay outside the two-phase region [26]. It is important to know the chemical composition of CO_2 and the impurities of the mixture to determine these conditions and ensure single-phase flow.

One way to estimate the phase behavior of CO_2 is through thermodynamic calculations. An equation of state (EOS) is a thermodynamic model which given pressure, temperature, and composition of a mixture, can be used to calculate its physical state and its properties.

The Span-Wagner EOS covers pure CO_2 from triple point to very high temperature and pressure with an accuracy similar to the experimental uncertainty and is currently considered state of the art for the calculation of physical properties of pure CO_2 [4, 13].

When it comes to mixtures, there is no universal equation of state which is ideal for all applications. Many EOS are available in commercial simulators as well as in various research groups. For the behavior of CO_2 mixtures, including impurities, the classical Peng-Robinson equation of state is often considered to be sufficiently accurate in the temperature, pressure and composition ranges for most engineering applications for CCUS [4, 14, 15]. For certain mixtures, those with water, association models such as SAFT may be more appropriate. A higher accuracy may be obtained for other mixtures if semi-empirical multiparameter mixture models such as GERG-2008 are employed, provided the model is employed within its accepted temperature, pressure, and composition range. The project CO_2Mix run by SINTEF Energy Research and Ruhr-Universität Bochum conducts experimental measurements to determine thermo-physical properties for CO_2-rich mixtures. The group is also developing a new highly accurate EOS called EOS-CG [29], which is intended for fiscal measurement. However, for design purposes and to calculate safety margins, the Peng-Robinson EOS is considered efficient also in the light of more computational robustness and availability in commercial simulation software.

In case the captured CO_2 contains impurities of H_2 or N_2, which have a critical temperature lower than CO_2, the phase diagram changes meaning that increased pressure is required to remain in liquid phase.

This is seen in Table 4 where increasing content of H_2 and N_2 increases the bubble point line and dew point line. In Table 4 the temperature is fixed at either 0 °C or 15 °C and the dew point pressure and bubble point pressure are calculated. The dew point is the point at which the first drop of a gaseous mixture begins to condense. The bubble point is the point at which the first drop of a liquid mixture begins to vaporize. For a mixture, here CO_2 with impurities, a two-phase region exists between the dew point and bubble point. As mentioned earlier, it is important to stay in a one-phase flow during pipeline transportation. In case of gaseous CO_2 mixtures, the pressure should be kept below the dew point. In case of liquid CO_2 mixtures, the pressure should be kept above the bubble point. In practice, some margin to the bubble point and dew point pressure is required to allow fluctuations in the operating pressure. As seen in the table below, the effect of impurities is more profound for the bubble point than for the dew point. The CO_2 captured by Wetsus in the ConsenCUS-project has an expected content of 1-2% of both N_2 and H_2 after drying[1]. To keep the fluid in liquid phase increased pressure is required for this mixture compared to pure CO_2.

Table 4 Dew point and bubble point pressure for CO_2 and CO_2 mixtures with N_2 and H_2. Calculated by Aspen HYSYS using Peng-Robinson EOS.

Mixture	**Dew and bubble point pressure at 0 °C [bar g]**		**Dew and bubble point pressure at 15 °C [bar g]**	
	Dew point	Bubble point	Dew point	Bubble point
CO_2 (100%)	33.5		49.7	
CO_2 mixture with 0.5mol% N_2	33.7	36.0	50.2	51.9
CO_2 mixture with 1.0mol% N_2	34.0	38.5	50.6	54.0
CO_2 mixture with 5.0mol% N_2	36.2	57.5	54.7	70.0
CO_2 mixture with 0.5mol% H_2	33.7	39.7	50.2	54.1
CO_2 mixture with 1.0mol% H_2	34.0	46.1	50.7	58.5
CO_2 mixture with 5.0mol% H_2	36.4	97.6	55.1	93.4
CO_2 mixture with 1.0mol% N_2 + 1.0mol% H_2	34.5	50.8	51.7	62.5

2.5.3 Impurities that enhance corrosion and cause material damage

Water is the most important impurity to control in CO_2 transportation [30]. The CO_2 stream should contain no free water at any location in the pipeline and during normal and upset operating conditions. Free water can cause corrosion in the presence of carbonic acid formed

[1] Informed September 2021. Object to change as the project involves.

by water and CO_2. The presence of small amounts of SO_2 or NO_x in the CO_2 stream can also cause formation of sulfuric acid and nitric acid, respectively, also leading to risk of corrosion. Research has investigated possible corrosion reactions when multiple impurities are present in dense CO_2 [31]. Detail on corrosion mechanism and material selection is however out of this scope.

As seen in Figure 6, the solubility of water in pure CO_2 decreases with pressure when CO_2 is in the vapor phase and increases when CO_2 is in liquid phase. The minimum solubility is observed just before the phase changes. If the water content in the CO_2 stream exceeds the solubility line, free water will exist, and a separate aqueous phase will occur [32]. This must be avoided and is often done by drying the gas. It is also seen in Figure 6 that the water content should be more strictly controlled for CO_2 transport at lower pressures and lower temperatures. The picture gets more complicated when CO_2 contains impurities. DNV's guidance note [5] states that *"There is limited available knowledge on water solubility models for CO_2 streams including other chemical compounds. The indicative solubility for pure CO_2* [Figure 6] *should not be taken as representative for a CO_2 stream with other chemical components".*

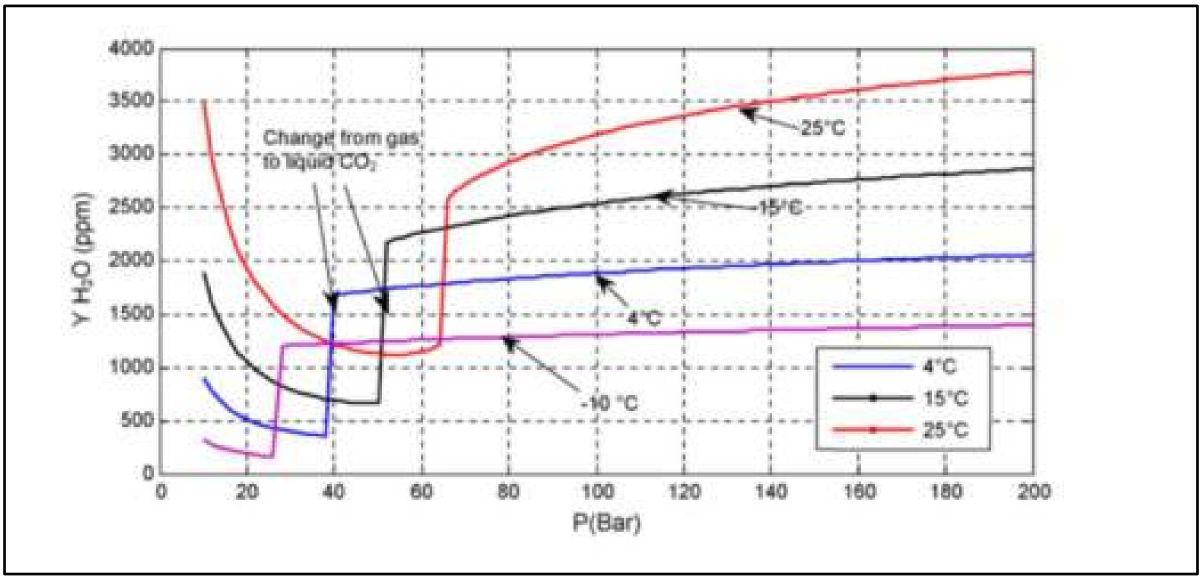

Figure 6 Water solubility in pure CO_2 for varying temperature as a function of pressure [23].

It is also important to limit water content to avoid formation of gas hydrate formation.
When there is a sufficient concentration of water molecules carried (dissolved) in the CO_2 at a given temperature and pressure, the H_2O and CO_2 molecules combine into a solid crystal structure - i.e. a gas hydrate. Gas hydrates are solid structures similar to water ice in their appearance and properties, in which guest molecules are situated in cavities formed by hydrogen-bonded water molecules [33]. However, the difference between the gas hydrate and

water ice is that the hydrate crystal structures are thermodynamically stable at conditions where water ice does not form. In addition, the formation of the hydrate solid, and subsequent drop-out from the CO_2-rich fluid, is sudden for small changes in system pressure for a given bulk H_2O concentration. The impact of this characteristic of the hydrate formation curve in H_2O + CO_2 mixtures is that a relatively short-term process disruption in the pipeline system can result in the drop-out of hydrates at locations where safety-critical equipment is installed. The formed hydrates could then accumulate within, for example, the sensing lines for critical pressure-sensing safety equipment, causing an undetected failure of the attached Safety Instrumented System. As hydrates can occur between other components in the CO_2-rich fluid, it is important to the reliability of the pipeline safety system that the hydrate curves for the transported fluid mixture are understood at the design phase and process units are installed to prevent the formation of hydrates during credible abnormal operating scenarios (e.g. maintenance activities).

All in all, drying of the CO2 stream is important for the operation of CO2 transportation. There are multiple water dehydration technologies, such as compression and cooling, adsorption on silica gel, molecular sieve or activated alumina [34].

2.5.4 Impurities of concern due to requirements at CO_2 utilization or storage site

The required CO_2 quality in CCUS value chain needs to be evaluated from case to case and based on cost-effective and safe operation. The requirement for CO_2 quality may be a result of the gas conditioning prior to transportation to comply with the requirement at the end user rather than the design requirement for the transport itself, e.g., pipeline or ship vessel.

The following will give examples of the CO_2 quality in existing or planned transportation systems. Table 5 lists CO_2 specifications for various CO_2 projects together with the CO_2 specification required for food and beverage application. Three selected CO_2 infrastructure projects are described in more details below.

The Northern Light CCS project in Norway is a joint venture between Equinor, Shell and TotalEnergies and will ship CO_2 from industrial sites near Oslo to an onshore terminal, and from there CO_2 is transported by pipeline to a permanent storage site in the seabed of the North Sea [35]. The CO_2 is transported in liquid form at a temperature around -28 °C and pressure at 15 bar g. When completed in mid-2024, a capacity of up to 1.5 million tonnes of CO_2 per year is expected. The allowable impurity levels are seen in Table 5 [17].

At the port of Rotterdam, a CCS project called Porthos is being developed. The project will transport CO_2 by pipeline, first 30 km onshore in gaseous phase at around 35 bar and then after compression to liquid phase at 130 bar further 22 km offshore. The CO_2 will be captured from various industrial sites such as Air Products and Shell and sent through the pipeline and stored in an empty gas field beneath the North Sea. A total amount of 37 million tonnes is planned to be stored over a 15-year period. The expected CO_2 specification is given in Table 5. A minimum CO_2 content of 95% is expected, and the sum of H_2, N_2, Ar, CH_4, CO and O_2 can be up to 4%, though with independent limits for each component. In October 2023 the Porthos project has taken the final investment decision and construction is expected to start in 2024 [36].

Kinder Morgan currently operates long-distance CO_2 pipelines in the U.S. where CO_2 from natural sources is transported to enhanced oil recovery. The CO_2 is transported at high pressures, typically around 150 bar g [37], which allows for a higher nitrogen content while still ensuring one-phase flow, as discussed in section 2.5.2. The specification considers fewer impurities than the CCS projects also given in the Table 5Table 5. The CO_2 is most often sourced from natural sources, and impurities like SO_x and NO_x, that are commonly present in flue gases from hard-to-abate industries considered in CCUS projects in Europe, are hence not present in the CO_2 specification [38].

As seen from Table 5, the limits of CO, NO_x, SO_x and H_2S is well below the limits for toxic hazards as stated by DYNAMIS in Section 2.5.1.

Table 5 CO_2 quality for selected references. Compounds not specified in the composition could still be present, but not specified as a requirement. The composition is either given mole basis or volume basis as noted.

	Unit	**Food and beverages application, EIGA, 2016**	**Northern Light, Norway, 2019**	**Porthos, NL, 2021**	**EOR onshore pipeline, Kinder Morgan, US, 2019**	**Fluxys Belgium March 2022**	**Open Grid Europe, Germany May 2022**	**Aramis, NL Feb 2023**	**Aramis, NL Feb 2023**
Transported by		-	Ship	Onshore and offshore pipeline	Onshore pipeline	Onshore pipeline	Onshore pipeline	Ship	Onshore pipeline
Phase			Liquid	Gas (onshore) Liquid (offshore)	Liquid	Gas	Liquid	Liquid	Gas
Operating pressure	bar g		13-18	35 (onshore) 130 (Offshore)	Typical 137-207 Minimum 89	20-33	80-90	13-18	
Operating temperature	°C		Around -26		Max 49	20-40			
Dewpoint (for all liquids)						< -10			< -10
Composition									
Composition	basis	*vol.*	*mole*	*mole*		*mole*	*vol.*	*mole*	*mole*
CO_2	%, min	99.9	99.81 (balance)	95	95	95	98	balance	95
H_2O	ppm	20	30	40	633	40	30	30	70
H_2	ppm		50	7500 (0.75%)		7500 (0.75%)	1%	500	7500 (0.75%)
O_2	ppm	30	10	40	10	40	30	10	40
N_2	%		50 ppm	2.4	4	2.4	2		2,5
Ar	%		100 ppm	0.4		0.4	0.25		0,4
SO_x	ppm	1	10	50		10	1	10	
H_2S	ppm	See note	9	5	20	5	10	5	5
Total sulphur	ppm	0.1		20	35	20 See note 5.3	30		20 See note 8.2

Table 5 cont.

	Unit	Food and beverages application,	Northern Light,	Porthos,	EOR onshore pipeline, Kinder Morgan	Fluxys Belgium	Open Grid Europe, Germany	Aramis, NL ship	Aramis, NL pipeline
CH_4	%	See note 1.1	100 ppm	1		1	0,25 See note 5.1		1
NO_x	ppm	2.5 NO + 2.5 NO_2	1.5	5		5	1	1.5	2.5
CO	ppm	10	100	750		750	100	1200	750
Amine	ppm		10	1		1	1	10	1
NH_3	ppm	2.5	10	3		3	10	10	3
Aromatic hydrocarbons	ppm	0.02	0.5 See note 5.2	0.1		0,1 See note 5.2			0,1
Propane and other aliphatic hydrocarbons			1100 See note 2.3	1200		1200			1200
Glycol			MEG: 0.0005 TEG: not allowed	See note 3.4					See note 8.3
Formaldehyde	ppm		20	10 (total aldehyde)		10 (total aldehyde)		20	10 (total aldehyde)
Acetaldehyde	ppm	0.2	20					20	
Methanol	ppm	10	30	620		620		40	620
Ethanol	ppm		1	20		20		20	20
HCN	ppm	0.5	100	20		2			2
Hg	ppm		0.0003			0,03	5 ppb	0,03	
Cd, Tl	ppm		0.03 See note 2.1			0,03		0,03	
Non-volatile residue (particulates)	ppm w/w	10	1 µm					See note 7.2	See note 7.2
Non-volatile organic residue (oil and grease)	ppm w/w	5							
Volatile organic components			10 See note 2.4	10 See note 3.5		10 See note 5.4			
References		[39]	[40, p. 30]	[41]	[42]	[43]	[44]	[45]	[45]

Notes:

1. EIGA Food and beverages application
   1.1. Total volatile hydrocarbons (calculated as methane): max 50 ppm of which max 20 ppm non-methane hydrocarbons.
   1.2. Total sulphur (as S): 0.1 ppm. If the total sulphur content exceeds 0.1 ppm as sulphur, then the species must be determined separately and the following limits apply: 0.1 ppm COS, 0.1 ppm H_2S, 1.0 ppm SO_2.
   1.3. Limit for NO/NO_2 is 2.5 ppm each.
   1.4. Limit for phosphine is 0.3 ppm and analysis necessary only for carbon dioxide from phosphate rock sources.
   1.5. Analysis for HCN necessary only for carbon dioxide from coal gasification sources.
2. Northern Light CCS
   2.1. Sum of cadmium and thallium must be less than 0.03 ppm.
   2.2. BTEX refers to Benzene, Toluene, Ethylbenzne and Xylene.
   2.3. Total amount of hydrocarbons not to exceed 1,100 ppm-mol. Individual limits for groups of HCs: C3 <1,100 ppm-mol, C4-C5 < 815 ppm-mol, C6-C7 < 75 ppm-mol, C8-C9 < 8 ppm-mol. C10+ not allowed.
   2.4. Total Volatile Organic Compounds (VOC) in addition to the ones listed separately in this specification, i.e., Ethanol, Methanol, Formaldehyde, Acetaldehyde, and BTEX, and includes the following components: 1-propanol < 1 ppm-mol, 2-butanol <1 ppm-mol, 1,2,4-trimethylbenzene <5 ppm-mol, Methyl acetate <10 ppm-mol, Acetone <10 ppm-mol, Hexanal <10 ppm-mol, Diethyl ether <10 ppm-mol, and Acetonitrile <10 ppm-mol. Other VOCs are not allowed.
3. Porthos CCS
   3.1. Sum of $[H_2+N_2+Ar+CH_4+CO+O_2]$ ≤4%
   3.2. Dew point limit for complete CO_2 composition should be less than -10 °C at 20 bar a.
   3.3. Includes COS, DMS, H_2S, SO_x, Mercaptan.
   3.4. To follow dew-point specification.
   3.5. Excluding methane, total aliphatic HC (C2-C10), methanol, ethanol and aldehydes.
4. Kinder Morgan EOR
   4.1. Oxygen must be limited, as it can cause overheat at the injection point for EOR due to exothermic reactions with hydrocarbons in the oil well [46].
5. Fluxys, Belgium
   5.1. Sum of $[H_2+N_2+Ar+CH_4+CO+O_2]$ ≤4%.
   5.2. To include C6-C10 and BTEX.
   5.3. Includes COS, DMS, H_2S, SO_x, Mercaptan.
   5.4. Excluding methane, total aliphatic HC (C2-C10), methanol, ethanol and aldehydes.
6. Open Grid Europe, Germany
   6.1. Total hydrocarbons
7. Aramis ship infrastructure
   7.1. Sum of $[H_2+N_2+Ar+CH_4+CO+O_2]$ ≤0,2%.
   7.2. This is the entry solids / dust specification for the envisaged Aramis stores. In order to achieve this, Aramis will request Aramis emitters to install dust removal facilities with a cut-off diameter of 10 micron as a

minimum. Furthermore, Aramis is planning to locate filters with cut-off diameter of 1 micron at optimal locations at the envisaged compressor and terminal stations.

8. Aramis pipeline infrastructure
   8.1. Sum of [H_2+N_2+Ar+CH_4+CO+O_2] ≤4%.
   8.2. Sum of [H_2S+COS+SO_x+DMS] ≤ 20 ppmmol.
   8.3. To follow dew-point specification.

3 Safety and risk in CO_2 transport

3.1 CO_2 sources

As described in Sections 2.1 and 2.2, a sufficiently high concentration of CO_2 in the air can acutely be toxic to life. However, the CO_2 captured from various industrial and natural sources always contains impurities, where many of those impurities are also acutely toxic to life (see, for example, Section 2.5.2). It is also clear from Section 2.5.3 that even "ppm" levels of impurities in the CO_2 fluid introduces a significant effect to the thermodynamic and thermophysical properties of the bulk fluid.

That the impurities could introduce both acute and chronic toxic effects on a community that is within the area affected by a CO_2 release of the size modelled in this study, is not well understood. Using the example of the Satartia event described in Section 2.3, many residents affected at the time of the incident continue to experience health problems to the present day [47].

It is thus important to understand how the various impurities interact within the released cloud and the concentration profiles therein when building the Case for Safety for a CO_2 pipeline or cryogenic storage facility. Unfortunately, the complexity of this aspect of the consequence modeling was not available within the computational tool selected for this study; therefore, this aspect of the safety analyses for the CCS value chain is recommended for further study.

3.2 Pipeline

When assessing the societal risks associated with a large release from a high pressure (dense phase) CO_2 pipeline, it is helpful to visualize the risk elements arranged as "bow-tie" of prevention and mitigation barriers on either side of the release event. A good example of a bow-tie representation of a CO_2 release event is provided in Figure 7. Please see reference [48] for details. Other examples of bow-tie diagrams related to CO_2 release events can be found in various literature (see, for example, [49]).

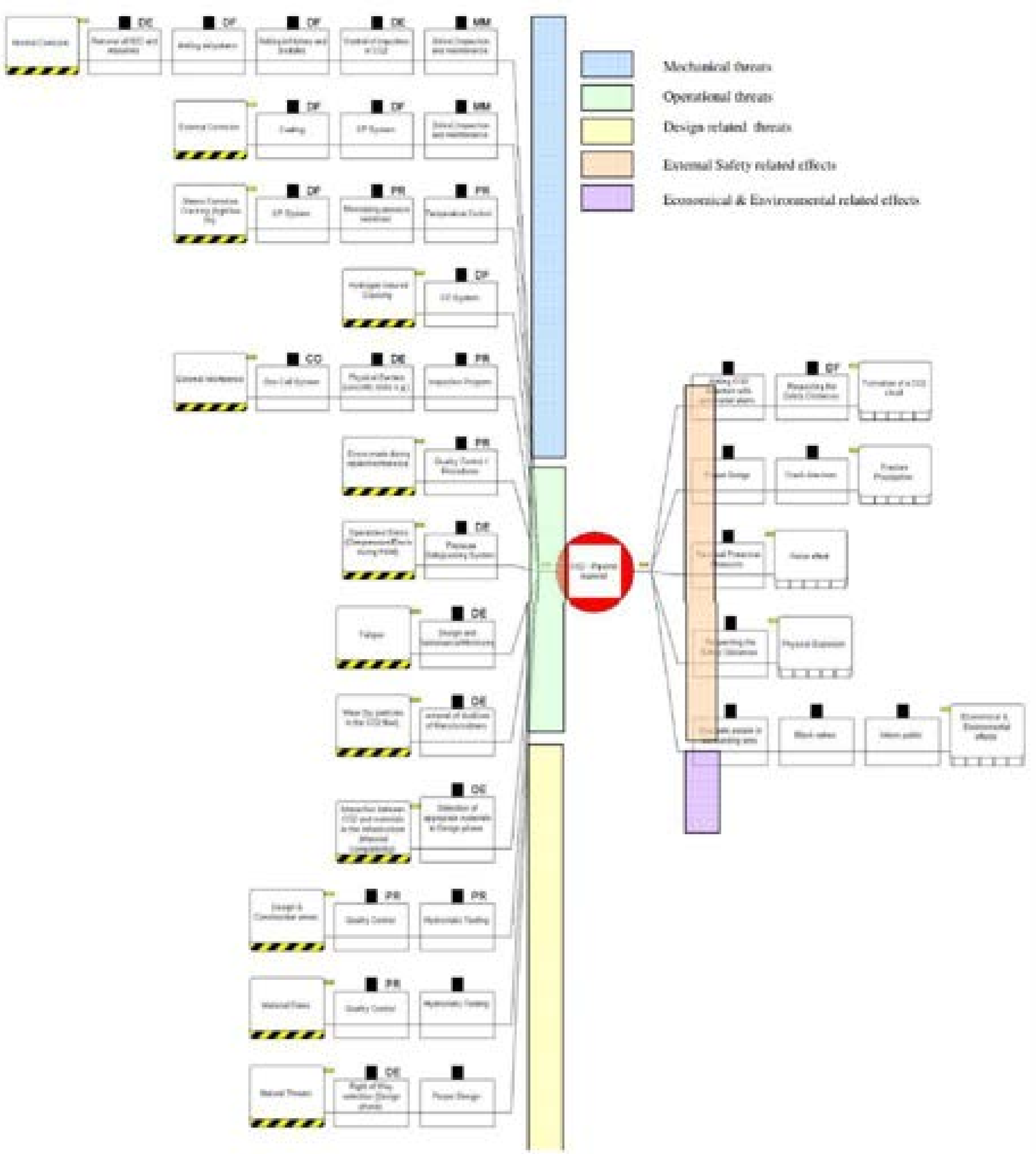

Figure 7 Example of the system barriers relevant to a CO_2 release event using the bow-tie representation [48]

The purpose of the bow-tie visualization is to highlight those barriers that require a high level of integrity or where additional barriers are required to either prevent the occurrence of the event or mitigate (reduce) the escalation of the event to more severe consequence. Thus, using the same methodology and procedure as applied to conventional natural gas transmission pipelines, the safety risk for every section of the CO_2 pipeline can be quantified and the resulting “risk to society” (Potential for Loss of Life (PLL) or Individual Risk per Annum (IRPA)) contours can be overlaid with the pipeline route. The overlaying of the risk contours highlights areas of concern to the affected community or communities in order to see whether an alternative routing should be considered, or additional barriers should be included in the pipeline safety system design. An example of a quantified risk determination in relation to population density is provided in [50], where this work also highlights the need to include the effects of topography adjacent to the modelled release point. Given the experience from the Satartia incident [47], it is necessary to include significant topography changes when modeling the dispersion of the cold, heavy CO_2 vented during an uncontrolled release event – i.e. the inclusion of the “ground effect” in the model.

When coupled with the bow-tie visualization of a CO_2 release event and the inclusion of a segmented pipeline design via the installation of safety valve stations, the quantified risk analysis results provide a robust and comprehensive perspective of the probability of a significant impact to communities along the pipeline route. The end goal of the pipeline safety assessment is thus to illustrate to all stakeholders that the pipeline design and operation fulfills the “societal contract” that the system safety risk is As Low As Reasonably Acceptable (ALARA). An example of this illustration is found in Figure 8.

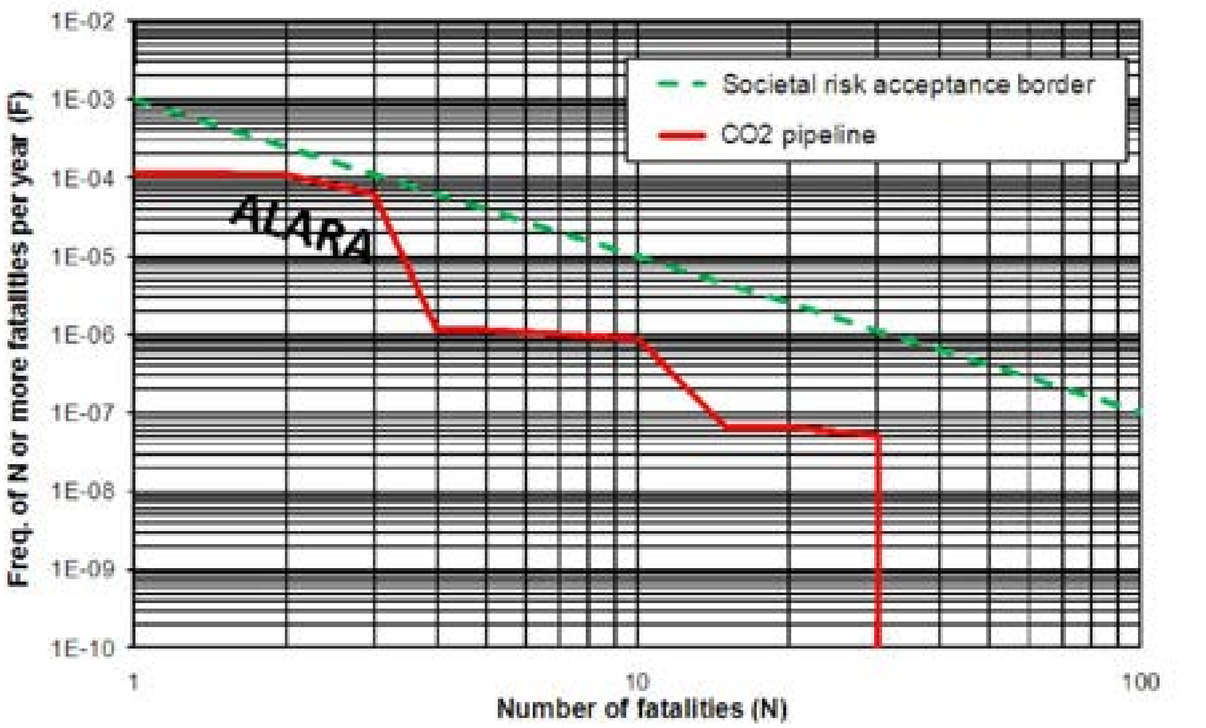

Figure 8 All barriers identified in the bow-tie of Figure 7 are included in the quantified risk analysis curve for the example CO_2 pipeline [51]. As the resulting risk curve is consistently below the “societal risk acceptance border”, the pipeline design meets the “societal risk contract” – or ALARA.

3.3 Road, rail and shipping

Regardless of the mode of surface transport – truck (road), railcar or ship – the surface transport of CO_2 involves the cooling of the CO_2 to the liquid state at a pressure above the triple point. At this condition, the CO_2 is classified as a cryogenic (inert) liquid within the applicable Transport of Dangerous Goods regulations similar to that applied to the transport of cryogenic liquid nitrogen (see, for example, the Class 120 fluid in [52]).

Given that the market for food grade CO_2 has been established for many decades, the actual and perceived safety risks associated with the truck and railcar transport of CO_2 are understood and normalized across many countries (see, for example, [53]). Given the cryogenic (low) temperature condition of the CO_2 liquid, there is a thermodynamic limitation to the amount and type of impurities that could stably exist in the liquid. Thus, the transport of non-food grade (impure) liquid CO_2 has the same risk level as that inherent with the decades-old truck and railcar transport of food-grade CO_2 liquids.

Contrary to the truck and railcar transport scenarios, the specific design for transport of cryogenic liquid CO_2 via a ship is relatively recent. Such ships have a total liquid storage volume of 7500 m^3 up to 22,000 m^3 distributed across 2, 3 or 4 cryogenic storage tanks [54]. As the temperature and pressure inside the tanks is similar to that of well-established Liquefied Petroleum Gas (LPG) ships, the safety risk associated with the shipping of cryogenic liquid CO_2 in such vessel is similar to that associated with the LPG ships, with the exception of the fire risk inherent with hydrocarbons.

3.4 Intermediate storage

Intermediate storage – the storage of CO_2 prior to further transport to the end destination – is more economic, by taking up less space, when the density CO_2 is high, e.g. cooled and pressurized to the liquid (cryogenic) state. At this condition, the tanks holding the cryogenic liquid can be in order of 3000m^3 or more. Thus, the safety risk of the contained volume of inert – yet potentially toxic – CO_2 is considered similar to that of other cryogenic inert liquids that are stored at such scale – e.g. liquid nitrogen. However, in contract to liquid nitrogen, a spill of liquid CO_2 is likely to persist longer at ground level due to the higher mass of CO_2 molecules relative to the surrounding air. For this reason, when evaluating the potential safety risk of a cryogenic liquid CO_2 facility, a reasonable proxy is either an LPG or LNG storage facility in terms of how the liquid pool from the spill vaporizes and the cold, heavy gas disperses (see, for example, [55]).

4 Failure frequencies

Failure frequencies is the approximation of the likelihood of an event, typically expressed as an annual probability. This section includes two main sections: First, a statistical analysis of the incident on U.S. onshore CO_2 pipeline using the incidents reported by PHMSA. This incident database also gives an overview of the causes of the incidents. Secondly, the failure frequencies reported for natural gas pipeline are presented since the statistical data set is much larger than for CO_2. This section also includes failure frequencies for storage tanks and some recommendations on failure frequencies applied in risk assessment.

4.1 Statistical analysis of incidents on U.S. onshore CO_2 pipelines

Every day CO_2 is transported in onshore pipelines in the U.S. The earliest pipelines were constructed in the 1970s and the main driver for CO_2 infrastructure is enhanced oil recovery – the extraction of crude oil by injection of CO_2 in oil fields. The CO_2 sources are primarily gas processing sites and natural sources, and the CO_2 is transported in dense with pressures typically above 90 barg.

The PHMSA is responsible for regulations on safe, reliable, and environmentally sound operation of pipelines in the U.S., including CO_2 pipelines. Loss of containment incidents must be reported to the PHMSA and the reports are publicly available. The length of CO_2 pipelines has been reported since 2004. There has been a steady development in the construction of onshore pipelines from 2004 to 2013, and their total length in 2022 was 8535 km (see Figure 9).

The total length of onshore natural gas transmission pipelines in the U.S is around 479,000 km [56]. It’s therefore important to highlight that the operating experience for CO_2 pipelines are limited compared to the hydrocarbon pipeline experience. The work package 8 in the ConsenCUS project concerns CCUS infrastructure in Europe and the purpose of this section is to discuss the expected failure rates on CO_2 onshore pipelines for CCUS in Europe.

The total length of gas transmission pipelines in the EU is around 200,000 km and the European Gas Pipeline Incident Data Group (EGIG) collects data from approximately 142,700 km of pipelines every year (the length has been steady since 2013). The level of experience for CO_2 onshore pipelines in Europe is currently very limited (OCAP operates 97 km pipeline of gaseous CO_2 [21]) and the data from the U.S.

reported by PHMSA will be used in the statistical analysis to discuss safety concerns in relation to CCUS in Europe.

The PHMSA database reports incidents on CO_2 pipelines since 1994 and the incidents are divided into the following main causes:

- Equipment failure
- Material failure of pipe or weld
- Incorrect operation
- Corrosion failure
- Other incident causes
- Excavation damage
- Natural force damage
- Other outside force damage

Each main cause is divided into some sub-causes, which can be seen in Appendix A.

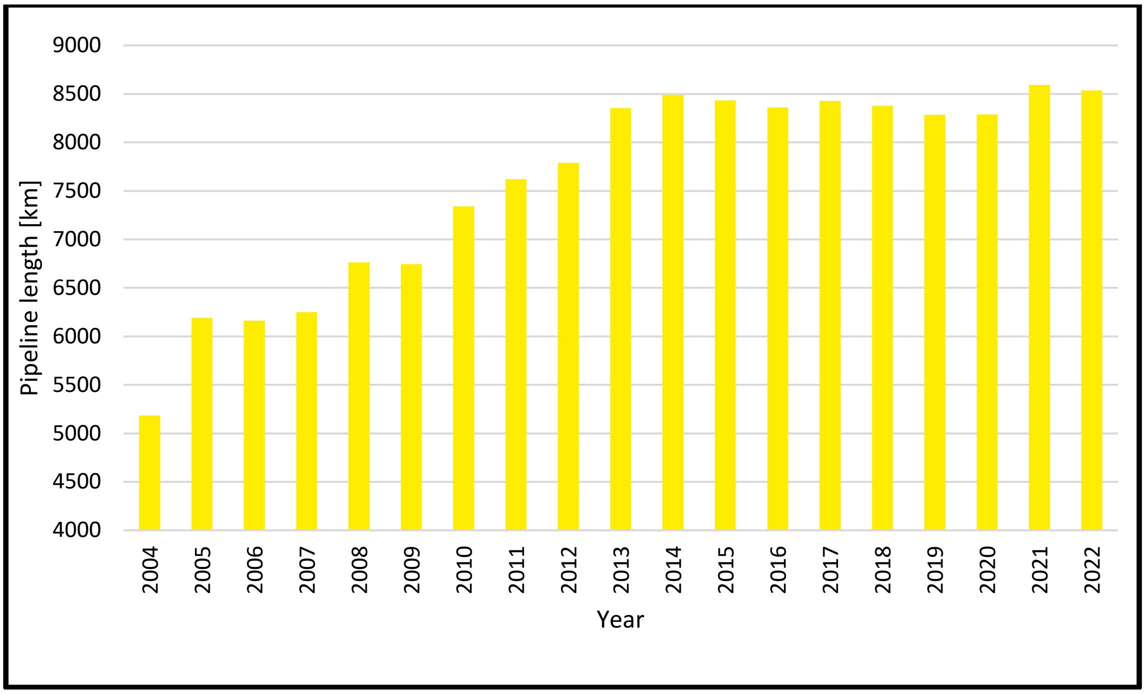

Figure 9 Total length of onshore CO_2 pipelines in the U.S from 2004 to 2022, based on data available from PHMSA.

4.1.1 Incident frequency

The PHMSA database was used to calculate the failure frequency for CO_2 onshore pipelines in the U.S. in the period of 1994 to 2021. Figure 10 shows the annual number of incidents reported to PHMSA in the period 1994 to 2021.

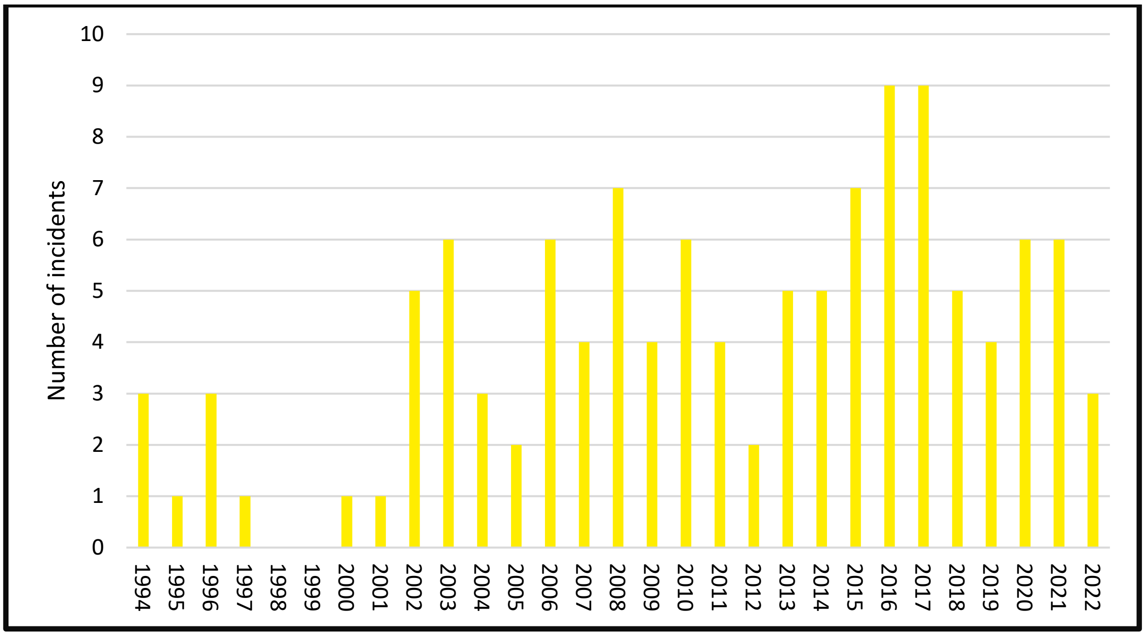

Figure 10 Number of incidents in the U.S. from 1994 to 2021 based on PHMSA database.

To find the failure frequency, the number of incidents is divided by the exposure. Exposure is the cumulative product of the total pipeline length recorded each year, and the number of years its different sections were in operation. For example, if 5000 km has been operating non-stop for 10 years, then the exposure equals 50,000 km·year. From 2004 the length of CO_2 pipelines was reported. Before 2004 the length of CO_2 pipelines was reported together with other hazardous chemicals. Hence, the failure frequency is calculated from 2004, where both the incident and length data are available, specifically for CO_2. A total number of 97 has been reported between 2004-2022. Figure *11* shows an incident frequency between 0.4 and 0.8 incidents per 1000 km per year between 2004 and 2022.

Note that the failure frequency does not tell anything about the severity of the incident.

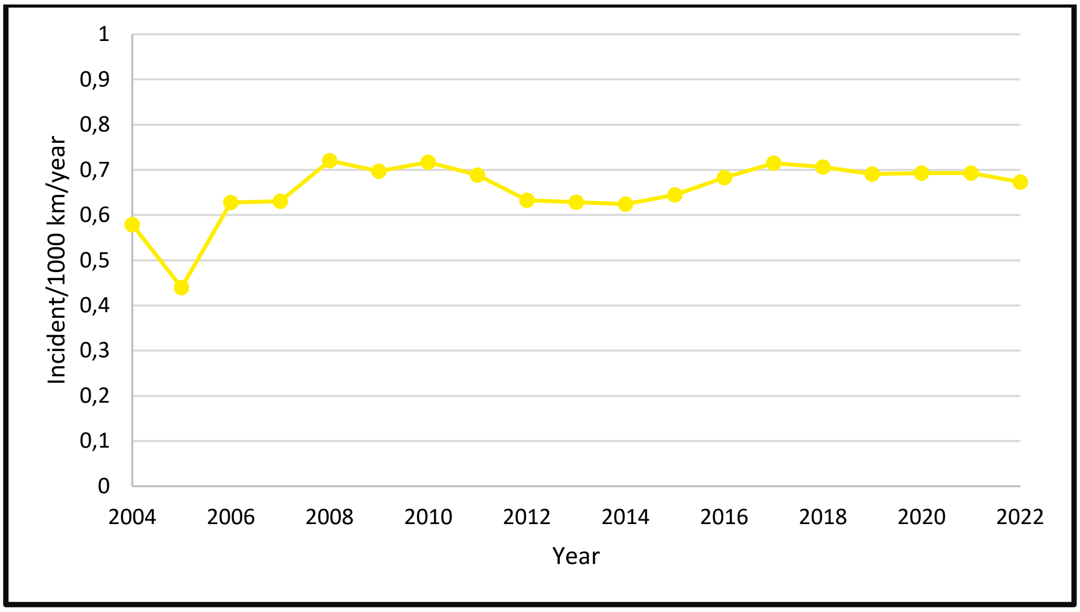

Figure 11 Incident frequency for CO_2 pipelines in the U.S., based on data from PHMSA from 2004-2022. The total number of incidents in this period was 97.

4.1.2 Cause of failure

The PHMSA database also provides the cause of the failure as described above and in Appendix A. Figure 12 shows the failure frequency based on each main cause reported. It is seen that equipment failure has the highest failure frequency, followed by incorrect operation and corrosion failure. Figure 13 shows the distribution of incident causes (2004-2022) in percentage.

Figure 12 shows no reported incidents caused by excavation damage from 2010 to 2022 and few reported from 2004-2022. The risk of excavation damage is the primarily risk in residual areas [57]. To compare the CO_2 pipeline infrastructure in the U.S. and the potential CCUS pipeline infrastructure in Europe, the location of the pipelines is important. Risk of excavation damage to pipelines is greater in urban sites, where multiple construction projects are happening near the gas infrastructure.

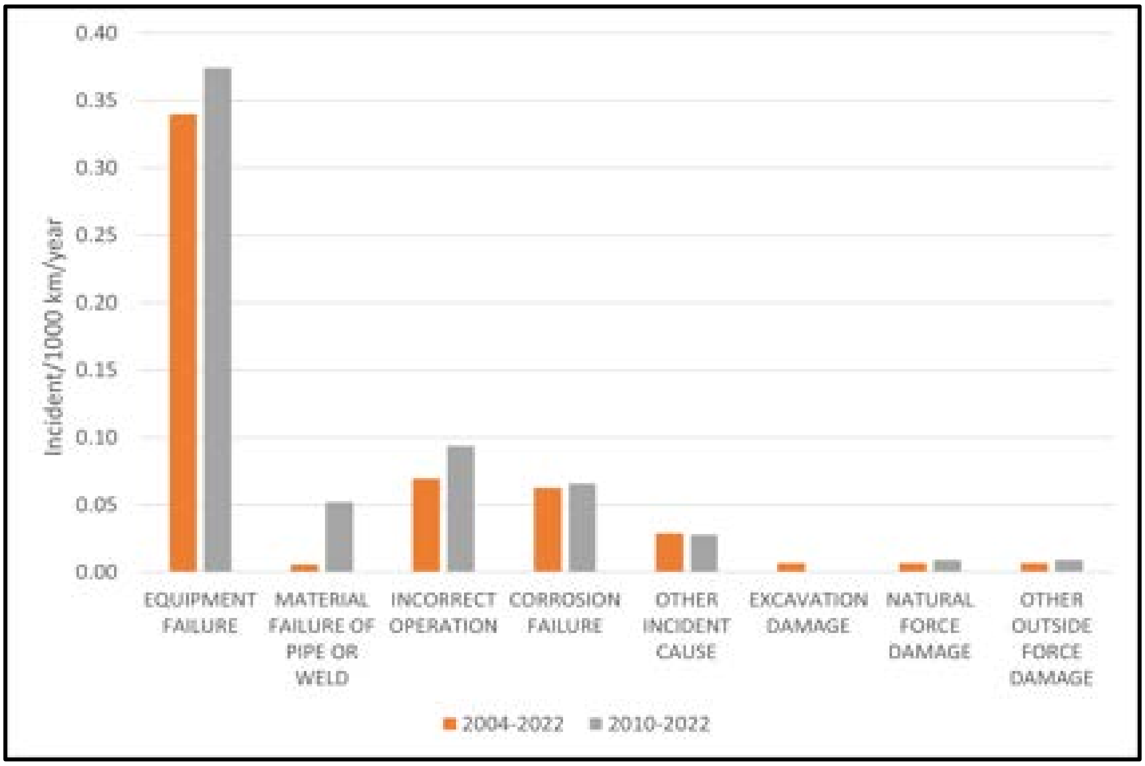

Figure 12 Failure frequency for CO_2 pipelines based on cause. Data from PHMSA database.

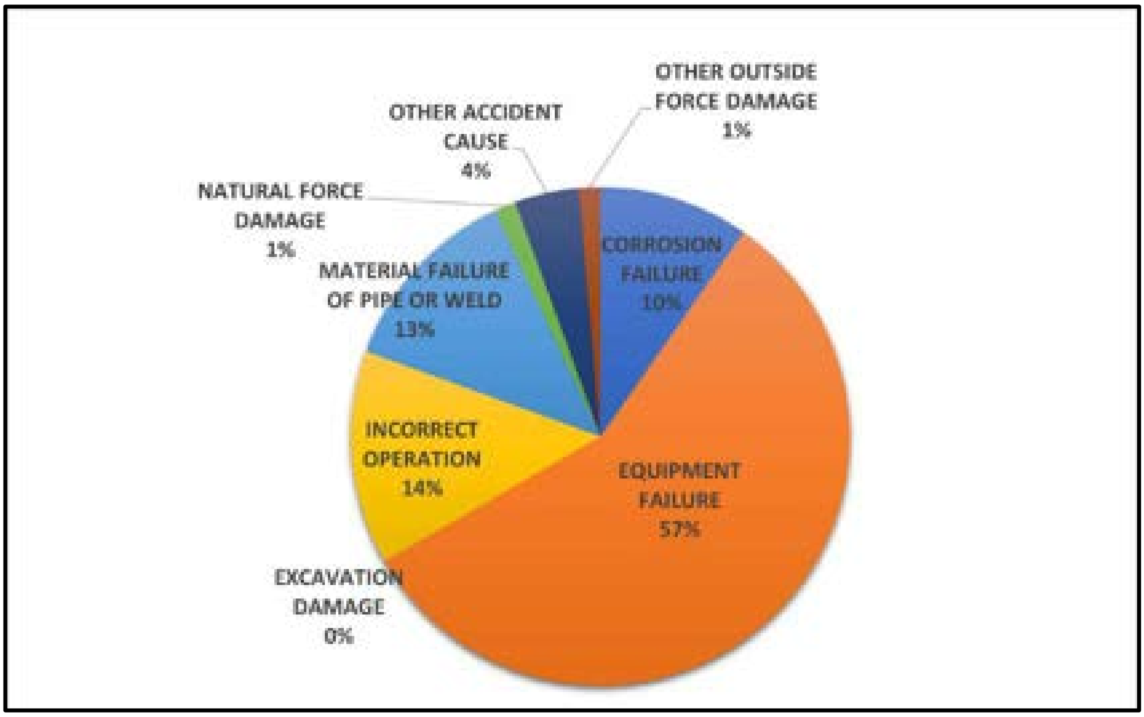

Figure 13 Distribution of incidents for CO_2 pipelines from 2004-2022. Data from PHMSA database.

Figure 14 shows a coarse overview of the pipeline locations in the U.S. and the population density given in number of people per km^2. It's evident that the CO_2 pipelines are mostly located in more rural areas with low population density, so the probability of excavation damage to the CO_2 pipelines will be lower here, compared to pipelines in densely populated areas.

The potential CO_2 pipeline infrastructure in Europe, such as the CO_2 clusters proposed in Work Package 8.4, will be in densely populated areas, see Figure 15. It is therefore reasonable to assume that the incident frequency caused by excavation damage will be higher than reported in the PHMSA database.

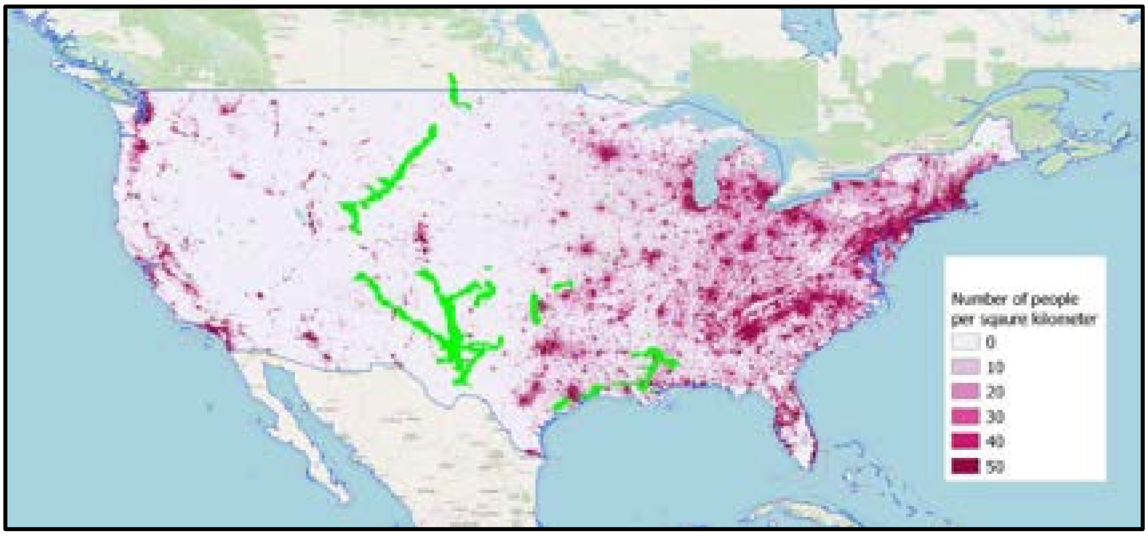

Figure 14 CO_2 pipelines (light green) in the U.S. and the population density (number of people per km^2). Population data taken from [41]. Pipeline map from PHMSA.

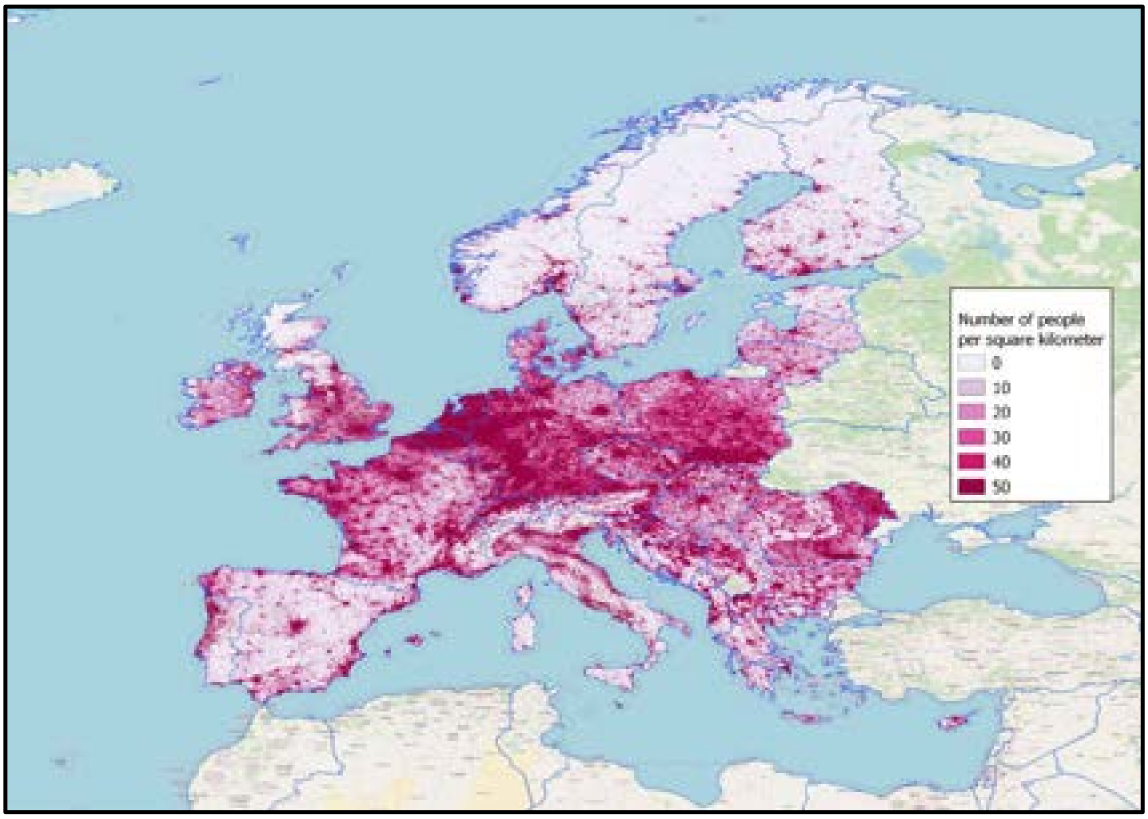

Figure 15 Population density in Europe (number of people per km^2). Population data taken from [41].

4.1.3 Pipeline incident frequency statistic for CO_2 vs. natural gas

It requires some caution and assumptions to compare the data available for the incident frequency statistics of CO_2 onshore pipelines in the U.S. with data available for natural gas pipelines in Europe. The overall aim is to give an estimate of the expected incident frequency for a potential CO_2 infrastructure for CCUS in Europe.

EGIG reports pipeline failure frequency and its causes from seventeen gas transmission system operators in Europe. The database started in 1970 and the latest report includes data until 2019. Incidents that lead to unintentional gas release must be reported, and the pipelines must fulfil the criteria of 1) being made of steel, 2) being onshore, 3) having a maximum operating pressure higher than 15 barg, and 4) being located outside the fence of a gas installation. The fifth and last criterion states that equipment failure shall not be included in the EGIG incident database, opposite to the PHMSA database. When equipment failure is omitted from the PHMSA database for CO_2, the causes and sub-causes reported are somewhat like the ones reported in EGIG. To compare the overall incident frequency for onshore pipelines, the incidents caused by equipment failures were omitted from the PHMSA database. The incident frequency for CO_2 onshore pipelines decreases from around 0.7 incidents per 1000 km·year (Figure *11*) to around 0.4 incidents/1000 km/year (Figure 16) when omitting the equipment failure cases. The incident frequency on European natural gas pipelines is taken from the EGIG report from 2004 to 2019. Figure 16 shows that the incident frequency is more than double for CO_2 averaging around 0.35-0.40 incidents/1000 km/year, compared to natural gas averaging around 0.15 incidents/1000 km/year in the most recent years. The comparison must be done with caution, since the exposure (km·year) is much larger for natural gas than CO_2. In other words, if the scales of these two pipeline networks were to be compared, the European natural gas pipelines would proportionally be considered even safer by exhibiting incident frequencies further below those of the CO_2 pipelines. However, scale was not taken into account during this comparison, so the two networks are only examined on the basis of 1000 km units, irrespective of their total size.

Figure 12 showed that the incidents caused by excavation work were almost zero, and Figure 14 showed that CO_2 pipelines are located mostly in rural areas in the U.S, where interferences from construction work is expected to be low. When looking at a potential CO_2 infrastructure for CCUS in Europe, it is worth to consider data from EGIG for incidents caused by external interferences. In the period 2010-2019 EGIG reported that 27% of the incidents was caused by “external interferences”. This is also linked to the population density in Europe (Figure 15) and a high level of construction work. The numbers from EGIG are about 0.035 external interference incidents/1000 km/year reported in the period 2010-2019. It is therefore plausible that an onshore CO_2 pipeline infrastructure will see the same level of incident frequency caused by external interferences as experienced for the national gas transmission system in Europe.

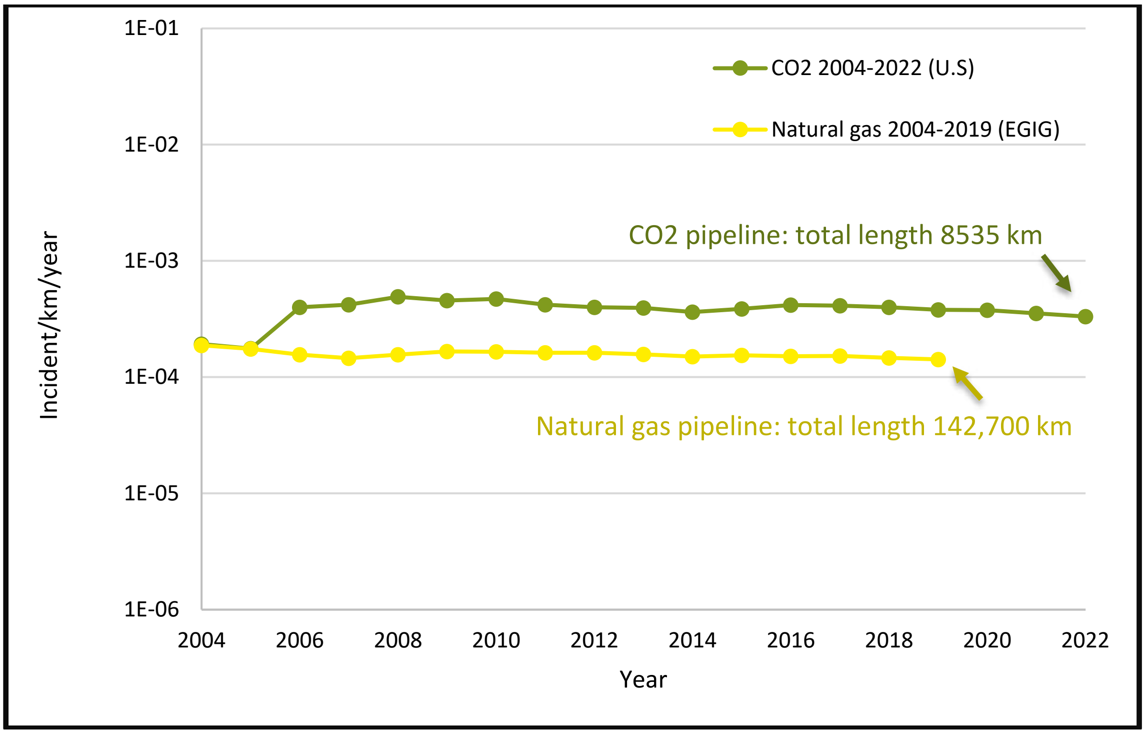

Figure 16 Incident frequency for CO_2 onshore pipelines in the U.S. (PHMSA database without equipment failure) and natural gas transmission system in Europe (EGIG report). Failure frequency is in the same order of magnitude. Note the difference in total length of pipeline.

The statistical analysis presented above can be summarized into the following items:

- Incident data for CO_2 pipelines are limited compared to the natural gas grid. In 2022 a total length of 8535 km CO_2 pipeline in the U.S. was reported. For comparison the incident data for European natural gas grid reported by EGIG in 2019 was 142,700 km. Comparing failure frequencies between CO_2 and natural gas pipeline should be done carefully.
- Based on the data available for the CO_2 onshore pipeline in the U.S., the overall primary incident frequency excluding equipment damage was around $3\text{-}5{\cdot}10^{-4}$ incident per year. This is in the same order of magnitude as EGIG reported for the natural gas transmission grid in Europe.
- Incidents caused by excavation damage on CO_2 pipelines could be expected to be in the same range as for the natural gas transmission grid operating today, around $3.5{\cdot}10^{-5}$ incidents/year.
- Incidents caused by equipment failure could be expected to be around $3{\cdot}10^{-4}$ incidents/year based on the US dataset.

As incident data for CO_2 pipeline transport are limited, the next section uses data for natural gas transport when comparing databases for incidents on pipelines.

4.2 Failure frequencies for natural gas pipelines

To facilitate onshore CO_2 pipeline transport, it is paramount to properly assess the risks of CO_2 releases from incidents and provide measures to ensure acceptable risk levels. Two databases for failure frequencies on natural gas pipelines are used: 1) the European Gas Pipeline Incident Data Group (EGIG) covering most of Europe and 2) the United Kingdom Onshore Pipeline Operators' Association (UKOPA) covering UK.

Based on EGIG data, the International Association of Oil & Gas Producers (IOGP) has recommended failure frequencies for safety assessment of onshore gas pipelines. The failure frequencies from EGIG and UKOPA together with recommendations from IOGP, where applicable, will be presented here. Criteria for an incident recorded in the EGIG database are:

- The incident must lead to an unintentional gas release.
- The pipeline must fulfil the following conditions:
    - To be made of steel
    - To be onshore
    - To have a maximum operating pressure higher than 15 barg
    - To be located outside the fence of a gas installation (this means that equipment failure such as compressors are not included in the database).

Similar for UKOPA the criteria are:

- An unintentional loss of product from the pipeline
- Within the public domain and outside the fences of installations
- Excluding associated equipment (e.g. valves, compressors) or parts other than the pipeline itself.
- Gas pipeline operating above 7 barg.

4.2.1 Overall failure frequencies for natural gas pipelines

Figure 17 Overall failure frequencies for natural gas pipeline based on pipe diameter. Figure 17 shows data from EGIG from 1970-2013 and more recently from 2010-2019 and from IOGP recommendations. It shows that the overall failure frequency decreases with increasing pipe diameter.

Data from EGIG shows decreasing failure frequencies over the last decades. This was attributed to a combination of better procedures for damage detection and prevention, technological developments, and measures to limit external interference.

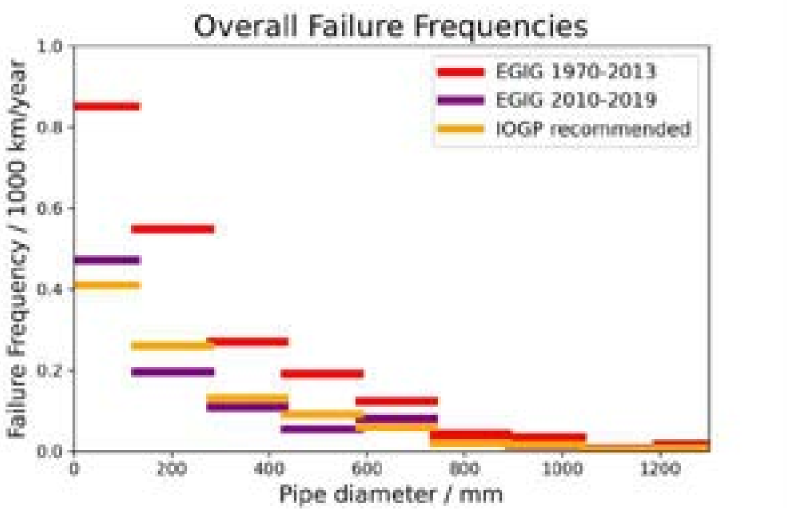

Figure 17 Overall failure frequencies for natural gas pipeline based on pipe diameter.

4.2.2 Cause of failure

From the EGIG report we get the incident distribution per cause from 2010-2019 for natural gas transmission pipelines. Note that equipment failure is not part of EGIG incident reporting. Corrosion and external interference account for about the same fraction of incidents. However, as also reported by EGIG, the corrosion incidents tend to have smaller leak sizes. External interference and ground movement accounts for the rupture incidents.

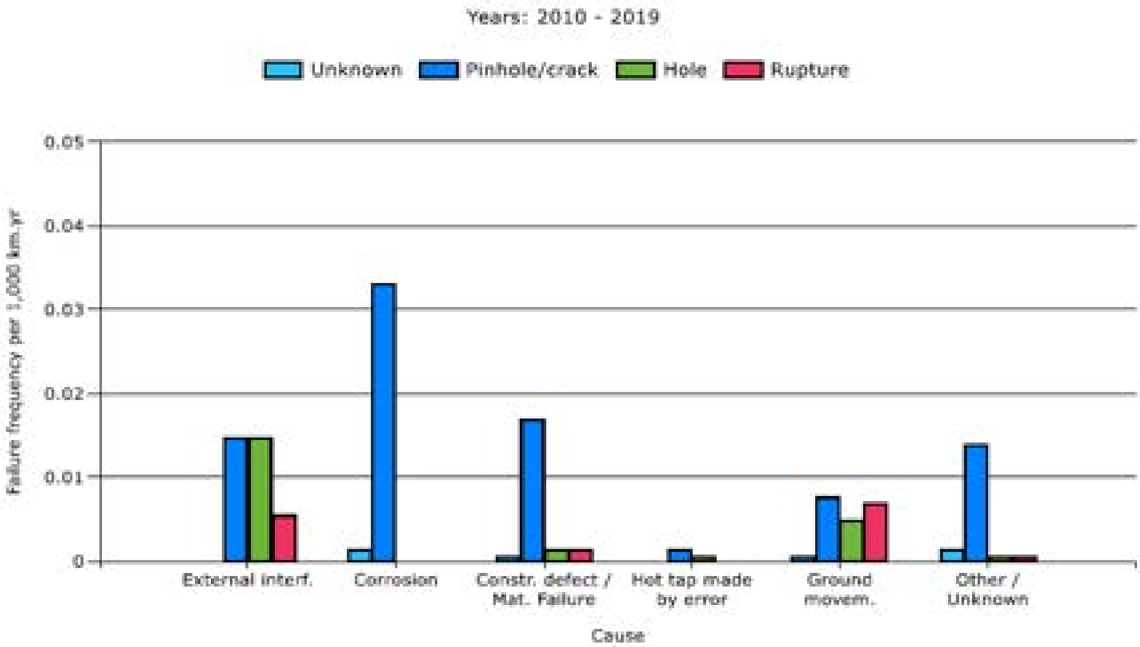

Figure 18 Cause of failure for natural gas pipeline. Data from EGIG [58].

4.2.3 Failure frequencies for external interference

Failure due to external interference (third party activity) should be independent of the gas type, and more or less directly transferable from natural gas pipelines to future CO_2 pipelines. UKOPA and EGIG have reported external interference failure frequencies for different pipe diameters and hole sizes, ranging from pinholes and holes (Figure 19 a) to full rupture of the pipeline (Figure 19 b). Lower failure frequencies are reported by UKOPA compared to EGIG for similar time periods. The system exposure is a factor 5 larger for EGIG compared to UKOPA, which means a larger statistical uncertainty for the latter. The failure frequencies are lower for large diameter pipelines compared to small ones, and for ruptures compared to holes and pinholes. This naturally leads to a significant statistical uncertainty for failure on large diameter pipelines, especially in the case of full ruptures.

The frequencies presented here can be used together with CO_2 consequence analyses to estimate the risk related to onshore CO_2 pipelines, bearing in mind the uncertainties of the databases.

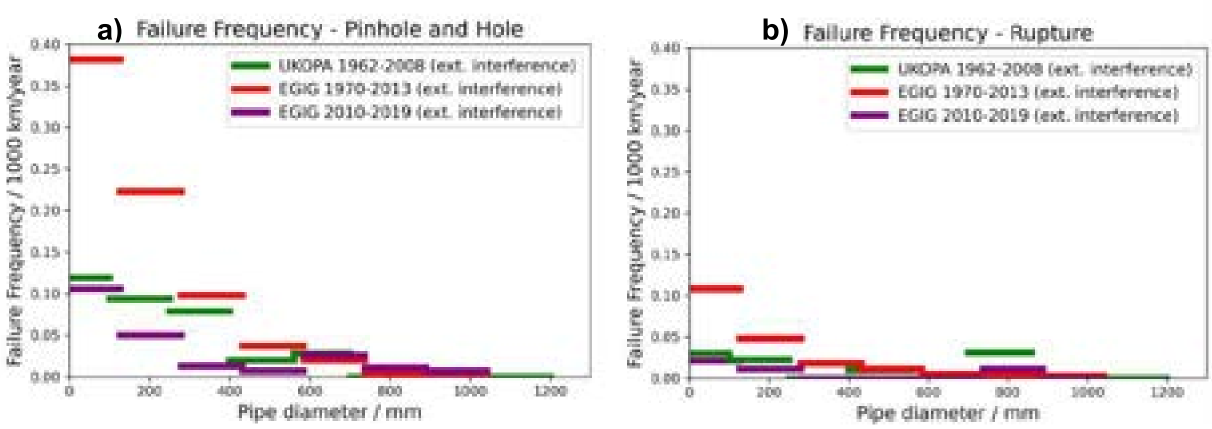

Figure 19 Failure frequencies for external interference for a) pinhole and hole and b) ruptures.

4.3 Failure frequencies for storage tanks

A key assumption applied to all “intermediate storage” risk models in this study is that the cryogenic liquid CO_2 tanks with a double-wall design, where both walls are construction of metal.

Thus, the frequency of a catastrophic failure based on Table 2.2 of [59] is $5.0x10^{-7}$ per tank per year. Assuming that there will be less than 10 tanks at any one site, the applied average failure frequency for a tank location for this study will be 1.0×10^{-6} per year.

4.4 Recommended failure frequencies for CO_2 transport

The dataset for failure frequencies for CO_2 pipeline transportation in the U.S. is limited compared to natural gas transmission pipelines. Since 2004 the reported number of incidents is 97 for a total pipeline length of 8535 km (2022-number). For comparison the total length of natural gas pipeline network in the EU is around 200,000 km. Keeping this in mind, a conservative comparison of the overall failure frequency was presented between the U.S. CO_2 pipeline and natural gas pipeline in Europe. The database for natural gas pipeline in Europe was selected since the CO_2 clusters relevant for the ConsenCUS project is within Europe. It was found that the overall failure frequency is in the same order of magnitude for both CO_2 and natural gas. Due to the limited size of the CO_2 failure frequency data set, it is not possible to evaluate the failure frequency based on a selected pipeline diameter. Therefore, the failure frequency data for the natural gas network has been applied in this work. As an example, the failure frequency from the EGIG database was selected for the base case in Section 5 of a 363.5 mm (16”) pipeline and given as 0.013/1000km·year. This value was applied to the risk assessment in Section 6.

5 Sensitivity analysis on consequence modeling

5.1 CO_2 pipelines

Consequence modeling can be used to estimate the hazard resulting from an event of release. Typically, a simulation tool is used to analyze the consequence of an accidental release of a chemical substance, such as a CO_2 release. It is important that the software is validated against experimental results. Simulation software for consequence modeling is a strong tool to give a general estimation of the consequence of a release for a two-dimension analysis. The purpose of the study overall in this report is to understand what two-dimension analysis can deliver in terms of insight to the consequence and risk associated with this type of system. Along with this objective, an additional objective is to understand when the modeling system provides an insufficiently detailed or unrealistic result for a more complex system.

In general, a consequence modeling is split into 1) a discharge calculation where the release from a vessel or pipe is modelled, 2) a dispersion calculation where the behavior of the released material is modelled such as the cloud formed after discharge, and finally 3) prediction of the effect such as the toxicity in case of CO_2. To compare cases, the toxic dose contours are compared typically at 0.1%, 1%, 10% and 99% lethality, respectively. The dangerous toxic load of a CO_2 release is calculated based on the Probit function as described in Section 2.2. The cloud width and length are reported at a height of 1 m from ground level, if not stated otherwise.

The software DNV Phast 9.0 was used for the modeling examples below. Details on the modeling approach can be found in Appendix B.

In this section, both CO_2 in gaseous and dense phase are considered. A pressure of 30 barg is considered for the gaseous CO_2 pipeline case and 120 barg for the dense CO_2 pipeline case. This is in line with typical operating conditions as seen in Figure 4. For the base case, the same pipe dimensions are modelled with both gaseous and dense CO_2 i.e. the inner pipeline diameter, release point, isolation valve spacing, isolation valve closure time, etc. are kept constant. Since the density of dense CO_2 is much larger than gaseous CO_2, the mass flow rate and amount of released CO_2 in a rupture event is much larger in dense phase CO_2 compared to gas phase CO_2.

The selected parameters for the base case are presented in Table 6. The purpose of this section is to present considerations and sensitivity analysis of selected parameters.

Summary of cases is presented in Appendix C.

Table 6 Parameters for base case onshore pipeline case with gaseous CO_2 and dense CO_2.

Basic of design	**Values**	
Case	Buried pipeline	
Media and phase	Gaseous CO_2 (assuming 100% purity)	Dense CO_2 (assuming 100% purity)
Operating flow rate	22 kg/s (80 ton/h or 0.7 MTPA)	168.6 kg/s (607 ton/h or 5.3 MTPA)
Temperature and pressure of CO_2	30 barg and 5 °C	120 barg and 5 °C
Mass of contained CO_2 between isolation valves (20 km)	155.9 tonnes	1,994 tonnes
Volume of contained CO_2 between isolation valves (20 km)	2075 m^3	2075 m^3
Release direction	Buried pipeline with vertical release	
Release point	Halfway between isolation valves	
Pipe inner diameter	363.5 mm (API 5L 16 inch SCH 80)	
Pipe roughness	0.045 mm (carbon steel)	
Pipe length	65 km	
Leak size	Full bore rupture, weld-to-weld distance 12 m (i.e. fracture length assumed to be 12 m)	
Weather	Neutral (Pasquil stability[2] D and wind speed of 4 m/s)	
Distance between isolation valves	20 km	
Response + valve closing time	60 s (assuming automatic leak detection system, i.e., instantaneous response)	
Depth of cover + soil type	1.2 m (clay)	
Terrain roughness	1 m (corresponding to suburbs, forests)	

[2] See Table 8 for definition.

Ambient temperature	9.85 °C
Relative humidity	70%
Additional consideration for above ground pipelines	
Case	Pipeline above ground
Release direction	Pipeline above ground with angled release of CO_2
Default release angle	30 degrees from horizontal
Depth of cover + soil type	None

The weather for the base case was selected to be at neutral weather stability and a wind speed of 4 m/s. Weather stability is elaborated in Section 5.1.2. The wind speed was selected as the most likely based on wind statistics for two locations in Denmark – see Appendix B.

The pipeline ruptures are always assumed to be halfway between isolation valve, corresponding to a "worst case" release scenario. This is illustrated in Figure 20 for a valve spacing of 20 km.

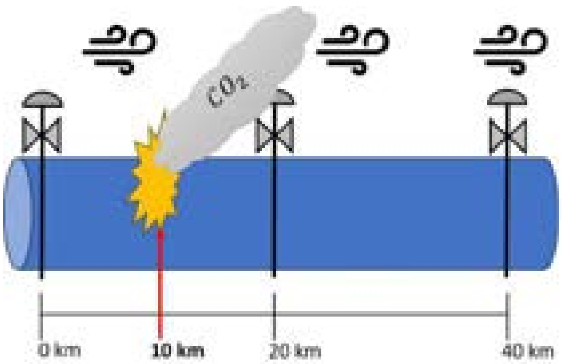

Figure 20 Illustration of pipeline rupture, halfway between isolation valves with 20 km spacing.

As a software limitation, the release direction is always simulated along the pipeline, never perpendicular to it (corresponding to the z-axis in Figure 21). For buried pipelines, only vertical and not angled releases are possible. However, for CO_2 pipelines above ground, angled release of CO_2 can be modelled between horizontal (x axis) and vertical (y axis) in any angle from 0 to 90 degrees, see Figure 21.
For the consequence modeling **the wind direction is always from west (left),** yet another limitation is that releases against the wind direction cannot be modelled in the consequence model.

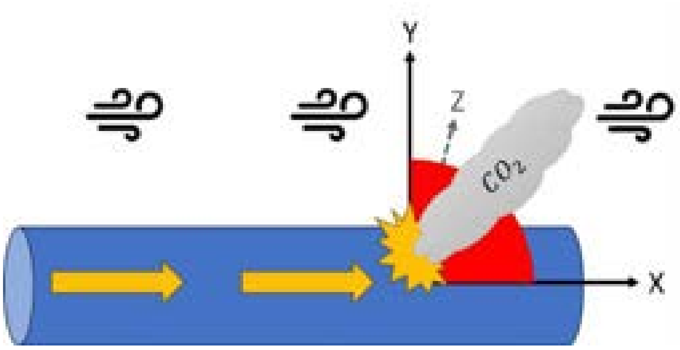

Figure 21 Illustration of a pipeline rupture with release along the pipeline (x-axis) with possible release angles (above ground pipeline only) between 0 and 90 degrees in the xy-plane as indicated by the red quarter circle.

Results from consequence modeling are displayed as side view dispersion (in the xy-plane in Figure 21, above ground rupture) at a given CO_2 concentration, typical at 4% unless otherwise stated, and as lethality curves at 1 m height from the ground (xz-plane in the illustration of a buried pipeline rupture in Figure 22).

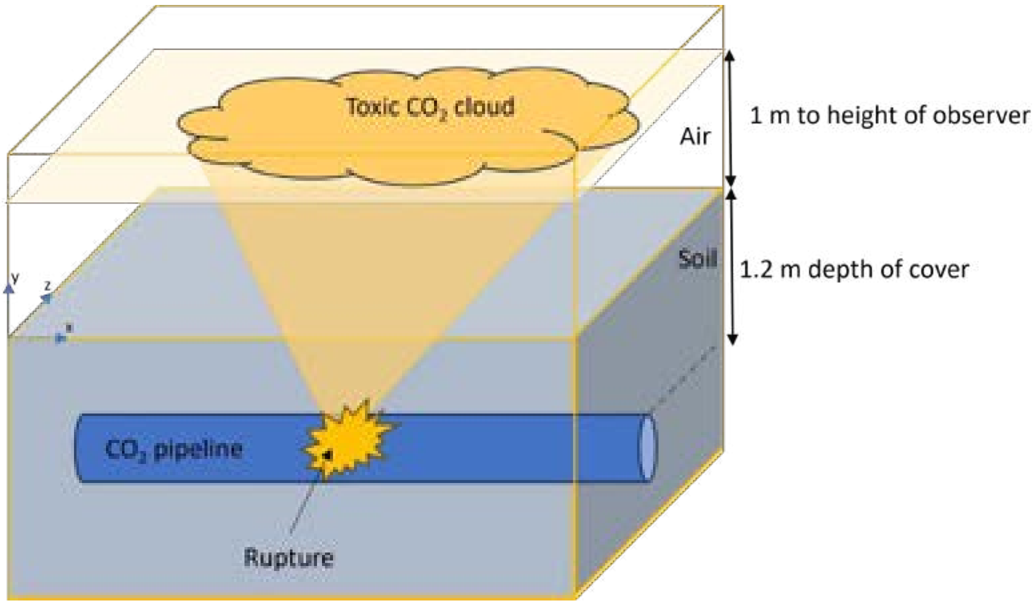

Figure 22 Illustration of the width and length of the toxicity cloud seen at 1 m height above the ground.

5.1.1 Base case scenarios

The consequence of a CO_2 buried pipeline rupture with the parameters in Table 6 are modelled. Figure 23 and Figure 24 show side views of dispersion of CO_2 at given concentrations (2, 4, and 10%) and toxicity curves for rupture of a gas (30 barg) and dense (120 barg) CO_2 pipeline, respectively, at lethality levels 0.1, 1, 10, and 99%. For the side views, the concentration curves are given at a specific time after each event. This time is by default the largest possible cloud area for the given concentrations. The specific time depends on input parameters, for example the valve spacing, and is provided for all reported consequence calculations in Appendix C. The dispersion curves for the gaseous pipeline rupture shows that the CO_2 doesn't reach ground level at concentration at or above 2%, except for the immediate (<10 m) vicinity of the rupture point. Hence, the release event is non-lethal at 1 m height outside the immediate vicinity of the rupture point, as seen from the lethality curves.

On the contrary, the dense phase rupture results in hazardous CO_2 concentrations at ground level at several hundred meters downwind from the rupture. This manifests as much larger lethality curves compared to gas phase rupture, with the 1% lethality curve reaching around 300 m downwind and around 150 m perpendicular to the pipeline. This difference is due to the much larger amount of CO_2 released from the dense phase pipeline. For the chosen weather condition, the dispersion of CO_2 follows the "conventional" behavior, i.e. rising as a vertical jet and then diluting downwind.

As shown in the next section, the weather stability will have an effect of the dispersion pattern.

Dry ice formation was not included in any of the models due to the limitation of the thermodynamic model applied in the tool.

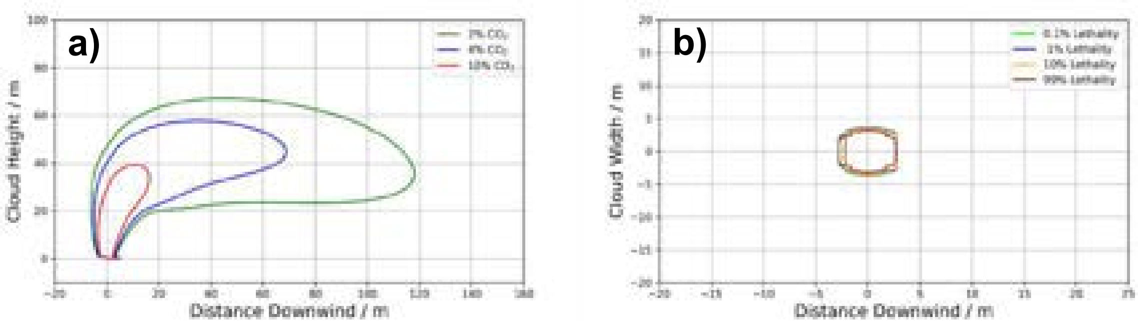

Figure 23 Rupture of a buried pipeline with 30 barg gaseous CO_2 for base case parameters a) Side views of dispersion at 2%, 4% and 10% CO_2 concentrations, b) Lethality contour curves at a height of 1 m above ground.

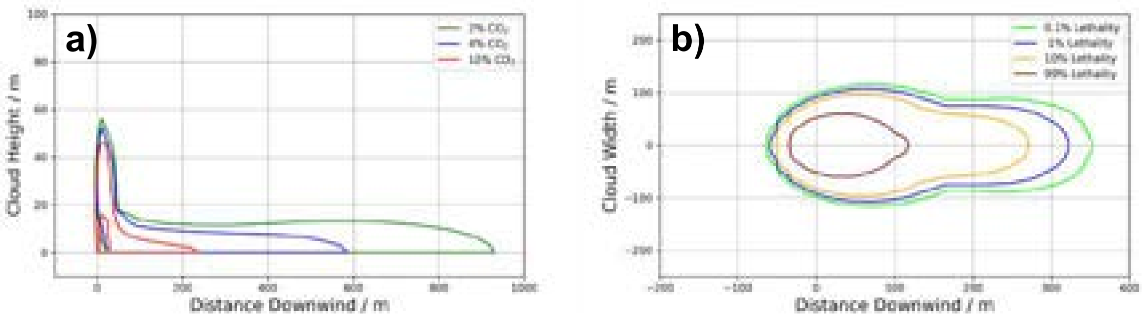

Figure 24 Rupture of a buried pipeline with 120 barg dense phase CO_2 for base case parameters a) Side views of dispersion at 2%, 4% and 10% CO_2 concentrations, b) Lethality contour curves at a height of 1 m above ground.

5.1.2 Weather conditions

The weather conditions will influence the dispersion of CO_2. Weather categories are defined by the wind speed (Table 7) and Pasquill stability class (Table 8). which are used in the dispersion calculation to account for the atmospheric stability. For example, a wind speed of 4 m/s and stability D is noted as weather category 4/D, and so forth. As a software limitation**, the wind direction is always from west in the consequence modeling.**

Appendix B presents weather statistics for two locations in Denmark: Aalborg Airport and Copenhagen Airport. The data shows that the most likely wind speed is around 4-6 m/s and likelihood of low wind speed, <1 m/s, is low. The weather statistics are used in the risk assessment in Section 6. For the consequence modeling in this section the weather category 4/D is chosen. Sensitivity analysis on different weather conditions is described in Section 5.1.2.1.

Table 7 Weather categories [60].

Wind speed	Day: Solar Radiation			Night: Cloud Cover	
(m/s)	Strong	Moderate	Slight	Cloudiness	Thinly overcast
< 2	A	A-B	B	F	E
2 -3	A-B	B	C	F	E
3 -4	B	B-C	C	E	D
4 -6	C	C-D	D	D	D
> 6	C	D	D	D	D

Table 8 Pasquill stability class [60].

Stability class	Definition
A	Very unstable
B	Unstable
C	Slightly unstable
D	Neutral
E	Slightly stable
F	Stable
G	Extremely stable (fog)

5.1.2.1 Effect of weather conditions on CO_2 buried pipeline ruptures

The effect of the weather conditions is shown in the following case. Figure 25 shows side view of CO_2 dispersion and 1% lethality curves for a rupture of a buried pipeline with 30 barg gas phase CO_2 and at various weather conditions. A large difference in the cloud shape is seen between 1 m/s and ≥2 m/s wind speeds. At more likely wind speeds (4 m/s), the CO_2 dilutes downwind to non-lethal levels before reaching the ground.

Figure 26 shows corresponding graphs for a 120 barg dense phase CO_2 pipeline rupture for same selected weather conditions. As given in Table 6, the inventory in the dense phase pipeline is around 13 times larger than the gas phase pipeline, so the release rate is much larger for the same pipeline geometry.

This simulation shows that CO_2 stays near the ground at low wind speed and stable weather conditions forming a kind of 'gas blanket' covering the ground. This is explained in more details in the next section.

Note: The relative humidity is 70% by default for all weather types. In general, a higher relative humidity results in larger toxicity clouds. However, the effect was found to be very limited for the selected base case (curves not shown).

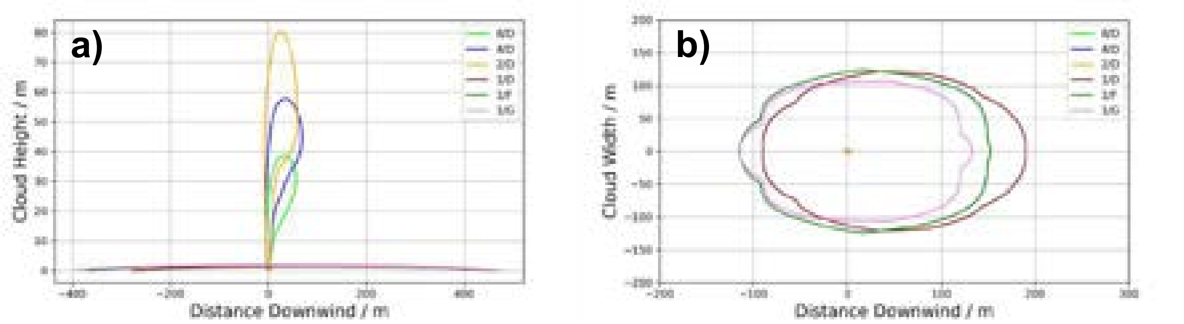

Figure 25 Rupture of a buried pipeline with 30 barg gaseous CO_2 at different weather conditions; a) Side views of dispersion at 4% CO_2, b) 1% lethality contour curves at a height of 1 m.

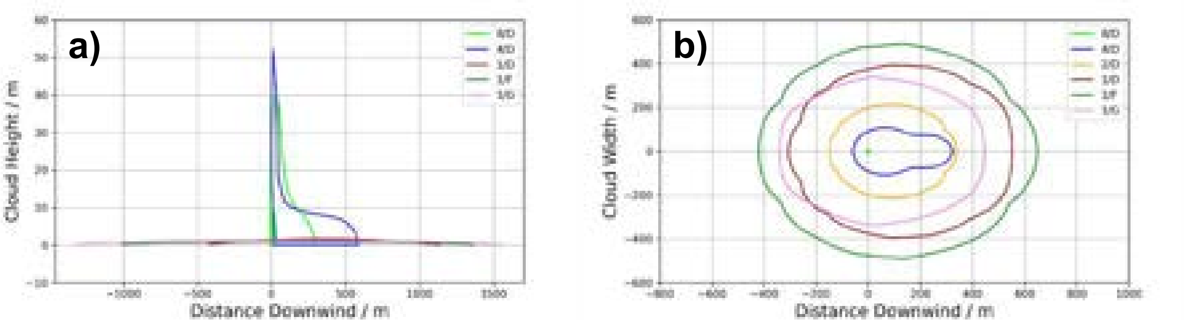

Figure 26 Rupture of a buried pipeline with 120 barg dense CO_2 at different weather conditions; a) Side views of dispersion at 4% CO_2, b) 1% lethality contour curves at a height of 1 m. For the weather condition 2/D, the CO_2 concentration was below 4% at the time of the side views.

5.1.2.2 Gas blanket modeling

It's evident from the figures above that the pattern of the release changes for low wind speeds. This can be characterized as a "gas blanket" on the ground. The software used for the modeling has recently been updated based on more data from experimental results, where the CO_2 released formed a “blanket” near the ground for low wind speed. The gas blanket model is activated for low wind conditions and large, low velocity releases of CO_2. The activation of the gas blanket model is crucial to the dispersion of CO_2. This can be seen from the side views of dispersion for different weather conditions in Figure 27, with each subfigure showing the dispersion from 1 second to 200 seconds after the rupture. This difference in dispersion behavior dictates the toxicity levels as seen in Figure 25 and Figure 26.

It should also be noted that as **a limitation of the modelling software, the gas blanket is only considered for buried pipelines**.

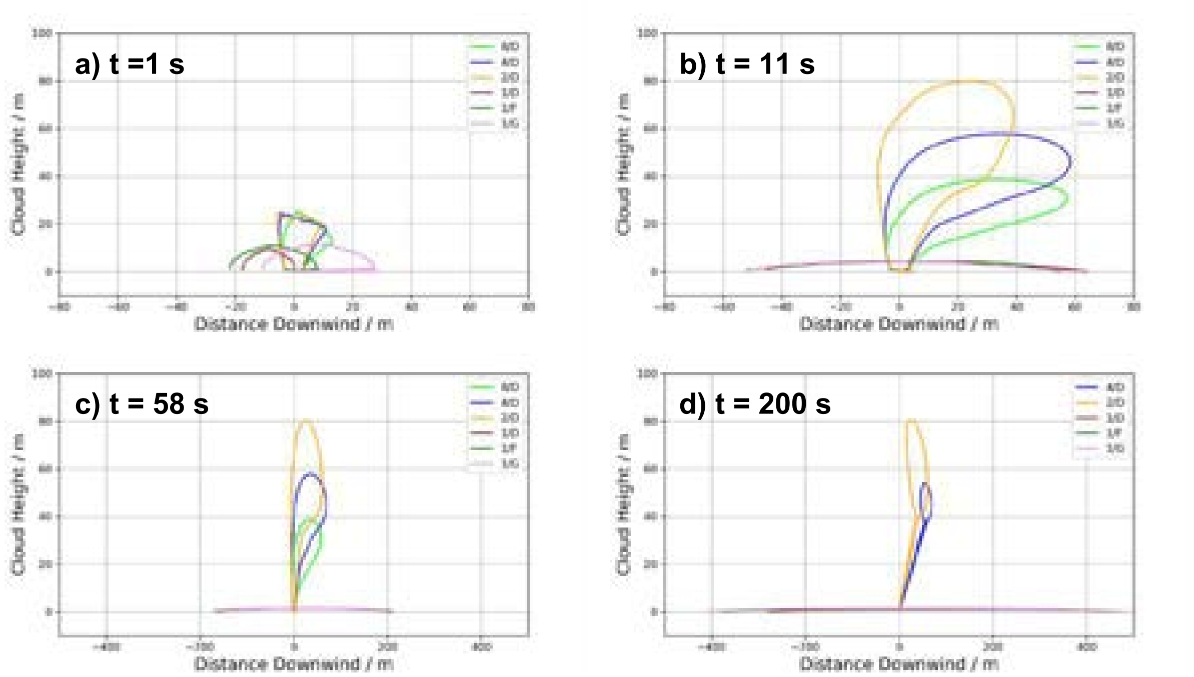

Figure 27 Rupture of a buried pipeline with 30 barg gaseous CO_2. Side view of dispersion (4% CO_2) at various weather conditions, with and without triggering the gas blanket model at various times; a) t = 1 s, b) t = 11 s, c) t = 58 s, and d) t = 200 s.

5.1.3 Terrain roughness parameters

Consequence modeling software typical assumes a **flat terrain**, i.e., no topography is considered. However, it is possible to adjust a uniform roughness of the terrain in the modeling. Low terrain roughness indicates e.g. open water or low crops whereas a high terrain roughness corresponds to for example forests, suburbs, or even city centers. Typical values are provided in Table 9. A large terrain roughness is expected to result in higher turbulence in the air when the released CO_2 reaches the surface. The terrain roughness expresses a uniform terrain variation. For the modeling in this report, a terrain roughness is set to 1 m in the base case, corresponding to e.g. suburbs. It’s evident that the parameter of terrain roughness is not detailed enough for a full risk evaluation in high populated areas with relatively high terrain roughness values. For this, more detailed information on distribution of e.g. buildings should be used for populated areas and one should consider three-dimension analysis where effects of obstacles and complexity of the geometry is studied.

Table 9 Typical terrain roughness lengths

Terrain roughness length	Terrain type
0.2 mm	Open water (e.g. sea)
5 mm	Mud flats or snow, no vegetation, no obstacles
100 mm	Low crops, occasional obstacles
500 mm	Parkland, bushes with numerous obstacles
1000 mm	Regular large obstacle coverage (e.g. forests, suburbs)
3000 mm	City centers with low and high rise buildings

Figure 28 shows the consequence modeling for the base case of a buried pipeline with gaseous CO_2 at varying terrain roughness of 5 mm, 100 mm, 1 m, and 3 m. The CO_2 is dispersed further downwind for a low terrain roughness compared to a high, due to a decrease in turbulence. The corresponding 1% lethality contour curves are shown in Figure 28 b. Regardless of terrain roughness, the CO_2 doesn't reach the ground at dangerous concentrations (4%), and hence there is no impact on the 1% lethality contours shown at 1 m height.

Figure 29 shows similar curves for the dense phase pipeline rupture. Again, a low terrain roughness means less turbulence and a larger distance downwind at selected 4% CO_2 concentration. However, in contrast to the gaseous pipeline rupture, the CO_2 reaches ground level at hazardous concentrations due to the much larger inventory released. The 1% lethality curves reach further downwind for low terrain roughness lengths where the CO_2 reaches further downwind due to less turbulence.

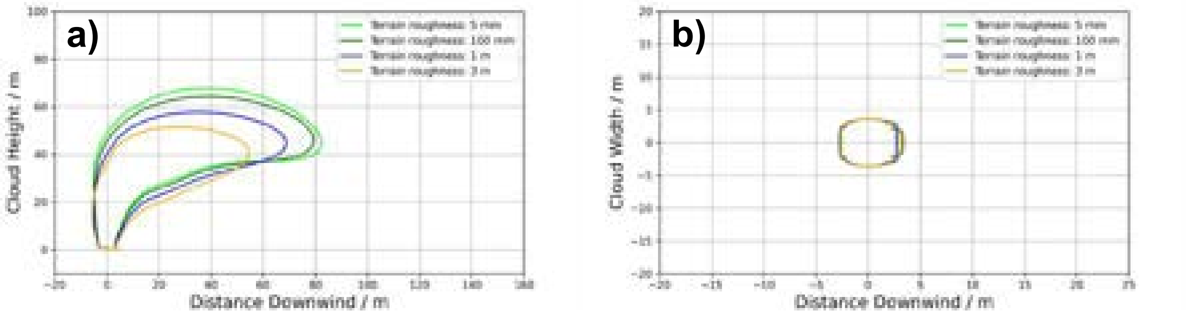

Figure 28 Rupture of a buried pipeline with 30 barg gaseous CO_2 at 4/D weather for various terrain roughness values. a) Side views of dispersion at 4% CO_2, b) 1% lethality contour curves at a height of 1 m.

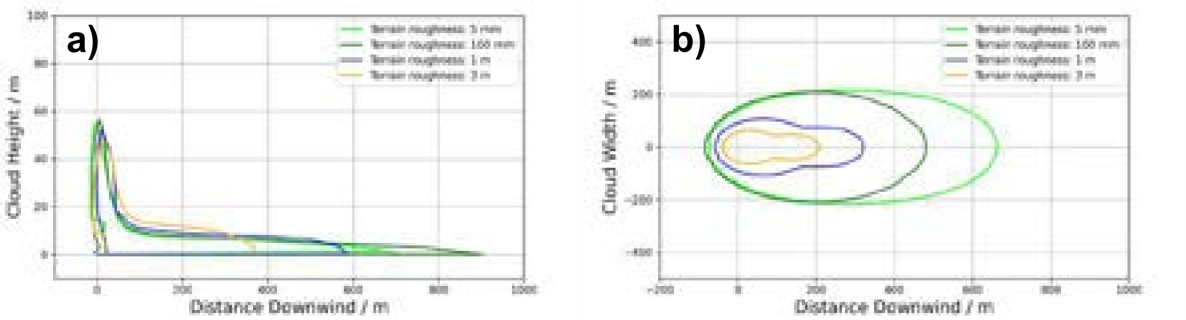

Figure 29 Rupture of a buried pipeline with 120 barg dense phase CO_2 at 4/D weather for various terrain roughness values. a) Side views of dispersion at 4% CO_2, b) 1% lethality contour curves at a height of 1 m.

5.1.4 Flow rate

For a selected pipeline dimension and the temperature and pressure of the CO_2, the flow rate inside the pipeline is also an input parameter to the consequence modeling. In this section, the effect of the flow rate on dispersion and toxicity is modeled. Figure 30 and Figure 31 show dispersion of CO_2 and corresponding 1% lethality contour curves for gas and dense pipeline ruptures, respectively, at two different flow rates. The results show that reducing the flow rate to the half has very little effect on the release of CO_2. This is valid for both gas and dense phase CO_2 releases. It should be kept in mind that for the base case in this report, the length of a segment is 20 km with closing time of the isolation valve of only 60 seconds. This means that the amount of CO_2 released during the event is almost the same between flowrates of 22 kg/s vs. 11 kg/s. Similar results are observed for dense phase. The difference would be more pronounced if the isolation valve closing time was longer.

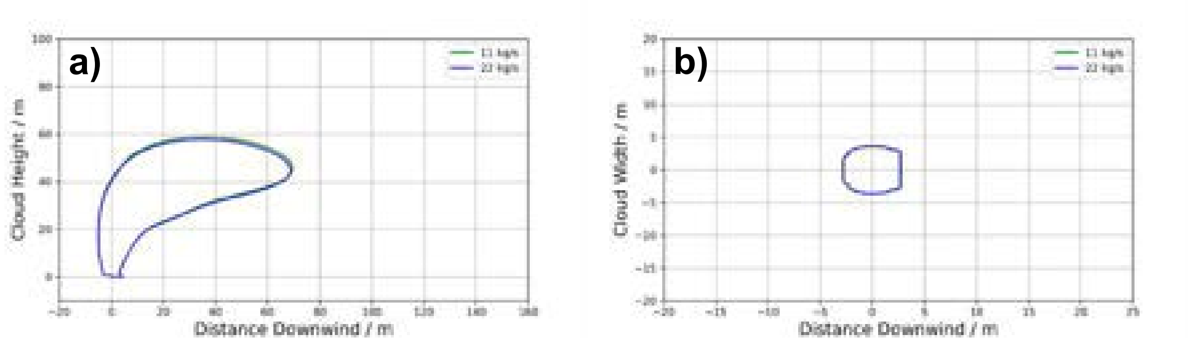

Figure 30 Rupture of a buried pipeline with 30 barg gaseous CO_2 at 4/D weather for different flow rates. a) Side views of dispersion at 4% CO_2, b) 1% lethality contour curves at a height of 1 m.

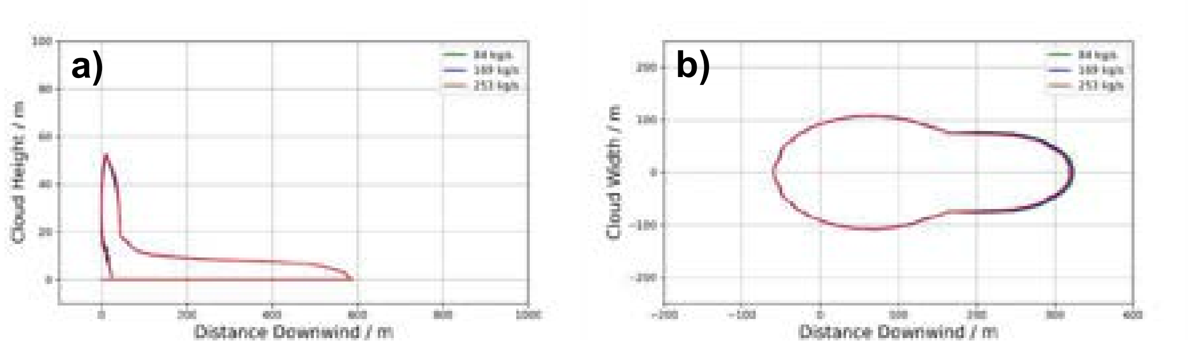

Figure 31 Rupture of a buried pipeline with 120 barg dense phase CO_2 at 4/D weather for different flow rates. a) Side views of dispersion at 4% CO_2, b) 1% lethality contour curves at a height of 1 m.

5.1.5 Distance between isolation valves and valves closing time

The distance between isolation valves will influence the amount of released CO_2 in a rupture scenario. Table 10 and Table 11 reports the mass of CO_2 released during a rupture event for gas and dense phase CO_2, respectively. The total mass of CO_2 contained between two isolation valves, prior to the rupture, is also provided. This total mass is referred to as static mass in the following text.

Figure 32 and Figure 33 show dispersion of CO_2 and corresponding 1% lethality contour curves with isolation valve spacing of 10 km, 20 km and 30 km for a gas and dense phase pipeline rupture, respectively. The valve closure time is kept to 60 seconds in all cases.
Installing isolation valves along a pipeline has large effect in minimizing the amount of CO_2 released in a rupture scenario, but changing the distance of 10 km, 20 km and 30 km, has only a small small effect on the dispersion, and hence the toxicity for the gas phase pipeline rupture. For the dense phase CO_2 pipeline, the area affected by the rupture can be slightly reduced by using valves every 10 km rather than every 20 or 30 km. This has some impact on the 1% lethality contour curve in the downwind direction.

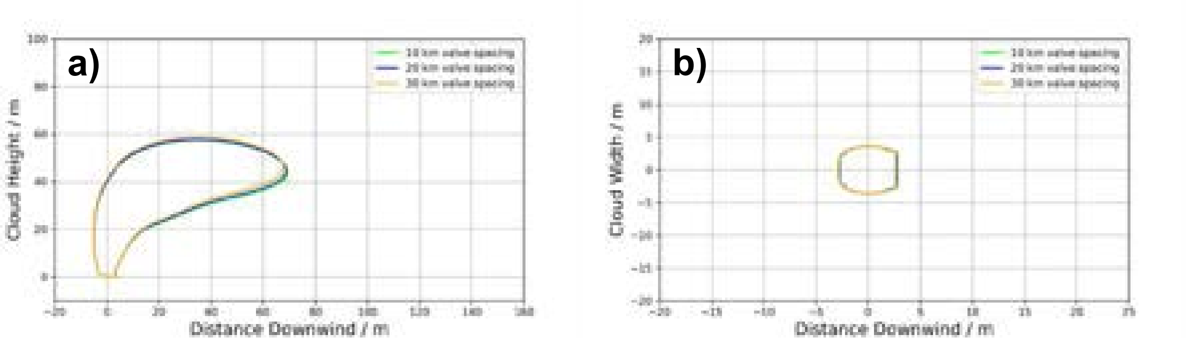

Figure 32 Rupture of a buried pipeline with 30 barg gaseous CO_2 at 4/D weather for different isolation valve spacing. a) Side views of dispersion at 4% CO_2, b) 1% lethality contour curves at a height of 1 m.

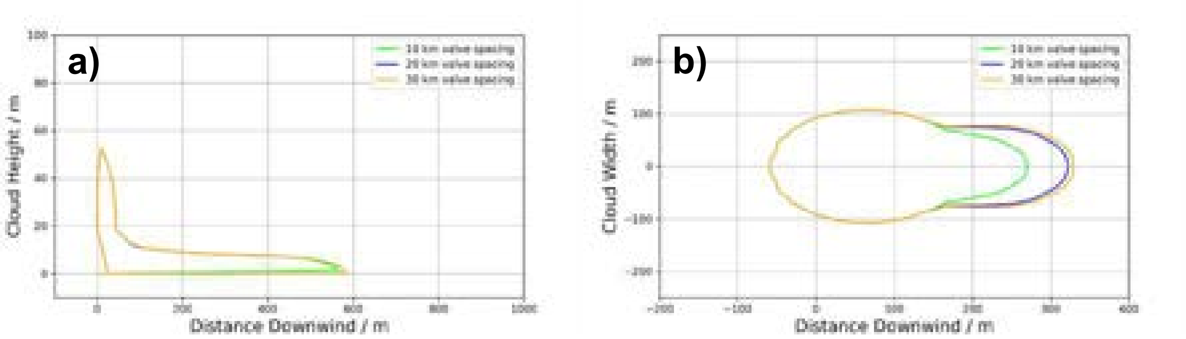

Figure 33 Rupture of a buried pipeline with 120 barg dense phase CO_2 at 4/D weather for different isolation valve spacing. a) Side views of dispersion at 4% CO_2, b) 1% lethality contour curves at a height of 1 m.

Effect of valve closing time:

For a given spacing of isolation valves, the valve closure time has a very small effect on the amount of CO_2 released during the event for the cases considered, see Table 10 and Table 11.
Static mass of CO_2 between valves before the release defines the minimum amount of CO_2 that will be released from t=0 to the end of the simulation time. Within the closing time of the valves additional CO_2 can be released. The difference between the released mass and the static mass values defines the mass of CO_2 that remains in the pipeline at the end of the simulation run because there is not enough pressure to completely empty the pipeline section.
The effects on the dispersion and lethality curves are minor for the closing time chosen in this study. This is shown in Figure 34 and Figure 35 for gas and dense buried pipeline ruptures, respectively, with isolation valve every 20 km in all cases. The closing time is set to 10 seconds, 30 seconds, and 60 seconds as input parameters. However, one should be aware of the selected time step in the calculation. For a specified closure time, the valve is assumed to close at the first time step after the set time (10, 30, or 60 s). The simulated valve closure time for each case is provided in Table 10 and Table 11.

While the dispersion of the gaseous pipeline is slightly affected for a very short closing time of 10.1 s compared to 60.1 s, no effect is evident in case of the dense phase pipeline rupture (real closure times of 10.9 s vs. 79.9 s). The negligible effect of the valve closure time can be attributed to the very small effect of valve closure time on the amount of CO_2, due to the relatively fast closing time in all cases (always <80 seconds).

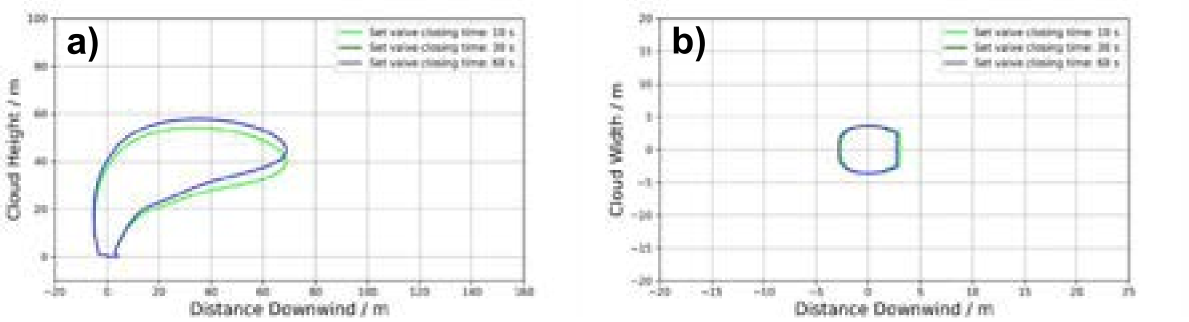

Figure 34 Rupture of a buried pipeline with 30 barg gaseous CO_2 at 4/D weather for different closing times of isolation valves. a) Side views of dispersion at 4% CO_2, b) 1% lethality contour curves at a height of 1 m.

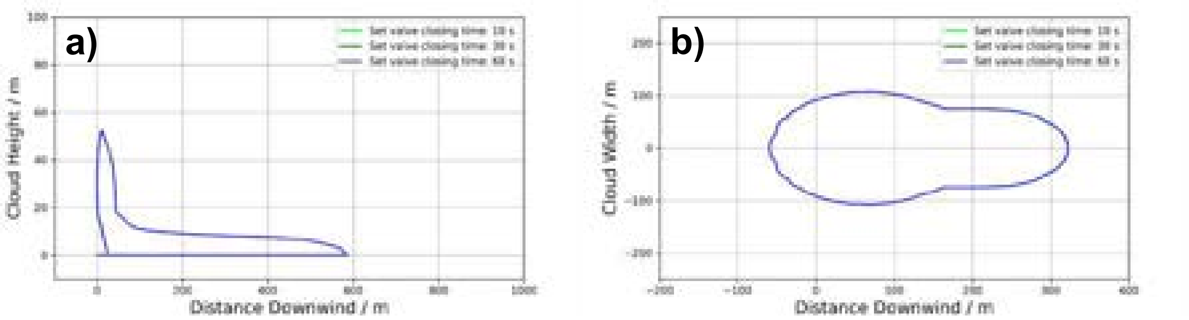

Figure 35 Rupture of a buried pipeline with 120 barg dense phase CO_2 at 4/D weather for different closure times of isolation valves. a) Side views of dispersion at 4% CO_2, b) 1% lethality contour curves at a height of 1 m.

Table 10 CO_2 gas phase releases for various valve spacing/closure times.

Valve specifications	Total mass of CO_2 released during rupture event (tonnes)	Static mass of CO_2 between valves before release (tonnes)	Total time of rupture event	Simulated valve closure time
Spacing: 30 km Closure time: 60 s	194.6	228.0	2743 s	60.1 s
Base case Spacing: 20 km Closure time: 60 s	138.1	155.9	1509 s	60.1 s
Spacing: 10 km Closure time: 60 s	77.0	79.8	545 s	60.1 s
Spacing: 20 km Closure time: 30 s	135.2	155.9	1518 s	32.4 s
Spacing: 20 km Closure time: 10 s	130.2	155.9	1526 s	10.1 s

Table 11 CO_2 dense phase release for selected valve spacing and closure times. 1 h is the limit for the total time of the event.

Valve specifications	Total mass of CO_2 released during rupture event (tonnes)	Static mass of CO_2 between valves before release (tonnes)	Total time of rupture event	Simulated valve closure time
Spacing: 30 km Closure time: 60 s	1769	2988	3600 s	79.9 s
Base case Spacing: 20 km Closure time: 60 s	1566	1994	3600 s	79.9 s
Spacing: 10 km Closure time: 60 s	861	998	2673 s	69.3 s
Spacing: 20 km Closure time: 30 s	1560	1994	3600 s	30.1 s
Spacing: 20 km Closure time: 10 s	1558	1994	3600 s	10.9 s

5.1.6 Burial depth and soil type for pipeline

The burial depth and soil type for the pipeline show an effect on the CO_2 dispersion and toxicity in the event of a rupture. Figure 36 and Figure 37 show the effect of selected burial depth and soil type for the base case for gaseous and dense CO_2, respectively. For the case of clay as soil type, a larger depth of cover leads to a slightly lower vertical jet. A larger depth of cover leads to a lower initial release velocity at ground level, i.e., due to a larger crater formation. A larger crater formation results in a larger loss of momentum, which in turns results in a lower vertical jet and hence a larger dispersion downwind.
At a constant depth of 1.2 m, the difference in dispersion between soil types of clay and sand is significant, especially for the dense phase rupture.
This is due to the lower bulk density of the sand leading to a larger crater and correspondingly a lower vertical jet velocity. Again, a lower vertical jet correlates with a larger dispersion of released CO_2 downwind, which has a significant effect on the lethality curves for the dense phase rupture. For gas phase rupture, the concentration at ground level is non-hazardous regardless of soil type and depth of cover.

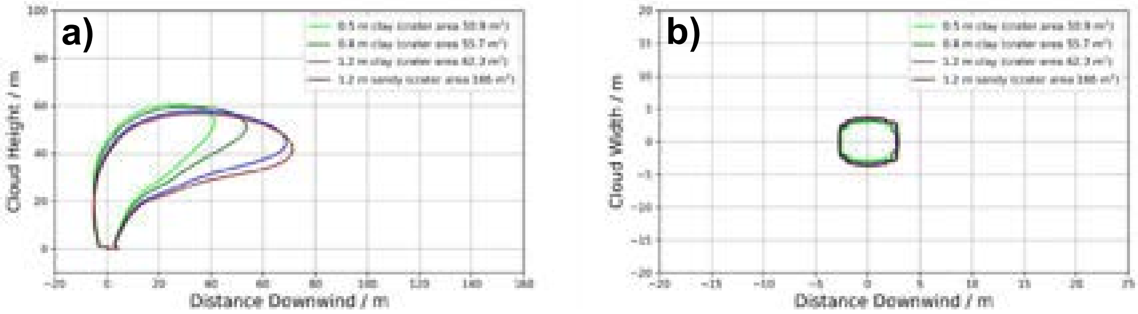

Figure 36 Rupture of a buried pipeline with 30 barg gaseous CO_2 at 4/D weather for different depth of covers and soil types. a) Side views of dispersion at 4% CO_2, b) 1% lethality contour curves at a height of 1 m.

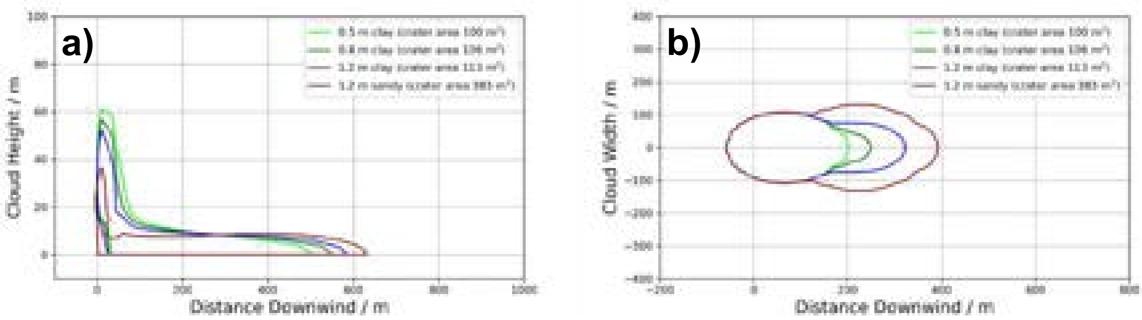

Figure 37 Rupture of a buried pipeline with 120 barg dense phase CO_2 at 4/D weather for different depth of covers and soil types. a) Side views of dispersion at 4% CO_2, b) 1% lethality contour curves at a height of 1 m.

5.1.7 Above ground ruptures

The above sections considered buried pipeline, which is foreseen to be the most likely case for CO_2 transportation in CCUS value chain in Europe. In this section pipelines above ground are modelled. Above ground pipeline could be relevant in confined spaces, such as in and out of compressor stations.

As CO_2 is a heavy gas it is of interest to see the effect if the pipeline rupture directs the CO_2 release in an angle from the ground. To and from a compressor station the pipeline will typical be horizontal and in the event of a release, there is not a soil layer to absorb the momentum energy at the time of the release. Therefore, at the start of a rupture event for an above ground piping, the momentum energy will cause the pipes to bend at the angles described in the graphs below.
In Figure 38 and Figure 39 the side views for a 4% concentration profile (subfigure a) and the 1% lethality curve (subfigure b) are shown for gaseous pipeline rupture and dense phase pipeline rupture, respectively, with an angle of release of 90° (vertical release from pipeline), 30° and 5°, respectively.

In Figure 40 side views and 1% lethality curves are compared for a buried and an above ground pipeline for gaseous CO_2. Above ground, where all momentum energy is directed upwards, the CO_2 dispersion reaches higher compared to the buried pipeline where some of the momentum energy is expelled by the crater formation. Due to this effect, downwind dispersion of CO_2 is limited compared to the buried pipeline rupture. However, the concentration of CO_2 does not reach hazardous concentrations at ground level, apart from the immediate site of the rupture. The small difference in the 1% lethality curves is due to crater formation in the case of the buried pipeline.

Figure 41 shows similar graphs for the case of dense phase CO_2. The same amount of fluid is released for both buried and non-buried pipeline, but for the buried pipeline, the momentum energy is expelled by the formation of the crater. Therefore, the fluid release is at ground level, leading to the large difference in lethality at 1 m.

The conclusion from this aspect of the study is that if the model does not account for critical parameters such as burial depth and soil type, for example, the results will be misleading and unrealistic for the simulated event.

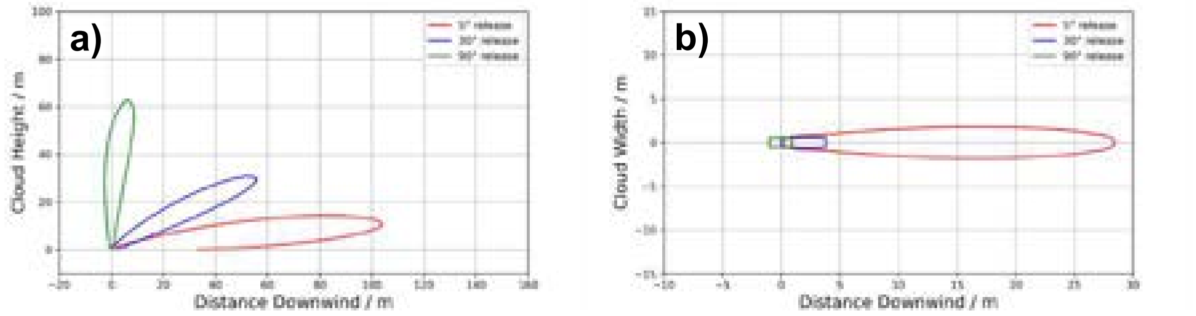

Figure 38 Above ground rupture of a pipeline with 30 barg gaseous CO_2 at 4/D weather for different release angles from horizontal. a) Side views of dispersion at 4% CO_2, b) 1% lethality contour curves at a height of 1 m.

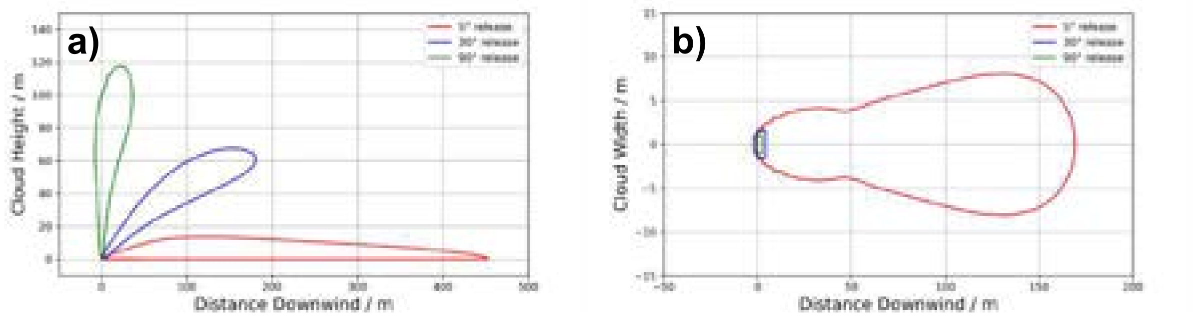

Figure 39 Above ground rupture of a pipeline with 120 barg dense phase CO_2 at 4/D weather for different release angles from horizontal. a) Side views of dispersion at 4% CO_2, b) 1% lethality contour curves at a height of 1 m.

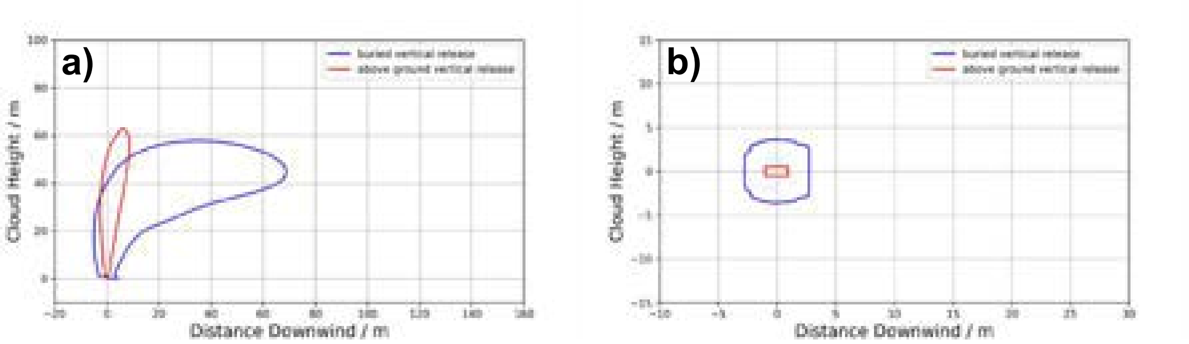

Figure 40 CO_2 pipeline rupture (gas phase) at 4/D weather, buried compared to above ground with vertical release. a) Side views of dispersion at 4% CO_2, b) 1% lethality contour curves at a height of 1 m.

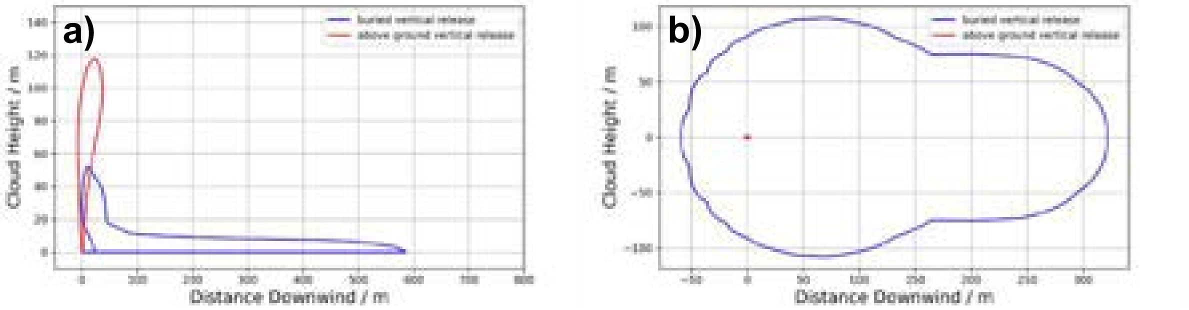

Figure 41 CO_2 pipeline rupture (dense phase) at 4/D weather, buried compared to above ground with vertical release. a) Side views of dispersion at 4% CO_2, b) 1% lethality contour curves at a height of 1 m.

5.1.8 Modeling CO_2 with impurities

As outlined in Section 2.5 the composition of CO_2 in CCUS value chain will not be 100% pure. So far, all consequence modeling in this section has been done for pure CO_2. It remains for the future work to model consequence for CO_2 with relevant impurities. However, as a software limitation we found that the gas blanket model applied at stable weather conditions and low wind speed described in Section 5.1.2.2 is only applicable for pure CO_2. Hence, one should be careful when modeling CO_2 with impurities and the selection of physical model.

5.2 Intermediate storage tanks

There will be a need for intermediate storage of CO_2 when looking at CCUS value chains. This could be at harbors before unloading or after offloading from ships or at the carbon capture site before truck offloading. There could also be a need when balancing hydrogen production made from renewable energy sources to produce for example electro fuels. As an example, the CCS-project Northern Light in Norway will transport CO_2 in ship cargo tanks at a pressure between 13 and 18 barg with corresponding equilibrium temperature [40]. The CO_2 will be transferred to onshore storage tanks at pressures between 13 and 18 barg [40]. Other references shows that there are some ongoing investigations to ship transport at low pressure (approx. 7 barg) with corresponding onshore storage facilities [61]. High pressure shipping (approx. 40 barg, +5 °C) is also a topic of investigation since cooling of the CO_2 can potentially be omitted [62]. Both the storage pressure and the tank volume will also be of interest when looking at the consequence of loss of liquid CO_2. Storage tanks will often consist of multiple, smaller tanks that can be filled sequentially through a manifold. The FEED study from a CCS project in Oslo, Norway, shows a design of 16 tanks each containing 342 m^3 [63]. The concept report from Northern Light shows 12 vertical tanks with the overall capacity of 9,150 m^3. This gives a volume of 763 m^3 for each tank [40]. The tanks are interconnected through valves and it's possible to close off a section in case of loss of material. The tank volume for this parameter study is chosen at 350, 750 and 3000 m^3. The larger size could imitate a failure in several tanks at the same time. The consequence of loss is calculated in this section and results are shown thought the lethality contour plots by comparing the parameters given in Table 12.

Table 12 Parameters for intermediate storage of CO_2. Base case values in bold.

Parameter	Values
Case	Pressure vessel (tank)
Tank volume	350, **750**, 3000 m^3
Media and phase	Liquid CO_2
Release point	1 m above ground
Temperature and pressure	+5 °C and 40 barg (high pressure shipping) **-28 °C and 15 barg (medium pressure shipping)** -50 °C and 7 barg (low pressure shipping)
Type of release	**Catastrophic rupture**
Weather	**4/D**

The assumptions described in Section 5.1 also applies in this section, i.e. base case parameters used for the consequence modeling of pipeline rupture were used for tanks as well (see Table 6 and Table 12). Only catastrophic rupture is considered, corresponding to "worst case" with regards to the consequences. Tank leaks and other failure modes could be considered in a future work.

For catastrophic ruptures, both the toxicity as well as the overpressure hazard from "a boiling liquid expanding vapor explosion" (BLEVE) event have impacts to the local population. Toxicity is described in the following section, and BLEVE in Section 5.2.2

5.2.1 Toxicity curves for rupture of CO_2 tanks

5.2.1.1 Base case, 750 m^3 tank

In the below graphs in Figure 42, the lethality contour plots for instantaneous tank rupture of liquid CO_2 are shown at the parameters from Table 12 at a height of 1 m above ground.

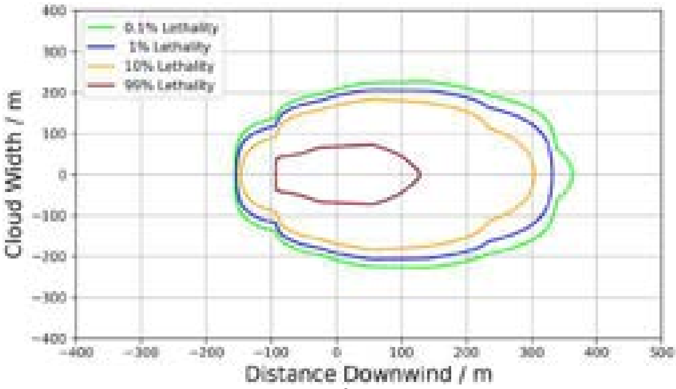

Figure 42 Tank rupture; 750 m^3, -28 °C / 15 barg. Lethality contour curves at observer height of 1 m.

5.2.1.2 Tank volume

In the below graphs in Figure 43, the lethality contour plots for instantaneous tank rupture of liquid CO_2 are shown at the base case parameters from Table 12 for storage at -28 °C / 15 barg, with variation of the tank volume. As expected, the consequence is much larger for a 3000 m^3 tank, containing more CO_2 and corresponding to a worst-case scenario with simultaneous rupture of several, interconnected tanks.

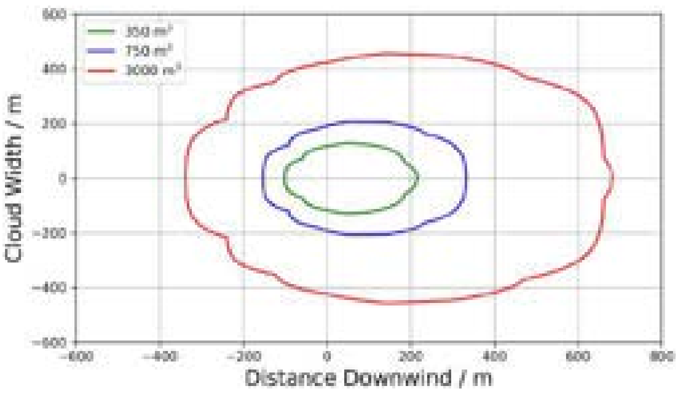

Figure 43 1% lethality curve for a tank rupture of 350 / 750 / 3000 m^3, respectively, and -28 °C / 15 barg. The lethality curve is observed at 1 m height.

5.2.1.3 Tank pressure and temperature

CO_2 shipping can be roughly divided into low, medium, and high pressure, as seen in Section 2.4 and Table 3. There are pros and cons transporting low- or high-pressure CO_2. For example, the cooling requirement can be limited or even avoided using high pressure CO_2 tanks (e.g., 40 barg, +5 °C). On the other hand, low pressure transport can lower the pressure limit requirements on the pressure vessel, reducing material costs – however, that means lowering the temperature (e.g., 7 barg and -50 °C). Figure 44 shows 1% lethality curves for different tank pressures of liquid CO_2, and corresponding equilibrium temperatures, for a tank volume of 750 m^3. The lethality curve is largest for low pressure conditions. Part of the difference in the lethality curves can be explained by the difference in mass released. A 750 m^3 tank contains 866 ton CO_2 at 7 barg / -50 °C compared to 672 ton at 40 barg / +5 °C. Another reason is the evaporation of cryogenic CO_2 as the colder the CO_2 the longer it stays near ground. The lower temperature cryogenic CO_2 causes local freezing of the ground, which then delays the conductive heat transfer to the pooling liquid. The delay of the heat input results in a significant decrease in pool boiling (evaporation) and thus a lower vapor generation compared with the higher-pressure CO_2 liquid release.

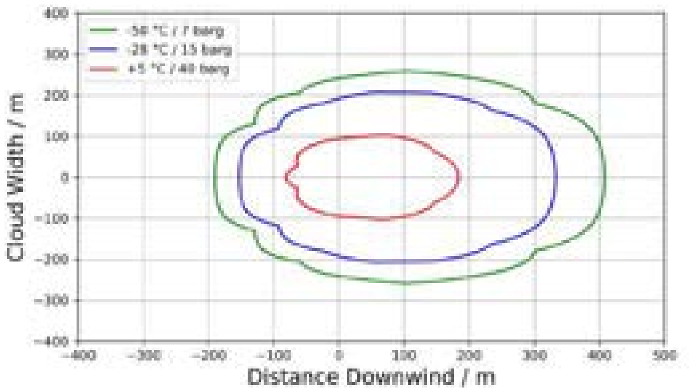

Figure 44 Tank rupture; 750 m^3 at 1% lethality at: -50 °C / 7 barg (green curve); -28 °C / 15 barg (blue curve); and +5 °C / 40 barg (red curve). Observed at 1 m height.

5.2.1.4 Rupture of CO_2 truck tank

Much smaller CO_2 volumes per tank will be transported by road (i.e. trucks) compared to shipping. Usual road tankers for LPG have capacities around 50 m^3. Figure 45 shows lethality curves for rupture of a tank with 50 m^3 of liquid CO_2 (-28 °C, 15 barg). The affected area is much smaller compared to large shipping tank ruptures (see Figure 45) and presents a significantly lower hazard compared to large containers for shipping and intermediate storage (harbor).

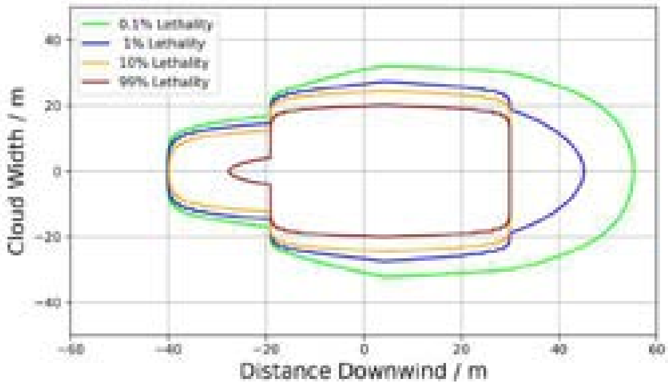

Figure 45 Tank rupture; 50 m³, -28 °C / 15 barg. Lethality contour curves at observer height of 1 m.

5.2.2 BLEVE for rupture of CO_2 tanks

A potential hazard for CO_2 pressure vessels is, in case the vessel is sealed off and heated, leading to an increase in pressure and the eventual failure of the tank due to overpressure. In such a case, a boiling liquid expanding vapor explosion (BLEVE) can occur, presenting a separate hazard. Probability of death from lung damage (hemorrhage) as a function of peak overpressure from the BLEVE shockwave has been determined by TNO from Probit-functions, with 50% lethality at 1.4 bar overpressure [64]. Figure 46 shows the full range of lethality levels due to lung hemorrhage caused by the shockwave.

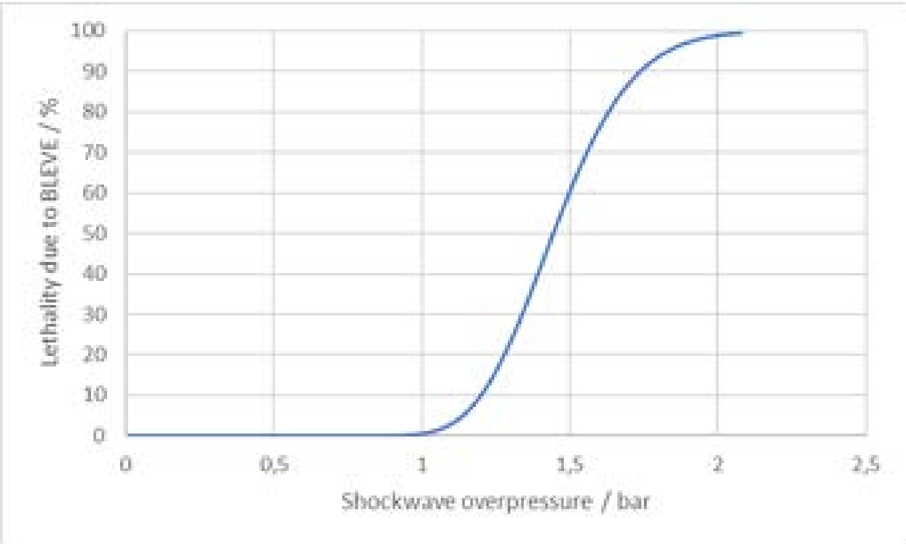

Figure 46 Lethality due to lung damage (hemorrhage) from a BLEVE event as function of shockwave overpressure.

The shockwave overpressures corresponding to 0.1, 1, 10, and 99% BLEVE lethality due to lung hemorrhage are 0.92, 1.03, 1.20, and 2.02 bar, respectively.

The parameters for the BLEVE consequence modeling are similar to the toxicity modeling of tank ruptures in Table 12, with a spherical tank geometry. The weather condition has no effect on BLEVE overpressure levels.

5.2.2.1 Base case, 750 m³ tank

Figure 47 shows overpressure levels from a BLEVE event of a 750 m³ CO_2 pressure vessel. The region inside the red circle (2.02 bar) represents the 99% fatal area, whereas the area outside the lime-green circle is safe, i.e., below 0.1% lethality. The overpressure levels are regular circles since the BLEVE event is modeled as a point source at the origin, which is different from a real event. A real event would involve the random and chaotic spreading of the cryogenic liquid over the area defined by the initial pressure wave. Clearly, this represents a limitation of the modeling software. The intermediate region will present a dangerous, but not necessarily fatal zone with gradually smaller overpressure levels moving outwards from the explosion. The region with 1% lethality level due to lung hemorrhage from the BLEVE event is 50 m (radius). This is much smaller than the 1% lethality curve from the toxicity of CO_2 itself (see Figure 47), which is between 300 m and 450 m depending on the direction.

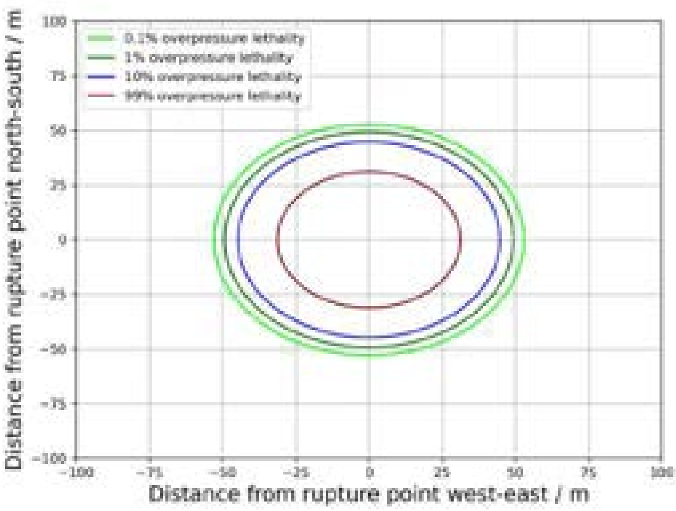

Figure 47 BLEVE overpressure levels from the explosion of a 750 m³ CO_2 tank (-28 °C / 15 barg) corresponding to 0.1, 1, 10, and 99% lethality due to lung hemorrhage.

5.2.2.2 BLEVE for different tank volumes

Figure 48 shows overpressure levels of 1.03 bar from BLEVE events of tanks with volumes 350, 750, and 3000 m³, corresponding to 1% lethality due to shockwave overpressure. Naturally, a larger tank results in a larger explosion and a larger affected area. For instance, a BLEVE of a 3000 m^3 CO_2 inventory, corresponding to rupture of multiple tanks simultaneously, leads to 1.03 bar overpressure (1% lethality) at ca. 80 m from the explosion compared to 50 m for a 750 m^3 tank (single tank) and below 40 m for a smaller 350 m^3 single tank. Regardless of volume, the 1% lethality levels are very small compared to those from the toxicity of CO_2 for equivalent volumes, see Figure 43.

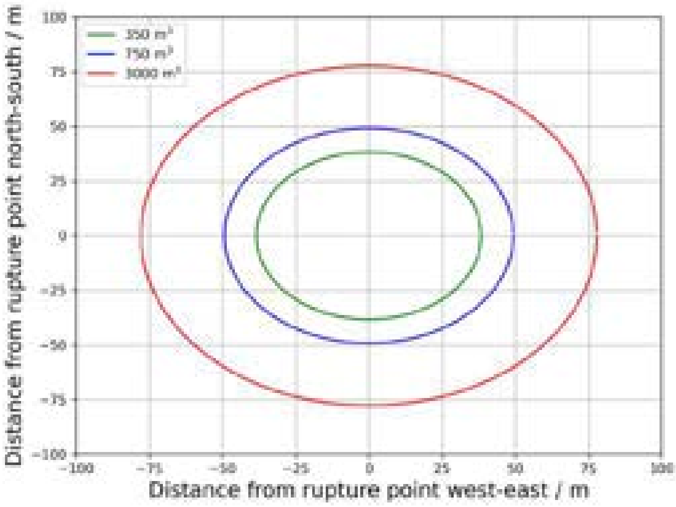

Figure 48 BLEVE overpressure level of 1.03 barg (corresponding to 1% lethality due to lung hemorrhage) from the explosion of CO_2 tanks with different volumes: 350, 750, and 3000 m^3, all at 15 barg / -28 °C.

5.2.2.3 BLEVE at varying tank pressure and temperature

Figure 49 shows overpressure levels of 1.03 bar from BLEVE events of 750 m^3 tanks with high-, medium-, and low-pressure CO_2 corresponding to conditions 40 barg / 5 °C, 15 barg / -28 °C, and 7 barg / -50 °C. It is seen that the BLEVE is most severe the higher the pressure. This is opposite the trend for the lethality due to the toxicity of CO_2. However, even for the high-pressure vessel, the 1% lethality contour due to toxicity, as see in Figure 44, is much larger compared to that from BLEVE overpressure.

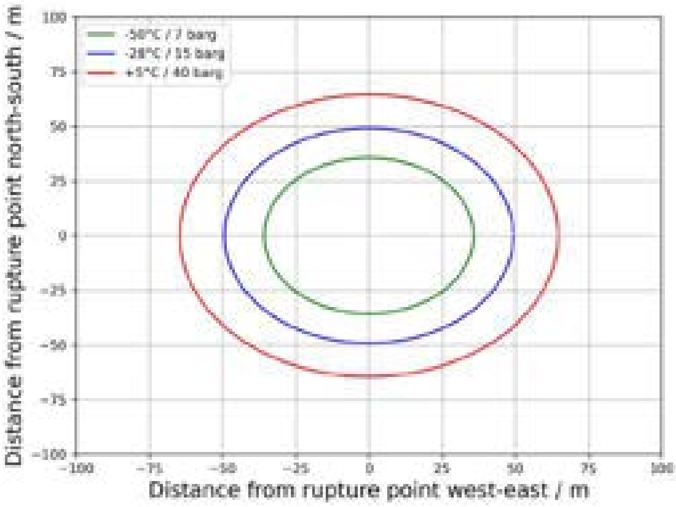

Figure 49 BLEVE overpressure level of 1.03 barg (corresponding to 1% lethality) from the explosion of 750 m^3 CO_2 tanks with different storage conditions: high pressure (40 barg / 5 °C), medium pressure (15 barg / - 28 °C), and low pressure (7 barg / -50 °C).

5.2.2.4 BLEVE for truck transport (50 m^3)

In addition to shipping of CO_2, trucks could be used for onshore transport of small volumes of CO_2. Figure 50 shows overpressure levels from a BLEVE event of a 50 m^3 CO_2 pressure vessel. The consequence of a BLEVE event is significantly smaller compared to large tanks used for shipping (750 m^3, Figure 47) and compared to the lethality due to the toxicity of CO_2 from rupture of an equivalent tank volume (Figure 45).

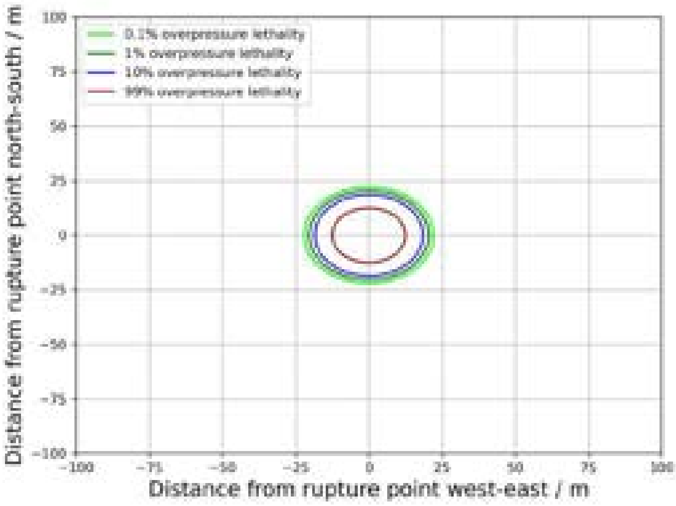

Figure 50 BLEVE overpressure levels from the explosion of a 50 m^3 CO_2 tank (-15 barg / -28 °C) corresponding to 0.1, 1, 10, and 99% lethality due to lung damage.

When comparing the impacts associated with the overpressure front and the toxicity of the CO_2 release, the BLEVE scenario will have a higher impact to persons in the immediate area of the event. However, the impact due to overpressure decreases exponentially with distance from the event. Therefore, a BLEVE type scenario is expected to have a limited impact on a community located at a reasonable distance from the event itself. At this distance, the toxicity of the release presents a higher impact to the community. Thus, only the toxicity is considered for the full risk assessment of tank ruptures in Section 6.

6 Risk assessment

6.1 Model considerations

A general expression of risk is:

$$\text{Risk} = \text{Frequency} \cdot \text{Consequence}$$

Where consequence is the probability of lethality of an event and frequency is the annual probability of the specific event.

The failure frequency term was elaborated in Section 4 with the recommendations in Section 4.4. The consequence term was elaborated in Section 5. The next task is to combine this together with weather statistics for a full risk assessment. The consequence modeling used one weather conditions for each run. In the risk assessment the weather statistics is added to consider the likelihood of the weather conditions at a given location. Details on the weather statistics is given in Appendix B.2 describing the use of the weather database from Danish Meteorological Institute (DMI) Open Data Source.

A simulation software, DNV Safeti, was used to give a general estimation of the risk associated with a CO_2 release for a two dimension analysis (2D). No effect of obstacles is considered.

The risk modeling gives contour curves around an event as an individual risk per year. The contour curves show the strip of land around the pipeline for a given individual risk per year. If the individual risk per year is acceptable, the area within this contour curve will be the width of the safe zone of the pipeline.

More details on the model setup are available in Appendix B.

Summary of cases is presented in Appendix C.

6.1.1 Base case

The defined base case for the pipeline risk assessment is based on the consequence modeling conducted in the previous section, specifically the pipeline specification provided in Table 6. The risk can be found by multiplying with the failure frequencies obtained from EGIG and provided in Section 4 (Figure 17). The risk for a full-bore rupture for onshore steel pipelines between 11 and 17 inches is 0.013/1000km·yr. Hence, this frequency is used for modeling the risk for the present pipeline dimensions

(16 inch). The frequency is normalized to the length of the pipeline segment, i.e., the distance between two isolation valves (20 km in the base case).

Notably, the weather is updated for the risk assessment. In contrast to the consequence modeling, which is conducted for one weather condition at a time and with the wind direction fixed (always from West), weather data described in Appendix B.2 is used for the risk assessment. Base case input parameters are provided in Table 13.

The failure rate of the isolation valve was assumed zero (no failure). It is for future works to include a failure frequency for the isolation valve.

Table 13 Definition of base case parameters for risk assessment of CO_2 pipeline ruptures

Parameter	Values
Consequence parameters	Similar to consequence modeling, see Table 6
Failure frequency pipeline	EGIG (11th report) and IOGP recommended, 0.013/1000km·yr for a 16-inch pipe Input risk parameter for pipeline with isolation valves every 20 km (base case): 2.6×10^{-4}/year
Weather data	From DMI open data – Copenhagen Airport 1 Jan. 2022 to 31. December 2023. Assuming Pasquil stability class D for all wind speeds [Ref 49]
Failure frequency isolation valve	0 (assumed not to fail)

Figure 51 shows risk contour curves expressed as individual risk per year for a base case gas and dense phase pipeline rupture (see Table 6). An individual risk below 10^{-6}/year corresponds to anywhere outside of the blue contour. If this individual risk is considered acceptable, a Right-of-Way of ca. 60 m for the gas phase and ca. 85 m for the dense phase pipeline would be sufficient to achieve broadly acceptable risk levels for this case.

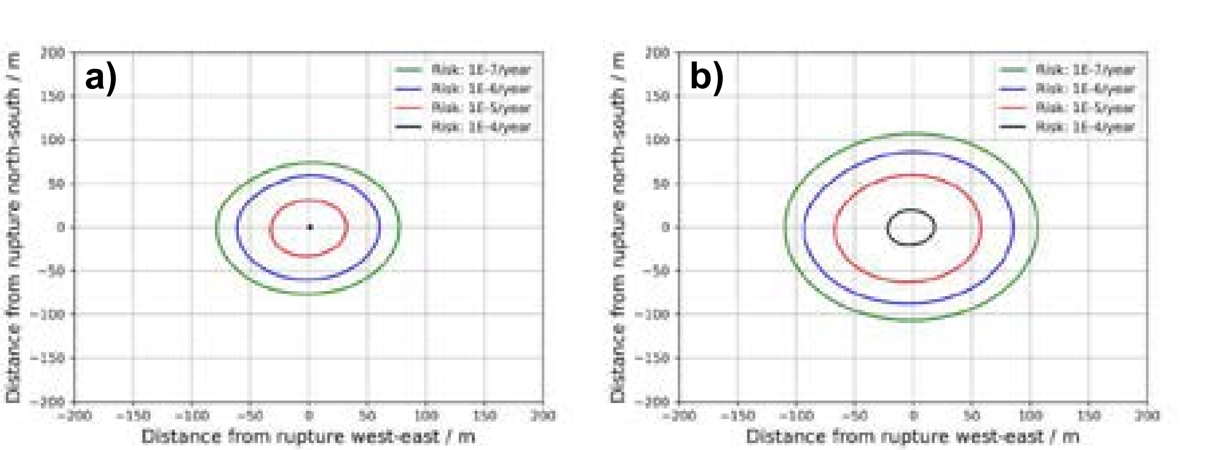

Figure 51 Individual risk per year (contour curves) for various distances from the rupture location for base case scenarios as defined in Table 13. a) 30 bar (gaseous) buried pipeline rupture, b) 120 bar (dense phase) buried pipeline rupture.

6.1.2 Weather conditions

Figure 52 shows risk contour curves for individual risk levels 1E-6/year, comparing 2 years of weather data (2022+2023) for two different locations in Denmark: Copenhagen Airport and Aalborg Airport, respectively. The results show small differences between the two locations. The individual risk is slightly higher in Aalborg compared to Copenhagen, most noticeable for the gas pipeline rupture. The difference is small considering the approximations in the modeling. Nevertheless, the results highlight the importance of using weather data representative for the location of interest when doing risk assessments on CO_2 pipelines.

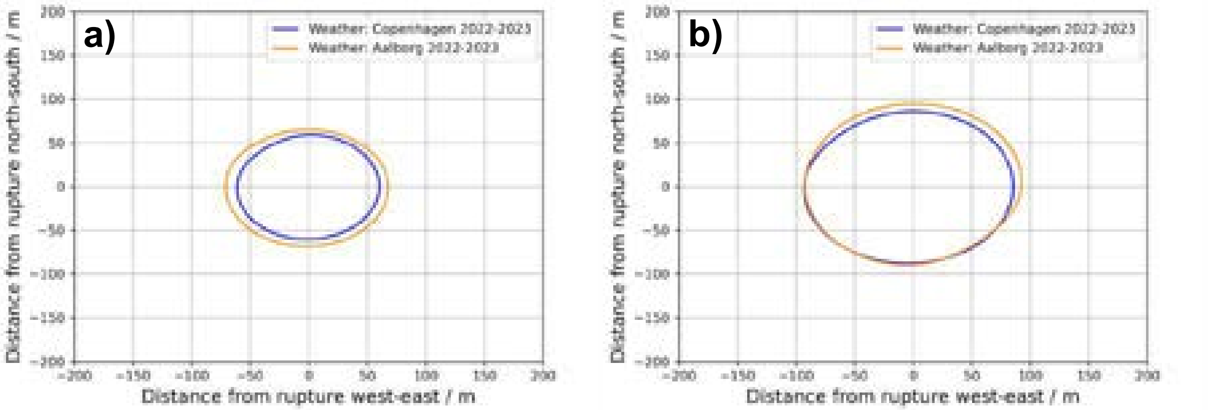

Figure 52 Risk contour curves at level 1E-6/year using weather data from either Copenhagen or Aalborg airport. a) 30 bar (gaseous) buried pipeline rupture, b) 120 bar (dense phase) buried pipeline rupture.

In addition to the location of the weather station, the chosen time interval for the weather data will influence the results of the risk assessment. Figure 53 shows risk contour curves for individual risk levels 1E-6/year, comparing 2 and 5 years of weather data for Copenhagen. The results show negligible differences between the two time periods, suggesting that 2 years of weather data is representative and appropriate for the risk assessment for this case.

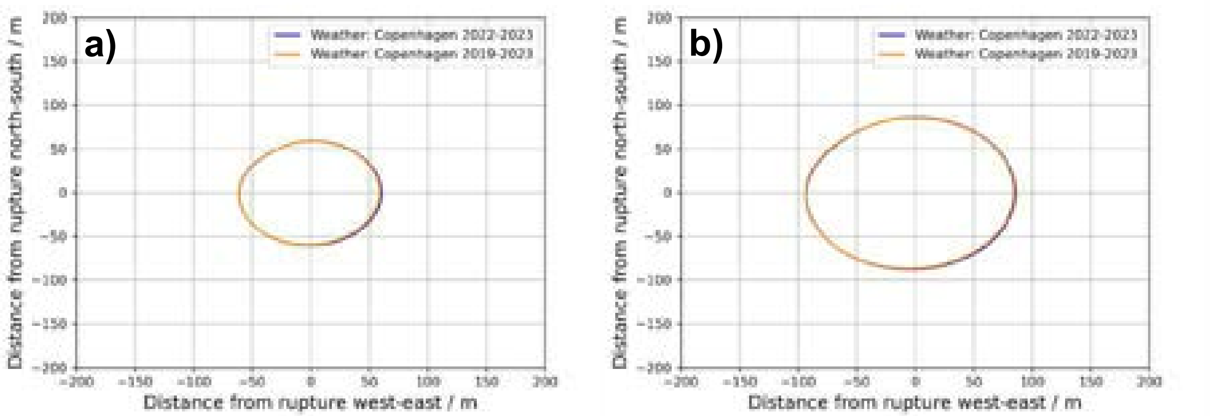

Figure 53 Risk contour curves at level 1E-6/year using weather data from Copenhagen from 2022-2023 or 2019-2023. a) 30 bar (gaseous) buried pipeline rupture, b) 120 bar (dense phase) buried pipeline rupture.

6.1.3 Effect of isolation valve spacing and closure time

When changing the valve spacing, the failure frequency also changes since this is given per kilometer per year as seen in Table 13. Failure frequencies for the studied isolation valve spacing are provided in Table 14.

Table 14 Failure frequency for pipeline with isolation valve spacing of 10, 20 and 30 km.

Distance between valve spacing	Failure frequency used in risk assessment
10 km	$1.3x10^{-4}$/year
20 km	$2.6x10^{-4}$/year
30 km	$3.9x10^{-4}$/year

Figure 54 shows risk contour curves (1E-6/year) for different isolation valve spacing for gas (a) and dense (b) CO_2 buried pipeline ruptures. For a given pipeline, a higher frequency of isolation valves leads to a decrease in 1E-6/year risk contours as expected but would increase the number of isolation valves and hence the cost of the pipeline.

Figure 55 shows 1E-6/year risk contour curves for different isolation valve closing time for gas (a) and dense (b) CO_2 buried pipeline ruptures, using a fixed valve spacing of 20 km between valves. The closing time of the isolation valves has a small effect on the risk. No effect is observed for the dense phase pipeline rupture, in agreement with the consequence modeling (Section 5.1.5).

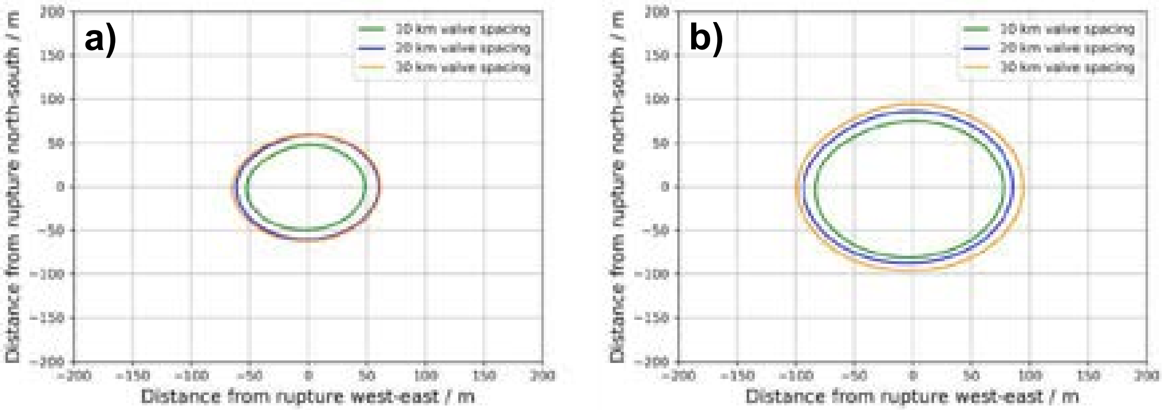

Figure 54 Risk contour curves at level 1E-6/year for different isolation valve spacing, using weather data from Copenhagen from 2022-2023. a) 30 bar (gaseous) buried pipeline rupture, b) 120 bar (dense phase) buried pipeline rupture.

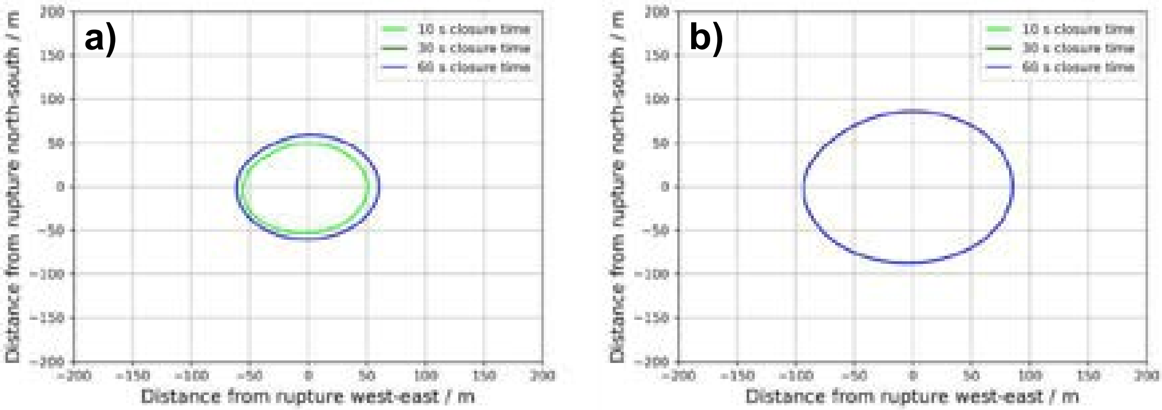

Figure 55 Risk contour curves at level 1E-6/year for different isolation valve spacing, using weather data from Copenhagen from 2022-2023. a) 30 bar (gaseous) buried pipeline rupture, b) 120 bar (dense phase) buried pipeline rupture.

6.2 Tank rupture

As it is assumed that the cryogenic storage tank is designed in accordance with Inherently Safer Principles [65], there will be a minimum of three layers of protection that must fail in order to create the operating condition required for a BLEVE event to occur. On a conservative basis, each layer has a probability of failure on demand of 10^{-2}, where the assumed demand rate is, at most, one demand per year. On this basis, the frequency for a BLEVE-type catastrophic rupture would be on average 10^{-6}/year. Therefore, the individual risk would reach this level for 100% lethality but will never be above it.
This value in a Danish context is considered broadly acceptable. Thus, the risk from a catastrophic tank rupture is acceptable in all cases. Future work could include risk assessment of various time-varying releases, including leaks, for an expanded QRA on pressure vessels.

7 Emergency management

7.1 Conventional approaches

The Emergency Response Services which is responsible for coordinating the response and minimizing the effects of an accident involving a pipeline system have historically derived their response plans from combination of the information contained in the national body guidebooks (see, for example, [52] and [66]) and the pipeline operator Emergency Response Plan (see, for example, [67]). However, the information contained in the documents are, generally, focused on describing the hazards and appropriate responses for natural gas, crude oil, and other hydrocarbon products due to the prevalence of such pipelines in the vicinity of communities for decades.

As a result of the length of time that hydrocarbon-containing pipelines have been operating near, or within, communities globally, there is a broad understanding by the communities of the balance between the “accident risk” and the “societal benefits” associated with this mode of energy transportation.

Although the transportation of CO_2 via a pipeline has been done for the past 20+ years, the small pipeline network relative to the natural gas and crude oil networks has resulted in a very limited number of readily available publications describing the guiding principles for responding to a large CO_2 release. In traditional sources of emergency response information (see, for example, [52]) could lead to a delayed, or insufficient response to an emergency (see, for example, [47]). Thus, it is necessary for the CO_2 pipeline operators and the local community Emergency Response Team leaders to engage with each other early in the pipeline design process for the purpose of clarifying the following points:

a) What type of event at the pipeline or associated process facility would require the involvement of the local Emergency Response Teams (ERTs)?
b) Upon notification of the event, should the ERTs refer to the minimum guidelines provided by the government safety agency?
c) Under what conditions would the minimum guidelines no longer apply and what should be the response?

As an example, the guidance provided in [52] for a CO_2 release (gas or cryogenic liquid) is to evacuate an area of at least 100 meters radius from the event location. Unfortunately, as illustrated in multiple plots throughout this report, and experienced by the community of Satartia [47], the “100m radius” guideline is likely to be inadequate.

Recognizing the gaps in the publicly available emergency response guidelines, industry groups have produced detailed emergency response planning guidelines specific to large-scale CO_2 systems. As an example, recently published guideline [68] included information critical to ensuring the effectiveness of ERTs that respond to a major event such as the rupture of a CO_2 pipeline.

7.2 Impacts of CO_2

Included in the guidance detailed in [68] are recommendations for leak detection, dispersion modeling, notification protocols and response actions. However, one of the key gaps in a document such as [68] is the “time” aspect of the event. There is a clear reason for this gap, as the time-based impacts associated with an event are specific to the event location, weather conditions, etc.

As an example, Figure 56 illustrates (base case simulation from Table 6) the progression of the CO_2-rich vapor cloud from the initial release to the time when the cloud is largely dispersed and no longer considered a hazard, where the difference between Figure 56 (a) and Figure 56 (b) is only the wind speed.

The primary conclusion from Figure 55(a) is that any person standing at a 100m distance from the release point would experience a CO_2 concentration in excess of 4% in the air within approximately 20s of the event occurrence (base case, full rupture), and that the hazardous CO_2 level at the 100m distance would persist for approximately 300s. But, in this time interval, the CO_2 concentration in the air would vary from the 4% and up to a maximum of 13.5% within 70s of the event start and then decrease again. This example thus highlights that a – necessarily – generalized guideline of a “100m safe distance” described in [52] should only be the first step in deriving a robust Emergency Response Plan with local ERTs for large-scale CO_2 transport systems.
To further reinforce the significant sensitivities associated with building an effective Emergency Response Plan; if there is a stronger wind as illustrated in Figure 55(b), a person standing at a 100m distance from the release point would not be adversely affected by CO_2 toxicity, as the wind prevents the CO_2 from reaching ground level throughout the simulated event time.

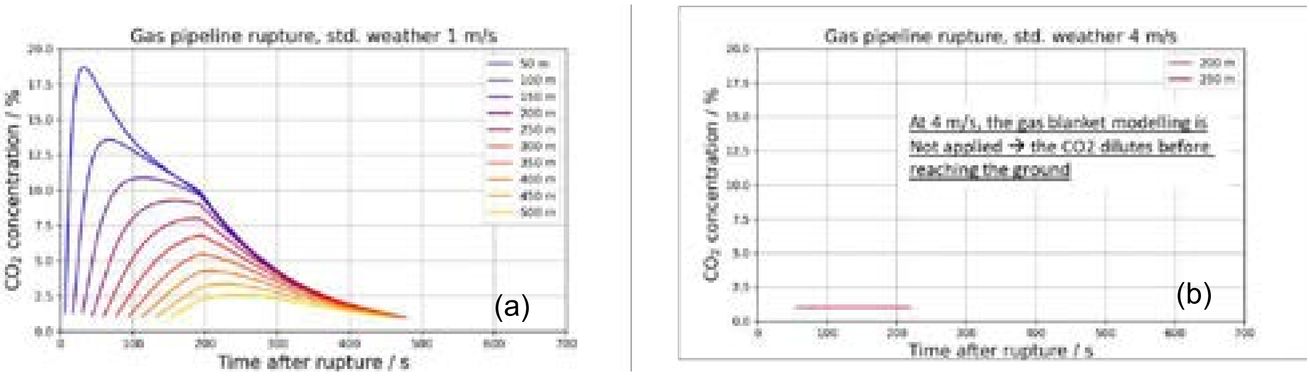

Figure 56 Plot of the progression of the CO_2 cloud at various distances from the release point. (a) Wind speed = 1 m/s and (b) Wind speed = 4 m/s

In addition, if the release event occurs at a point along a pipeline transporting dense phase (or supercritical) CO_2 fluid, the progression of the released cloud is likely to follow a concentration path as illustrated in Figure 56. The concentration contours illustrated in Figure 57 highlight that there is a short time window post-release where the CO_2 falls to concentrations less than 4%. However, within 50-60s the cold gas falls to ground level and remains until it warms sufficiently to disperse to low concentrations.

Thus, Figure 57 illustrates three key characteristics of a release from a dense phase pipeline system:

1. The released gas can persist at ground level for >10 minutes even with a wind speed of 4 m/s.
2. The ground level CO_2 concentration is such that persons within the described distances will be negatively affected.
3. The response time of the local ERTs will be impaired if specific safety equipment is not deployed prior to the response.
4. Although not modeled, there is an expectation that dry ice would collect in the vicinity of the rupture point and thus delay the emergency crews in creating a safe area due to the subliming dry ice to gaseous CO_2.

Points (1) and (2) above have been described at length previously. Point (3) is primarily related to the ability of the ERTs to mobilize and maintain a presence within the emergency area. Previous studies have highlighted that when high concentrations of inert gases are drawn into an internal combustion engine – either diesel or gasoline – with the air, the engine performance degrades quickly and eventually stalls [69], [70], [71]. Thus, even though the ERTs responding to the emergency event will have Self-Contained Breathing Apparatus (SCBA) available to eliminate the acute toxic effects of the CO_2 in the air, the ERTs may be unable to respond due the failure of the ERT vehicles.

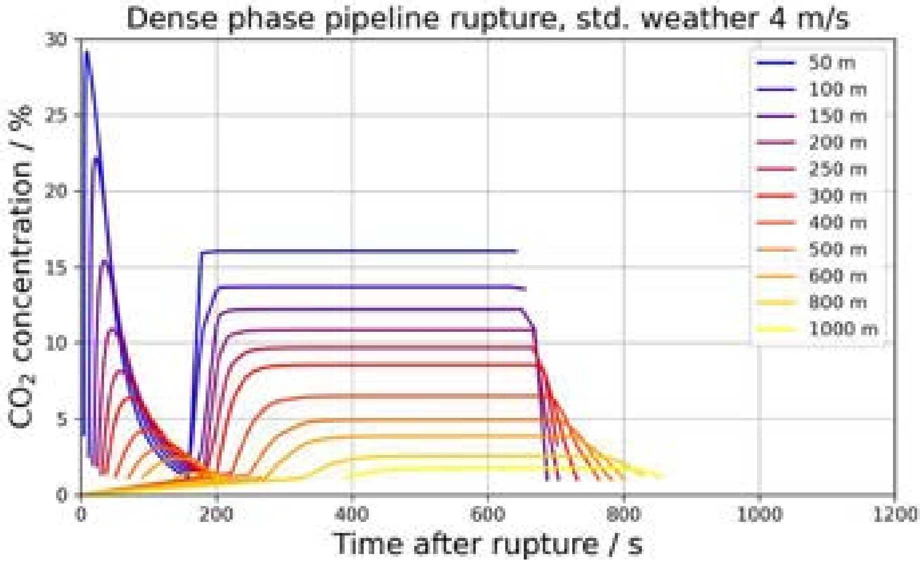

Figure 57 Plot of the progression of the CO_2 cloud at various distances from the release point of dense CO_2 for a wind speed of 4 m/s.

7.3 Recommendations

The recommendations relevant to Emergency Response Plan development are summarized by the following:

1. Initiate the development of the company-specific Emergency Response Plan using the most recent versions of the guiding documents produced by industry groups and government agencies.
2. Engage with the local community ERTs early in the design phase for the pipeline and/or storage facility to ensure a transparent understanding of the event types and the time-based evolution of the hazards with each event.
3. Ensure that the time-based "event response" plots are based on credible and easily referenced and understandable scenarios which the ERTs can use for internal training and community outreach engagements.
4. Highlight early in the engagement with local community ERTs under which scenarios, if any, alternative safety equipment will be required – e.g. electric emergency vehicles, large-capacity SCBA units, etc.
5. Internalize the learnings from historically relevant events to ensure that critical parameter sensitivities inherent with a CO_2 release event are robustly challenged and referenced within the joint company / community Emergency Response Plan.

8 Conclusions and future work

Transporting CO_2 – as like any other gas or liquid – induces a risk to human health and environment in case of a leakage. Transporting CO_2 by pipeline or truck is not a new task since it has been practiced for decades, especially for pipeline transport in the U.S. However, the scale of CCUS is foreseen to become a new, large industry in Europe and the mitigation measures to avoid a leakage of CO_2 is key to the success of the CCUS value chain and towards the goal of Net Zero emissions.

Risk is the combination of the probability of an incident to happen and the consequence of the event. Both topics as well as considerations for an emergency response plan in case of an incident was investigated in this report.

Based on a comparison between the U.S. CO_2 pipeline and the European natural gas transmission pipeline the overall failure frequency on pipelines, excluding equipment failure, was given as incident per kilometer per year. It was found that the overall failure frequency was within the same order of magnitude for the two fluids. Given the limited dataset on CO_2 incident statistics, the data set for natural gas transmission pipeline was applied by account for the fact that the failure frequency will decrease with increasing pipeline diameter.

For the cases considered, the CO_2 can reach as far away as 1000 m from the release point. The CO_2 can travel this distance due to the auto refrigeration effects during the release of the high-pressure CO_2 to atmospheric pressure. The simulation results have shown that wind has a significant impact on the ground effect or persistence of the CO_2 as it disperses from the release point. Therefore, the time factor for a CO_2 release should be included in the development of an emergency response plan.

A consequence model should account for critical parameters such as burial depth and soil type to avoid results that could be misunderstood or unrealistic for the simulated event.

Simulation results for the selected cases highlight the sensitivity of weather conditions and valve station placement on the risk curves. The results indicate that the risk curves are more sensitive to weather conditions than valve spacing.

The acceptability of the calculated risk is country and company specific. Given the general nature of the report objectives an assessment of the cost-benefit associated with safety risk has been deferred. It is recommended that a path to achieving acceptable risk should include the learnings from historically relevant events to ensure that critical parameter sensitivities inherent with a CO_2 release event are robustly challenged and referenced within the design process and the joint company / community Emergency Response Plan. In addition, it is also clear that existing public available guidance for emergency response purposes should be reviewed in parallel with consequence modeling to ensure the effective response to any release event.

Based on others research it is evident that the impurities in the CO_2 stream can have an effect on the material integrity of the pipeline. It remains for future work to include impurities in the consequence modeling.
This report included only CO_2 release from a rupture. For future work it will be of value to include release from a leakage of a pipeline or a tank.

.

9 References

[1] ‘SI 24 / 17 - Carbon Dioxide Physiological Hazards -“Not just an asphyxiant!”’ EUROPEAN INDUSTRIAL GASES ASSOCIATION AISBL. Accessed: Feb. 17, 2022. [Online]. Available: https://www.eiga.eu/publications/?_sf_s=Carbon%20Dioxide%20Physiological%20Hazards%20%E2%80%9CNot%20just%20an%20asphyxiant!%E2%80%9D

[2] ‘General hazards of Carbon Dioxide’. Accessed: Dec. 19, 2021. [Online]. Available: https://www.hse.gov.uk/carboncapture/carbondioxide.htm

[3] ‘Methods of approximation and determination of human vulnerability for offshore major accident hazard assessment’. Accessed: Dec. 19, 2021. [Online]. Available: https://www.hse.gov.uk/foi/internalops/hid_circs/technical_osd/spc_tech_osd_30/spctecosd30.pdf

[4] ‘Assessment of the Dangerous Toxic Load (DTL) for Specified L...’ Accessed: Dec. 19, 2021. [Online]. Available: https://www.hse.gov.uk/chemicals/haztox.htm

[5] DNV-GL, *Design and operation of carbon dioxide pipelines*, 2021st ed. in DNVGL-RP-F104.

[6] dr. P.A.M. Uijt de Haag, dr. B.J.M. Ale, ‘Guidelines for quantitative risk assessment’.

[7] ‘PHMSA Failure Investigation Report - Denbury Gulf Coast Pipelines, LLC | PHMSA’. Accessed: Jan. 02, 2023. [Online]. Available: https://www.phmsa.dot.gov/news/phmsa-failure-investigation-report-denbury-gulf-coast-pipelines-llc

[8] ‘PHMSA Announces New Safety Measures to Protect Americans From Carbon Dioxide Pipeline Failures After Satartia, MS Leak | PHMSA’. Accessed: Jan. 02, 2023. [Online]. Available: https://www.phmsa.dot.gov/news/phmsa-announces-new-safety-measures-protect-americans-carbon-dioxide-pipeline-failures

[9] ‘OCAP levert zuivere CO2 aan glastuinbouwers via een pijpleiding’, The Linde Group. Accessed: Aug. 15, 2022. [Online]. Available: https://www.ocap.nl/nl/index.html

[10] ‘Casus: Lekkage van een OCAP CO2-leiding’, BrandweerNederland.nl. Accessed: Aug. 15, 2022. [Online]. Available: https://www.brandweernederland.nl/casus-lekkage-van-een-ocap-co2-leiding/

[11] Energy Institute (Great Britain), Ed., *Technical guidance on hazard analysis for onshore carbon capture installations and onshore pipelines: a guidance document*, 1st ed. London : Energy Institute, 2010.

[12] F. Hedlund, ‘The extreme carbon dioxide outburst at the Menzengraben potash mine 7 July 1953’, 2012, doi: 10.1016/J.SSCI.2011.10.004.

[13] G. Kling *et al.*, ‘The 1986 Lake Nyos Gas Disaster in Cameroon, West Africa’, *Science*, vol. 236, pp. 169–75, May 1987, doi: 10.1126/science.236.4798.169.

[14] P. Paul Shiladitya |. Shepherd, Richard |. Woollin, ‘Selection of materials for high pressure CO2 transport’. Accessed: Sep. 04, 2023. [Online]. Available: https://www.twi-global.com/technical-knowledge/published-papers/selection-of-materials-for-high-pressure-co2-transport.aspx

[15] K. Patchigolla and J. E. Oakey, ‘Design Overview of High Pressure Dense Phase CO2 Pipeline Transport in Flow Mode’, *Energy Procedia*, vol. 37, pp. 3123–3130, Jan. 2013, doi: 10.1016/j.egypro.2013.06.198.
[16] National Petrolum Council, ‘Meeting the Dual Challenge - a Roadmap to At-Scale Deployment of Carbon Capture, Use, and Storage.’, 2019. Accessed: Jan. 17, 2024. [Online]. Available: https://dualchallenge.npc.org/files/CCUS_V1-FINAL.pdf
[17] J. Barrie, K. Brown, P. Hatcher, and H. Schellhase, ‘Carbon dioxide pipelinesA preliminary review of design and risks’, in *Greenhouse Gas Control Technologies 7*, vol. I, Elsevier, 2005, pp. 315–320. doi: 10.1016/B978-008044704-9/50032-X.
[18] ‘Technology Data - Carbon capture, transport and storage’, Danish Energy Agency and Energinet, Nov. 2023.
[19] I. Phillips, ‘ZEP/CCSA Shipping Guidance Note’.
[20] ‘Maritime Transport of CO2’, Danish Technological Institute and Maersk Broker Advisory Services A/S, 2022. [Online]. Available: https://maerskbroker.com/wp-content/uploads/2022/11/Maritime-Transportation-of-CO2-ENG.pdf
[21] S. P. Peletiri, N. Rahmanian, and I. M. Mujtaba, ‘CO2 Pipeline Design: A Review’, *Energies*, vol. 11, no. 9, Art. no. 9, Sep. 2018, doi: 10.3390/en11092184.
[22] P. Paul Shiladitya |. Shepherd, Richard |. Bahrami, Amir |. Woollin, ‘Material selection for supercritical CO2 transport’. Accessed: Sep. 04, 2023. [Online]. Available: https://www.twi-global.com/technical-knowledge/published-papers/material-selection-for-supercritical-co2-transport.aspx
[23] R. Barker, Y. Hua, and A. Neville, ‘Internal corrosion of carbon steel pipelines for dense-phase CO_2 transport in carbon capture and storage (CCS) – a review’, *Int. Mater. Rev.*, vol. 62, no. 1, pp. 1–31, Jan. 2017, doi: 10.1080/09506608.2016.1176306.
[24] P. Myles and P. Shirley, ‘Quality Guidelines for Energy System Studies: CO2 Impurity Design Parameters (NETL-PUB-22529). National Energy Technology Laboratory’, netl.doe.gov. Accessed: Apr. 12, 2023. [Online]. Available: https://www.netl.doe.gov/projects/files/QGESSCO2ImpurityDesignParameters_Update_010119.pdf
[25] M. Bilio, S. Brown, M. Fairweather, and H. Mahgerefteh, ‘CO2 pipelines material and safety considerations’, no. 155, p. 7, 2009.
[26] S. Westman *et al.*, ‘Vapor-liquid equilibrium data for the carbon dioxide and nitrogen (CO2+N2) system at the temperatures 223, 270, 298 and 303 K and pressures up to 18 MPa’, *Fluid Phase Equilibria*, vol. 409, Sep. 2015, doi: 10.1016/j.fluid.2015.09.034.
[27] C. Huh, S.-G. Kang, M.-I. Cho, and J.-H. Baek, ‘Effect of water and nitrogen impurities on CO2 pipeline transport for geological storage’, *Energy Procedia*, vol. 4, pp. 2214–2221, 2011, doi: 10.1016/j.egypro.2011.02.109.
[28] B. Wetenhall, J. M. Race, and M. J. Downie, ‘The Effect of CO2 Purity on the Development of Pipeline Networks for Carbon Capture and Storage Schemes’, *Int. J. Greenh. Gas Control*, vol. 30, pp. 197–211, Nov. 2014, doi: 10.1016/j.ijggc.2014.09.016.
[29] S. W. Løvseth, ‘Equations of State for CCS: Can We Trust Them?’, #SINTEFblog. Accessed: Dec. 21, 2021. [Online]. Available: https://blog.sintef.com/sintefenergy/ccs/equations-of-state-ccs-can-we-trust-them/

[30] A. Brown, C. Eickhoff, J. E. A. Reinders, I. Raben, M. Spruijt, and F. Neele, ‘IMPACTS: Framework for Risk Assessment of CO2 Transport and Storage Infrastructure’, *Energy Procedia*, vol. 114, pp. 6501–6513, Jul. 2017, doi: 10.1016/j.egypro.2017.03.1786.

[31] B. H. Morland, ‘Corrosion in CO2 transport pipeline: Formation of corrosive phases in dense phase CO2’, 2020, Accessed: Jan. 12, 2022. [Online]. Available: https://www.duo.uio.no/handle/10852/72169

[32] R. Barker, Y. Hua, and A. Neville, ‘Internal corrosion of carbon steel pipelines for dense phase CO_2 transport in Carbon Capture and Storage (CCS) - A review’, *Int. Mater. Rev.*, vol. 62, Maj 2016, doi: 10.1080/09506608.2016.1176306.

[33] A. Jäger, V. Vinš, R. Span, and J. Hrubý, ‘Model for gas hydrates applied to CCS systems part III. Results and implementation in TREND 2.0’, *Fluid Phase Equilibria*, vol. 429, pp. 55–66, Dec. 2016, doi: 10.1016/j.fluid.2016.08.027.

[34] Z. Abbas, T. Mezher, and M. R. M. Abu-Zahra, ‘CO2 purification. Part I: Purification requirement review and the selection of impurities deep removal technologies’, *Int. J. Greenh. Gas Control*, vol. 16, pp. 324–334, Aug. 2013, doi: 10.1016/j.ijggc.2013.01.053.

[35] ‘Northern Lights’, Northern Lights. Accessed: Jan. 10, 2022. [Online]. Available: https://northernlightsccs.com/

[36] ‘CO2 reduction through storage beneath the North Sea’, Porthos. Accessed: Jan. 10, 2022. [Online]. Available: https://www.porthosco2.nl/en/

[37] ‘Carbon Dioxide (CO2) Operations | Kinder Morgan’. Accessed: Jan. 07, 2022. [Online]. Available: https://www.kindermorgan.com/Operations/CO2/Index#tabs-co2_supply

[38] M. Vitali, C. Zuliani, F. Corvaro, B. Marchetti, A. Terenzi, and F. Tallone, ‘Risks and Safety of CO2 Transport via Pipeline: A Review of Risk Analysis and Modeling Approaches for Accidental Releases’, *Energies*, vol. 14, no. 15, Art. no. 15, Jan. 2021, doi: 10.3390/en14154601.

[39] EIGA, ‘DOC 70/17 - Carbon Dioxide Food and Beverages Grade, Source Qualification, Quality Standards and Verification’. EUROPEAN INDUSTRIAL GASES ASSOCIATION AISBL, 2016.

[40] ‘Northern Lights Project Coencept report . RE-PM673-00001’. Equinor, 2019. Accessed: Jan. 10, 2022. [Online]. Available: https://ccsnorway.com/app/uploads/sites/6/2020/05/Northern-Lights-Project-Concept-report.pdf

[41] ‘Porthos CO2 specification’. Porthos CO2 Transport and Storage, Sep. 30, 2021. Accessed: Jan. 07, 2021. [Online]. Available: https://www.porthosco2.nl/wp-content/uploads/2021/09/CO2-specifications.pdf

[42] J. Glass, ‘CO2 Pipelines - New Technologies & Economics for Carbon Capture / Sequestration - Kinder Morgan CO2 Company’, Mar. 29, 2019. [Online]. Available: https://energyatkenanflagler.unc.edu/wp-content/uploads/2019/04/Glass-CO2-Pipelines.pdf

[43] ‘CO2: Preparing to build the network’. Accessed: May 08, 2023. [Online]. Available: https://www.fluxys.com/en/energy-transition/hydrogen-carbon-infrastructure/carbon_preparing-to-build-the-network

[44] TES and OGE, ‘Open Grid Europe: CO2-Spezifikation’. Accessed: May 11, 2023. [Online]. Available: https://co2-netz.de/en#co2grid

[45] ‘CO_2 specifications for Aramis transport infrastructure’, Aramis CCS. Accessed: May 08, 2023. [Online]. Available: https://www.aramis-ccs.com/news/co2-specifications-for-aramis-transport-infrastructure
[46] ‘Quality Guidelines for Energy System Studies: CO2 Impurity Design Parameters’, netl.doe.gov. Accessed: Jan. 11, 2022. [Online]. Available: https://www.netl.doe.gov/energy-analysis/details
[47] D. Zegart, ‘Gassing Satartia: How A CO2 Pipeline Explosion Affected This Mississippi Town’, HuffPost. Accessed: Jan. 06, 2022. [Online]. Available: https://www.huffpost.com/entry/gassing-satartia-mississippi-co2-pipeline_n_60ddea9fe4b0ddef8b0ddc8f
[48] ‘WP3.2 – Societal and environmental aspects of CO2 transport through pipelines: risk characterization and management’, *CO2Europipe Proj. No 226317*, 2011.
[49] ‘CO2RISKMAN’, DNV. Accessed: Mar. 23, 2023. [Online]. Available: https://www.dnv.com/Default
[50] D. Lisbona, A. McGillivray, J. L. Saw, S. Gant, M. Bilio, and M. Wardman, ‘Risk assessment methodology for high-pressure CO2 pipelines incorporating topography’, *Process Saf. Environ. Prot.*, vol. 92, no. 1, pp. 27–35, Jan. 2014, doi: 10.1016/j.psep.2013.09.003.
[51] M. Nyborg, K. Arvidsson, J. Johansson, S. Liljemark, and L. Olsson, ‘Risk analysis methodology for CO2 transport including quantified risk calculation’, *Energy Procedia*, vol. 4, pp. 2816–2823, 2011, doi: 10.1016/j.egypro.2011.02.186.
[52] Transport Canada / United States Department of Transport / Secretaría de Communicaciones y Transportes, *Emergency Response Guidebook*, vol. 2020.
[53] Asia Industrial Gases Association, ‘AIGA 040_06 Good practices guide for loading & unloading of cryogenic liquid tankers_reformat Jan 12.pdf’. [Online]. Available: https://www.asiaiga.org/uploaded_docs/AIGA%20040_06%20Good%20practices%20guide%20for%20loading%20&%20unloading%20of%20cryogenic%20liquid%20tankers_reformat%20Jan%2012.pdf
[54] ‘HD KSOE secures order for world’s largest liquefied CO2 carrier - KED Global’. Accessed: Mar. 15, 2024. [Online]. Available: https://www.kedglobal.com/shipping-shipbuilding/newsView/ked202307190011
[55] S. Peng, D. Zhou, and B. Xie, ‘Analysis of LNG Storage Tank Safety: A Comprehensive Model Approach with ANP and Normal Cloud’, *Appl. Sci.*, vol. 12, no. 23, Art. no. 23, Jan. 2022, doi: 10.3390/app122311941.
[56] ‘Annual Report Mileage for Natural Gas Transmission & Gathering Systems | PHMSA’. Accessed: Aug. 01, 2023. [Online]. Available: https://www.phmsa.dot.gov/data-and-statistics/pipeline/annual-report-mileage-natural-gas-transmission-gathering-systems
[57] BSI, *Pipeline systems - Steel pipelines on land. Guide to the application of pipeline risk assessment to proposed developments in the vicinity of major accident hazard pipelines containing flammables. Supplement to PD 8010-1:2004*. in PD 8010-3:2009+A1:2013. 2009.
[58] ‘11th Report of the European Gas Pipeline Incident Data Group’, EGIG. Accessed: May 13, 2023. [Online]. Available: https://www.egig.eu/reports
[59] ‘Risk assessment data directory - Storage incident frequencies’, IOGP Publications library. Accessed: Mar. 15, 2024. [Online]. Available:

https://www.iogp.org/bookstore/product/risk-assessment-data-directory-storage-incident-frequencies/
[60] NOAA Air Resources Laboratory, ‘Pasquill Stability Classes’. Accessed: May 15, 2023. [Online]. Available: https://www.ready.noaa.gov/READYpgclass.php
[61] ‘DNV and partners launch CETO joint industry project (JIP) to develop low pressure solutions for CO2 ship transport’, DNV. Accessed: Aug. 07, 2023. [Online]. Available: https://www.dnv.com/news/dnv-and-partners-launch-ceto-joint-industry-project-jip-to-develop-low-pressure-solutions-for-co2-ship-transport-214449
[62] ‘CO2 Shipping’, Goal7. Accessed: Jan. 05, 2024. [Online]. Available: https://www.goalsev.com/thought-leadership/co2-shipping
[63] Fortum Oslo Varme, ‘Quantitative Risk Assessment (QRA) for CCS plant’.
[64] TNO, ‘Methods for the determination of possible damage to people and objects resulting from releases of hazardous materials (Green Book)’, *Inst. Voor Milieu-En Energietechnologie TNO Prins Maurits Lab.*, 1992, Accessed: Mar. 21, 2023. [Online]. Available: https://repository.tno.nl/islandora/object/uuid%3Ab1a78c99-eaba-4e74-9d5e-981a6093fe2e
[65] P. R. Amyotte and F. I. Khan, ‘The role of inherently safer design in process safety’, *Can. J. Chem. Eng.*, vol. 99, no. 4, pp. 853–871, 2021, doi: 10.1002/cjce.23987.
[66] Pipeline Association for Public Awareness, ‘Pipeline Emergency Response Guidelines’, 2020.
[67] Marathon Pipe Line LLC, ‘Guidelines for pipeline emergencies’, 2020.
[68] American Petroleum Institute / Liquid Energy Pipeline Association / National Association of State Fire Marshals, ‘Carbon dioxide (CO2) emergency response tactical guidance document – best practice guidelines for preparedness and initial response to a pipeline release of carbon dioxide (CO2)’, Nov. 2023.
[69] V. Giurcan, D. Razus, M. Mitu, and V. Schröder, ‘Limiting Oxygen Concentration and Minimum Inert Concentration of Fuel-air-inert Gaseous Mixtures Evaluation by means of Adiabatic Flame Temperatures and Measured Fuel-air Lower Flammability Limits’, 2013. Accessed: Mar. 15, 2024. [Online]. Available: https://www.semanticscholar.org/paper/Limiting-Oxygen-Concentration-and-Minimum-Inert-of-Giurcan-Razus/bf6f3376a975d1864628b5081eb6354c2799ad2a
[70] Z. Zheng and M. Yao, ‘Mechanism of Oxygen Concentration Effects on Combustion Process and Emissions of Diesel Engine’, *Energy Fuels*, vol. 23, no. 12, pp. 5835–5845, Dec. 2009, doi: 10.1021/ef900676h.
[71] C. Çinar, T. Topgül, M. Ciniviz, and C. Haşimoğlu, ‘Effects of injection pressure and intake CO2 concentration on performance and emission parameters of an IDI turbocharged diesel engine’, *Appl. Therm. Eng.*, vol. 25, no. 11, pp. 1854–1862, Aug. 2005, doi: 10.1016/j.applthermaleng.2004.10.011.
[72] ‘Hazardous Liquid/CO2 Accident Report Instructions F 7000-1 | PHMSA’. Accessed: Apr. 12, 2023. [Online]. Available: https://www.phmsa.dot.gov/forms/hazardous-liquidco2-accident-report-instructions-f-7000-1
[73] M. Vitali, C. Zuliani, F. Corvaro, B. Marchetti, and F. Tallone, ‘Statistical analysis of incidents on onshore CO2 pipelines based on PHMSA database’, *J. Loss Prev. Process Ind.*, vol. 77, p. 104799, Jul. 2022, doi: 10.1016/j.jlp.2022.104799.

Appendix A Definition of failure cause

The list below is reproduced from PHMSAs definition of failure cause. The categories are given in the instructions for filling out accident reports. The apparent cause is selected from a list of main cause and sub-causes [72]. The list has also been given in [73]. There has been some adjustment to the categories over the years, and the main purpose of the list is to give an overview of the causes and sub-causes. The right column in the table shows if the sub-cause is included in EGIGs database and in which category. It's seen that the equipment failure is not part of EGIGs database.

PHMSA incident cause	**PHMSA sub-cause**	**Included in EGIG category (yes/no)**
Corrosion failure	External corrosion	Yes “Corrosion”
	Internal corrosion	Yes “Corrosion”
Natural force damage	Natural force damage	Yes “Ground movement”
	Earth movement (not due to heavy rains/floods)	Yes “Ground movement”
	Lightning	Yes “Other and unknown”
	Temperature including thermal stress and frozen components	No
	High winds	No
	Other natural force damage	Yes “Ground movement”
Excavation damage	Excavation damage	Yes “External interference”
	Excavation damage by operator (first party)	Yes “External interference”
	Excavation damage by third party	Yes “External interference”
	Previous damage due to excavation activity	No

Other outside force damage	Nearby industrial, man-made or other fire/explosion as primary cause of accident	No
	Damage by car, truck, or other motorized vehicle/equipment not engaged in excavation	No
	Damage by boats, barges, drilling rigs, or other maritime equipment or vessels set adrift, or which have otherwise lost their mooring	No
	Routine or normal fishing or other maritime activity not engaged in excavation	No
	Electrical arching from other equipment or facility	No
	Previous mechanical damage not related to excavation	No
	Intentional damage	No
	Other outside force damage	
Material failure of pipe or weld	Design-, construction-, installation-, or fabrication-related	Yes “Construction defect/material failure”
	Original manufacturing-related	Yes “Construction defect/material failure”
	Environmental cracking-related	Not known
Equipment failure	Malfunction of control/relief equipment	No
	Pump or pump-related equipment	No
	Failures of fittings or connectors	No
	ESD system failure	No
	Other equipment failure	No
Incorrect operation	Errors by facility personal	Yes “Other and unknown”
	Improper selection or installation of equipment	Yes “Other and unknown”
	Improper valve selection or operation	Yes “Other and unknown”
	Inadvertent over-pressurization	Yes “Other and unknown”
	Other incorrect operation	Yes “Other and unknown”
Other accident cause	Miscellaneous	Yes “Other and unknown”

	Unknown	Yes “Other and unknown”

Appendix B Risk assessment recipe

This section describes the method used to conduct the risk assessment in this report. The model requires data, and all models are based on assumptions and model considerations.
In this section the data included in the modeling is presented and categorized into either 1) critical assumption, 2) available information, 3) model construction or 4) simulation setup. By defining this, it should be possible to replicate the results for other researchers.

The quantitative risk assessment follows a data flow as outlined in the Figure 58 and described in the following subsections.

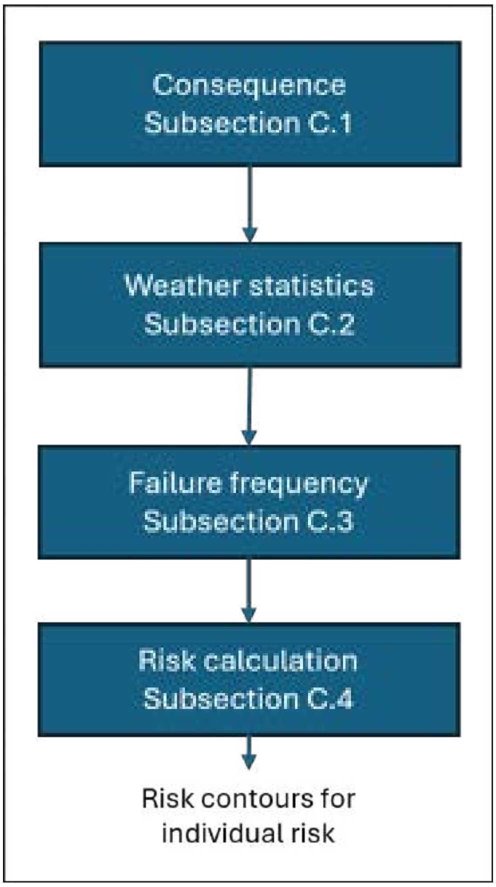

Figure 58 Data flow for quantitative risk assessment

B.1 Consequence analysis

1. Key assumption

- 100% pure CO_2
- No dry ice solid deposition effect
- Wind direction is always from west
- No cross winds. The release direction is always simulated along the pipeline, never perpendicular to it
- Flat topography considered
- One predominant soil type
- Ambient temperature of 9.85 ºC
- Relative humidity of 70%
- Atmospheric pressure X

2. Available information

- Line pipe dimensions in accordance with API5L documentation

3. Model construction

- Model build in accordance with recommendations contained in SA-01 Phast Training, ver. 3, 22-08-14
- Thermodynamic properties: DIPPR base for pure CO_2.

4. Simulation execution

- Execution time is 3600 seconds
- Valve closure time is calculated using time step plus the defined closure time
- All simulations completed on Lenovo ThinkPad T14
- Phast and Safeti version 9.0
- Output format: MS Excel-files with
    - Concentration profile at 4% CO_2
    - Toxicity profile 0.1%, 1%, 10%, and 99% lethality.

Table 15 List of parameters for consequence modeling

Parameter	Unit	Value	Parameter variation	Default value?	Comment	Assumption	Information avail.	Model constr.	Simulation setup
Case specific input parameters - pipeline									
Media		100% pure CO_2		no	assuming 100% purity	x			
Operating flow rate	kg/s	22	11; 84; 169; 253	no		x			
Temperature	°C	5		no		x			
Pressure	barg	30	120	no		x			
Pipe inner diameter	mm	363.5		no	API 5L 16 inch SCH 80		x		
Pipe roughness	mm	0.045		no	carbon steel		x		
Pipe length	km	65		no		x			
Release direction		Buried pipeline with vertical release	Above ground with angled release	no		x			
Release point				no	Halfway between isolation valves	x			
Leak size		Full bore rupture		no	weld-to-weld distance 12 m (i.e. fracture length assumed to be 12 m)	x			
Weather		4/D	8/D; 2/D; 1/D; 1/F; 1/G	no		x			
Distance between isolation valves	km	20	10; 30	no		x			
Response + valve closing time	s	60	10; 30	no		x			
Depth of cover	m	1.2	0.8; 0.5	no		x			
Soil type		Clay	Sand; Mixed	no		x			

Terrain roughness	m	1	0.005; 0.1; 3	no		x			
Release elevation	m	0		yes		x			
Breach sizing method		Actual size		yes		x			
Time averaging – duration of interest	s	3600		yes					x
Time averaging – method for calculating average rate		Average between 2 times		yes					x
First time value for rate between two times	s	0		yes					x
Second time value for rate between two times	s	20		yes					x
Type of terrain for dispersion		Land		yes		x			
Crater modeling – accident type for buried sections		Full bore rupture						x	
Probit function								x	
Case specific input parameters – Tank									
Media		CO_2		no		x			
Tank volume	m^3	750	350; 3000	no		x			
Release point above ground	m	1		no		x			
Temperature	°C	-28	-50; 5	no		x			
Pressure	barg	15	7; 40	no		x			
Type of release		Catastrophic rupture		no		x			
Weather		4/D		no		x			
Elevation for release	m	1		no		x			
Type of terrain for dispersion		Land		yes		x			
Type of pool substrate and bunds		Concrete, no bund		yes		x			
Max distance option		From minimum overpressure		yes		x			
Minimum distance	m	0		yes		x			
Number of distance points		100		yes				x	
BLEVE blast parameter – air or ground burst		Ground burst		yes				x	

BLEVE blast parameter – Ideal gas modeling		Model as real gas		yes				x	
Other parameters									
Discharge parameters				yes				x	
Dispersion parameters				yes				x	
Weather parameters								x	
Surface parameters				yes	Expect surface roughness length – see case specific input			x	
Pool vaporization parameters				yes				x	
Toxic parameters				yes				x	
Explosion parameters		0.92; 1.03; 1.2; 2.02		yes				x	
Fire ball and BLEVE blast parameters				yes				x	
General parameters				yes				x	
General risk parameters				yes				x	
Grid parameters				yes				x	

B.2 Weather statistics

Wind quantification is important for the dispersion calculations and an input parameter in the risk modeling.

1. Key assumption

Period for wind data: 2 years from 2022-01-01 to 2023-12-31.
Weather stability D: was assumed for all wind speeds.
Wind direction: the data consists of the latest 10 minutes' mean wind direction measured 10 m over terrain.
Wind speed: the data consists of the latest 10 minutes' mean wind speed measured 10 m over terrain.

2. Available information

The wind statistics were selected for Danmark and based on the weather database from Danish Meteorological Institute (DMI) Open Data Source.
Link to data base: https://opendatadocs.dmi.govcloud.dk/DMIOpenData
API: Meteorological Observations

Query parameters	Input
`limit`	300000
`stationID`	06180 = Copenhagen Airport 06030 = Aalborg Airport
`datetime`	1) 2 years: 2022-01-01 to 2023-12-31 2) 5 years: 2019-01-01 to 2023-12-31
`parameterID`	1) Wind speed (“wind_speed”) 2) Wind direction (“wind_dir”)

More guidance can be found here:
https://opendatadocs.dmi.govcloud.dk/en/APIs/Meteorological_Observation_API
(Assessed February 28, 2024)

3. Model construction

The wind speed was divided into 6 wind speed ranges: 0-1 m/s 1-2 m/s, 2-4 m/s, 4-6 m/s, 6-8 m/s and >8 m/s. The wind direction was divided into 8 wind sectors: North, Northwest, West, Southwest, South, Southeast, East, and Northeast.
For each wind speed range, the **mean wind speed** was calculated and used as input parameter in the risk modeling.

4. Simulation setup.

The wind data was collected and analyzed using Python 3.0. A query string was defined with the parameters listed above and send to the receiving server. Data is returned in a ‘FeatureCollection’ object. Based on the data on wind speed and wind direction, wind roses – using the `WindroseAxes` function - for selected location and period is generated, as seen in Figure 59 and Figure 60. As seen from the figures the wind roses are almost identical for the two periods for each selected location in Denmark (Copenhagen vs. Aalborg). Table 16 gives the data in a table-format and the calculated mean wind speed for each range.

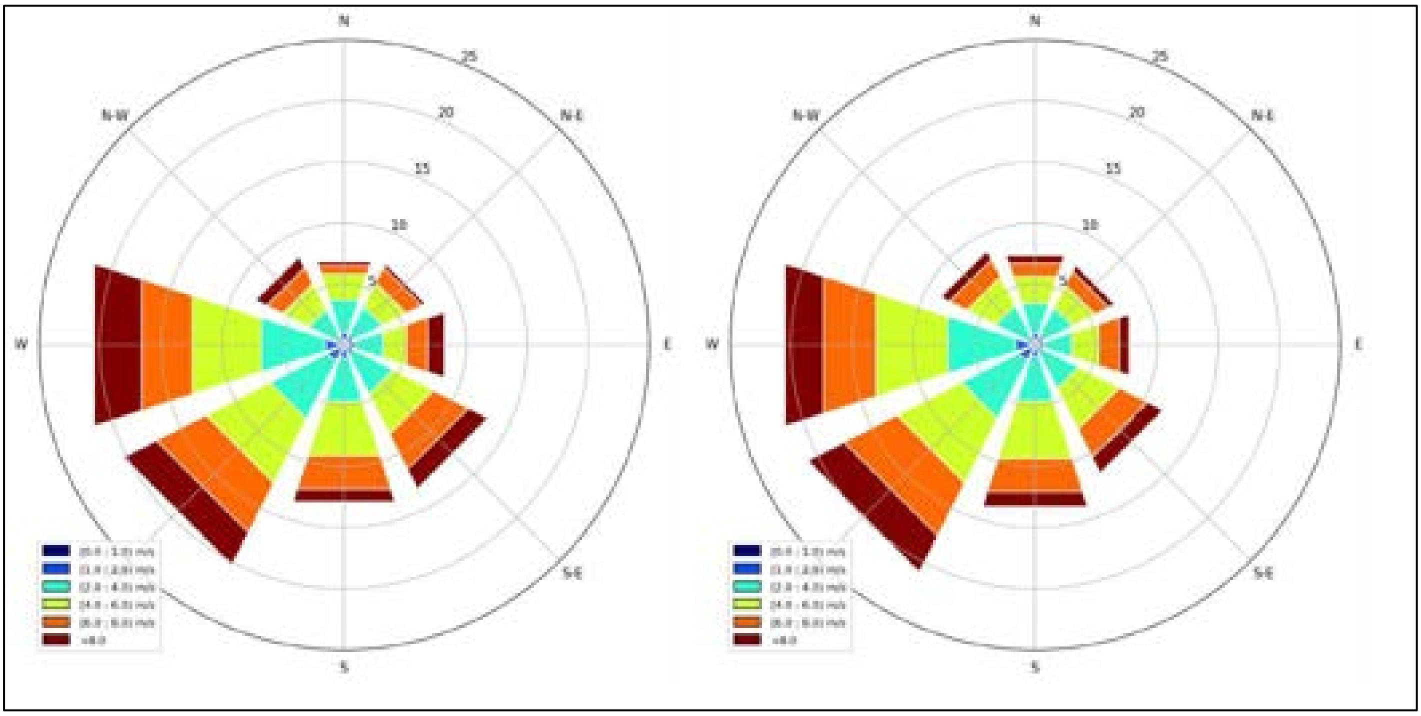

Figure 59 Wind roses for Copenhagen Airport for 2 years 2022-2023 (left) and 5 years 2019-2023 (right).

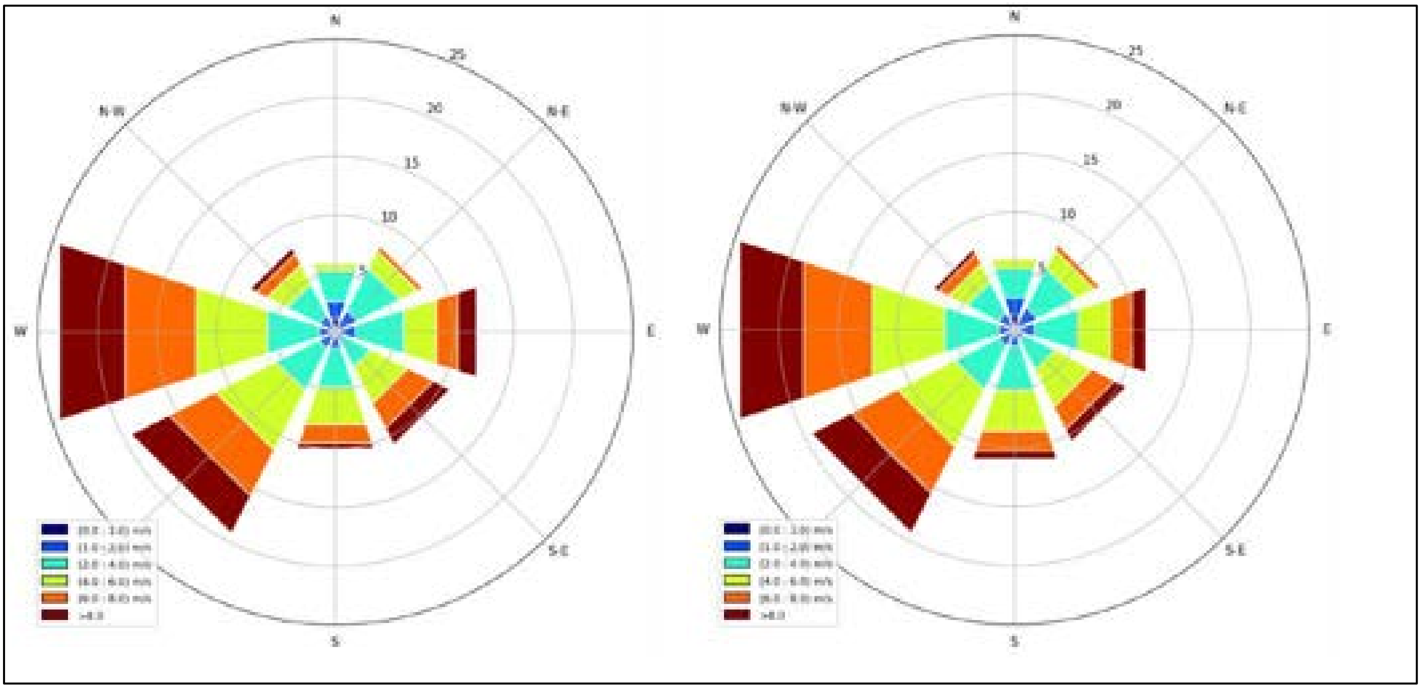

Figure 60 Wind roses for Aalborg Airport for 2 years 2022-2023 (left) and 5 years 2019-2023 (right).

Table 16 Wind data for Copenhagen Airport 2022-2023 and 2019-2023 and Aalborg Airport 2022-2023.

Copenhagen Airport Wind data 2022-2023										
index	N	NE	E	SE	S	SW	W	NW	Mean wind speed	
0-1 m/s	0.40	0.15	0.16	0.15	0.25	0.31	0.26	0.15	<1	**0.43**
1-2 m/s	0.61	0.74	0.78	0.77	0.81	1.17	1.31	0.54	>=1 to <2	**1.31**
2-4 m/s	2.87	2.62	2.38	3.58	3.79	5.30	5.54	2.55	>=2 to <4	**2.91**
4-6 m/s	2.22	2.20	2.07	3.72	4.68	5.91	5.95	2.39	>=4 to <6	**4.86**
6-8 m/s	0.75	1.42	1.77	3.21	2.92	4.55	4.35	1.48	>=6 to <8	**6.86**
>8 m/s	0.35	0.35	1.49	1.79	1.06	3.02	4.14	1.01	>8	**9.71**

Copenhagen Airport Wind data 2019-2023										
index	N	NE	E	SE	S	SW	W	NW	Mean wind speed	
0-1 m/s	0.40	0.15	0.13	0.13	0.22	0.28	0.23	0.14	<1	**0.43**
1-2 m/s	0.56	0.69	0.69	0.65	0.73	1.19	1.38	0.59	>=1 to <2	**1.31**
2-4 m/s	2.63	2.59	2.33	3.21	3.88	5.29	5.87	2.89	>=2 to <4	**2.92**
4-6 m/s	2.32	2.05	2.35	3.77	4.94	5.94	6.21	2.65	>=4 to <6	**4.85**
6-8 m/s	1.13	1.28	1.72	2.58	2.89	4.87	4.55	1.59	>=6 to <8	**6.86**
>8 m/s	0.66	0.55	0.88	1.46	1.29	3.34	3.32	0.81	>8	**9.59**

Aalborg Airport Wind data 2022-2023										
index	N	NE	E	SE	S	SW	W	NW	Mean wind speed	
0-1 m/s	1.18	0.38	0.30	0.25	0.32	0.31	0.24	0.23	<1	**0.36**
1-2 m/s	1.54	1.66	1.45	0.60	1.11	1.22	1.19	1.30	>=1 to <2	**1.31**
2-4 m/s	2.75	4.02	4.27	2.51	3.49	4.07	4.56	3.01	>=2 to <4	**2.86**
4-6 m/s	0.62	1.70	2.89	3.49	3.40	5.74	6.30	1.92	>=4 to <6	**4.85**
6-8 m/s	0.14	0.45	1.88	2.40	1.65	4.38	6.25	1.05	>=6 to <8	**6.84**
>8 m/s	0.00	0.08	1.68	1.55	0.51	3.57	5.83	0.56	>8	**9.95**

Aalborg Airport Wind data 2019-2023										
index	N	NE	E	SE	S	SW	W	NW	Mean wind speed	
0-1 m/s	1.29	0.38	0.29	0.23	0.29	0.29	0.24	0.25	<1	**0.35**
1-2 m/s	1.55	1.75	1.42	0.63	1.11	1.21	1.15	1.33	>=1 to <2	**1.31**
2-4 m/s	2.61	3.74	3.91	2.94	3.94	4.19	4.83	2.95	>=2 to <4	**2.87**
4-6 m/s	0.82	1.74	2.95	3.54	3.69	5.47	6.45	1.79	>=4 to <6	**4.84**
6-8 m/s	0.15	0.49	1.91	2.17	1.76	4.41	6.15	0.97	>=6 to <8	**6.85**
>8 m/s	0.01	0.06	1.20	1.11	0.70	3.77	5.73	0.43	>8	**9.87**

B.3 Failure frequency

- Please see Section 4.2
- Isolation valve failure rate is set to zero

B.4 Risk calculation

Methodology in accordance with Section 13.1 using data from Section 13.1 through Section 13.3.

Output format: csv-files with risk contours of Location Specific Individual Risk at 1E-4/yr, 1E-5/yr, 1E-6/yr, and 1E-7/yr.

Appendix C Summary of cases

Summary of cases for consequence modelling

Gaseous (30 bar) CO2 buried pipeline rupture

Number of varied parameters from base case	Parameter varied	Weather	Terrain roughness	Mass flow rate	Isolation valve spacing	Valve closure time	Depth of cover + soil type	Time for reported side view	Total mass of released CO2	Total time of event	Initial mass of CO2 between valves	Simulated valve closure time
0	BASE CASE	Multiple	1000 mm	22 kg/s	20 km	60 s	1.2 m clay	193.3 s	138 ton	1509 s	156 ton	60.1 s
1	Terrain roughness	4D	3000 mm	22 kg/s	20 km	60 s	1.2 m clay	193.3 s	138 ton	1509 s	156 ton	60.1 s
1		4D	100 mm	22 kg/s	20 km	60 s	1.2 m clay	193.3 s	138 ton	1509 s	156 ton	60.1 s
1		4D	5 mm	22 kg/s	20 km	60 s	1.2 m clay	193.3 s	138 ton	1509 s	156 ton	60.1 s
1	Mass flow rate	4D	1000 mm	11 kg/s	20 km	60 s	1.2 m clay	195.5 s	144 ton	1536 s	156 ton	60.1 s
1	Valve spacing	4D	1000 mm	22 kg/s	30 km	60 s	1.2 m clay	288.1 s	195 ton	2743 s	228 ton	60.1 s
1		4D	1000 mm	22 kg/s	10 km	60 s	1.2 m clay	187.7 s	77 ton	545 s	80 ton	60.1 s
1	Valve closure time	4D	1000 mm	22 kg/s	20 km	30 s	1.2 m clay	186.5 s	135 ton	1518 s	156 ton	32.4 s
1		4D	1000 mm	22 kg/s	20 km	10 s	1.2 m clay	200.8 s	130 ton	1526 s	156 ton	10.1 s
1	Depth of cover + soil type	4D	1000 mm	22 kg/s	20 km	60 s	0.8 m clay	193.3 s	138 ton	1509 s	156 ton	60.1 s
1		4D	1000 mm	22 kg/s	20 km	60 s	0.5 m clay	193.3 s	138 ton	1509 s	156 ton	60.1 s
1		4D	1000 mm	22 kg/s	20 km	60 s	1.2 m sandy	193.3 s	138 ton	1509 s	156 ton	60.1 s
2	Valve spacing + closure time	4D	1000 mm	22 kg/s	10 km	10s	1.2 m clay	183.7 s	69 ton	548 s	80 ton	10.1 s

Gaseous (30 bar) CO2 above ground rupture

Number of varied parameters from base case	Parameter varied	Weather	Terrain roughness	Mass flow rate	Isolation valve spacing	Valve closure time	Angle of release	Time for reported side view	Total mass of released CO2	Total time of event	Initial mass of CO2 between valves	Simulated valve closure time
0	BASE CASE	4D	1000 mm	22 kg/s	20 km	60 s	30 degrees	193.3 s	138 ton	1509 s	156 ton	10.6 s
1	Angle of release	4D	3000 mm	22 kg/s	20 km	60 s	5 degrees	193.3 s	138 ton	1509 s	156 ton	10.6 s
1		4D	250 mm	22 kg/s	20 km	60 s	90 degrees (vertical)	193.3 s	138 ton	1509 s	156 ton	10.6 s

Dense (120 bar) CO2 buried pipeline rupture

Number of varied parameters from base case	Parameter varied	Weather	Terrain roughness	Mass flow rate	Isolation valve spacing	Valve closure time	Depth of cover + soil type	Time for reported side view	Total mass of released CO2	Total time of event	Initial mass of CO2 between valves	Simulated valve closure time
0	BASE CASE	Multiple	1000 mm	169 kg/s	20 km	60 s	1.2 m clay	652.9 s	1,566 ton	3600 s (1h limit)	1,994 ton	79.9 s
1	Terrain roughness	4D	3000 mm	169 kg/s	20 km	60 s	1.2 m clay	652.9 s	1,566 ton	3600 s (1h limit)	1,994 ton	79.9 s
1		4D	100 mm	169 kg/s	20 km	60 s	1.2 m clay	652.9 s	1,566 ton	3600 s (1h limit)	1,994 ton	79.9 s
1		4D	5 mm	169 kg/s	20 km	60 s	1.2 m clay	652.9 s	1,566 ton	3600 s (1h limit)	1,994 ton	79.9 s
1	Mass flow rate	4D	1000 mm	84 kg/s	20 km	60 s	1.2 m clay	655.4 s	1,560 ton	3600 s (1h limit)	1,994 ton	72.2 s
1		4D	1000 mm	253 kg/s	20 km	60 s	1.2 m clay	649.2 s	1,568 ton	3600 s (1h limit)	1,994 ton	78.1 s
1	Valve spacing	4D	1000 mm	169 kg/s	30 km	60 s	1.2 m clay	737.7 s	1,769 ton	3600 s (1h limit)	2,988 ton	79.9 s
1		4D	1000 mm	169 kg/s	10 km	60 s	1.2 m clay	358.9 s	861 ton	2873 s	998 ton	69.0 s
1	Valve closure time	4D	1000 mm	169 kg/s	20 km	30 s	1.2 m clay	650.5 s	1,560 ton	3600 s (1h limit)	156 ton	30.1 s
1		4D	1000 mm	169 kg/s	20 km	10 s	1.2 m clay	651.3 s	1,558 ton	3600 s (1h limit)	156 ton	10.9 s
1	Depth of cover + soil type	4D	1000 mm	169 kg/s	20 km	60 s	0.8 m clay	652.9 s	1,566 ton	3600 s (1h limit)	1,994 ton	79.9 s
1		4D	1000 mm	169 kg/s	20 km	60 s	0.5 m clay	652.9 s	1,566 ton	3600 s (1h limit)	1,994 ton	79.9 s
1		4D	1000 mm	169 kg/s	20 km	60 s	1.2 m sandy	652.9 s	1,566 ton	3600 s (1h limit)	1,994 ton	79.9 s
2	Valve spacing + closure time	4D	1000 mm	169 kg/s	10 km	10s	1.2 m clay	358.7 s	852 ton	2883 s	998 ton	12.1 s

Dense (120 bar) CO2 above ground rupture

Number of varied parameters from base case	Parameter varied	Weather	Terrain roughness	Mass flow rate	Isolation valve spacing	Valve closure time	Angle of release	Time for reported side view	Total mass of released CO2	Total time of event	Initial mass of CO2 between valves	Simulated valve closure time
0	BASE CASE	4/D	1000 mm	169 kg/s	20 km	60 s	30 degrees	452.9 s	1,388 ton	3600 (1 h limit)	1,994 ton	79.9 s
1	Angle of release	4/D	3000 mm	169 kg/s	20 km	60 s	5 degrees	452.9 s	1,388 ton	3600 (1 h limit)	1,994 ton	79.9 s
1		4/D	250 mm	169 kg/s	20 km	60 s	90 degrees (vertical)	452.9 s	1,388 ton	3600 (1 h limit)	1,994 ton	79.9 s

Tanks (Toxicity and BLEVE overpressure)

Number of varied parameters from base case	Parameter varied	Weather	Terrain roughness	Tank volume	Mass of contained CO2	Tank pressure/ temperature
0	BASE CASE	4/D	1000 mm	750 m3	800 ton	15 barg/-28 C
1	Variation of tank volume	4/D	1000 mm	50 m3	53 ton	15 barg/-28 C
1		4/D	1000 mm	350 m3	374 ton	15 barg/-28 C
1		4/D	1000 mm	3000 m3	3,202 ton	15 barg/-28 C
1	Variation of tank pressure/temperature	4/D	1000 mm	750 m3	673 ton	7 barg/-50 C
1		4/D	1000 mm	750 m3	889 ton	45 barg/+5 C

Summary of cases for full risk assessment

Gaseous (30 bar) CO2 buried pipeline rupture

Number of varied parameters from base case	Parameter varied	Failure frequency	Weather data	Terrain roughness	Mass flow rate	Isolation valve spacing	Valve closure time	Depth of cover + soil type
0	BASE CASE:	2.6E-4/ year	Copenhagen, 2022-2023, stability D	1000 mm	22 kg/s	20 km	60 s	1.2 m clay
1	Weather station	2.6E-4/ year	Aalborg, 2022-2023, stability D	1000 mm	22 kg/s	20 km	60 s	1.2 m clay
1	Weather - time period	2.6E-4/ year	Copenhagen, 2019-2023, stability D	1000 mm	22 kg/s	20 km	60 s	1.2 m clay
1	Valve spacing	3.9E-4/ year	Copenhagen, 2022-2023, stability D	1000 mm	22 kg/s	30 km	60 s	1.2 m clay
1		1.3E-4/ year	Copenhagen, 2022-2023, stability D	1000 mm	22 kg/s	10 km	60 s	1.2 m clay
1	Valve closure time	2.6E-4/ year	Copenhagen, 2022-2023, stability D	1000 mm	22 kg/s	20 km	30 s	1.2 m clay
1		2.6E-4/ year	Copenhagen, 2022-2023, stability D	1000 mm	22 kg/s	20 km	10 s	1.2 m clay
2	Valve spacing AND closure time	1.3E-4/ year	Copenhagen, 2022-2023, stability D	1000 mm	22 kg/s	10 km	10s	1.2 m clay

Dense (120 bar) CO2 buried pipeline rupture

Number of varied parameters from base case	Parameter varied	Failure frequency	Weather data	Terrain roughness	Mass flow rate	Isolation valve spacing	Valve closure time	Depth of cover + soil type
0	BASE CASE:	2.6E-4/ year	Copenhagen, 2022-2023, stability D	1000 mm	169 kg/s	20 km	60 s	1.2 m clay
1	Weather station	2.6E-4/ year	Aalborg, 2022-2023, stability D	1000 mm	169 kg/s	20 km	60 s	1.2 m clay
1	Weather - time period	2.6E-4/ year	Copenhagen, 2019-2023, stability D	1000 mm	169 kg/s	20 km	60 s	1.2 m clay
1	Valve spacing	3.9E-4/ year	Copenhagen, 2022-2023, stability D	1000 mm	169 kg/s	30 km	60 s	1.2 m clay
1		1.3E-4/ year	Copenhagen, 2022-2023, stability D	1000 mm	169 kg/s	10 km	60 s	1.2 m clay
1	Valve closure time	2.6E-4/ year	Copenhagen, 2022-2023, stability D	1000 mm	169 kg/s	20 km	30 s	1.2 m clay
1		2.6E-4/ year	Copenhagen, 2022-2023, stability D	1000 mm	169 kg/s	20 km	10 s	1.2 m clay
2	Valve spacing AND closure time	1.3E-4/ year	Copenhagen, 2022-2023, stability D	1000 mm	169 kg/s	10 km	10s	1.2 m clay